# Flensburg University of Applied Sciences

# B A C H E L O R – T H E S I S

**Topic**: Comparative Evaluation of Joint Leak Tightness for Two Steam Turbine Casing Geometries

**By:** Jochen Homann

**Student number:** 510886 (Flensburg UAS)

**Course of studies:** Renewable Energy Engineering (Flensburg UAS)
Energy Technology (Kymenlaakso UAS)

**First evaluator:** Prof. Dr.-Ing. Ilja Tuschy (Flensburg UAS)

**Second evaluator:** Merja Mäkelä, Lic. Tech. (Kymenlaakso UAS)

**Date of issue**: 15.06.2015

**Date of submission:** 15.08.2015

**Jochen Homann**

# Comparative Evaluation of Joint Leak Tightness for Two Steam Turbine Casing Geometries

Bachelor thesis submitted within the context of a bachelor´s degree in cooperation with:

MAN Diesel & Turbo SE
Engineering MARC Steam Turbine
Hermann-Blohm-Straße 5
20457 Hamburg

Industrial supervisors: Dr.-Ing. Claus Fost; Florian Brahm, M.Eng.

# Preface

This bachelor thesis is written as the final deliverable for my bachelor double degree in Renewable Energy Engineering and Energy Technology. My home university is the Flensburg University of Applied Science and my host university is the Kymenlaakso University of Applied Science.

Within the scope of a prior internship at MAN Diesel & Turbo I became acquainted with steam turbines, joint leak tightness and have completed some preparatory work which is included in this thesis. This preparatory work contained initial training for the employed program Creo Simulate as well as the general construction of the basic model.

I would like to thank all my colleagues and friends who supported me during this time. My special thanks go to my industrial supervisors, Claus Fost and Florian Brahm as well as to my university supervisors Ilja Tuschy and Merja Mäkelä. It would not have been possible to write this thesis without your support.

Conclusively I can say that I am satisfied with my work and it makes me proud that MAN Diesel & Turbo applied for a patent based on my work outlined in this thesis.

Hamburg, August 2015

# Table of Contents

# List of Figures

**Appendix A**



**Appendix B**

# List of Tables

**Appendix A**

**Appendix B**

# List of Symbols

The following symbols are used throughout this thesis:

| Symbol | Designation |
|---|---|
| $A_D$ | sealing area (at most interface area less the through-hole for the bolt) |
| $A_p$ | pressureised area |
| a | distance of the substitutional line of action of the axialload $F_A$ from the axis of the imaginary laterally symmetrical deformation body |
| $b_T$ | depth of the interface area (x direction) |
| $b_1$ | width of the partial seal face |
| $b_2$ | width of the partial seal face |
| $c_F$ | rigidity of the flange material |
| $c_S$ | rigidity of the bolt material |
| $c_T$ | width of the interface area perpendicular to the depth $b_T$ (y direction) |
| $D_{DH}$ | head of a bolt diameter |
| d | bolt diameter = outside diameter of thread (nominal diameter) |
| $d_{af}$ | diameter of the reduction surface for position the expansion sleeve |
| $d_{DH}$ | internal diameter of expansion sleeve |
| $d_h$ | hole diameter of the clamped parts |
| $d_y$ | horizontal distance between point of intersection of the tangents of the round and inner edge |
| e | horizontal distance between bolt axis and inner suface |
| F | load, general |

| | |
|---|---|
| $F_A$ | axial load, a component, directed in the bolt axis and proportionally related to the bolt of a working load $F_B$ in any direction |
| $F_B$ | working load at a joint in any direction |
| $F_K$ | clamp load |
| $F_{Kab}$ | clamp load at the opening limit |
| $F_{Kerf}$ | clamp load required for sealing functions, friction grup and prevention of one-sided opening at the interface |
| $F_{KP}$ | minimum clamp load for ensuring a sealing function |
| $F_{KQ}$ | minimum clamp load for transmitting a transverse load and/or a torque by friction grip |
| $F_{KR}$ | residual clamp load at the interface |
| $F_{KR\ (Rest)}$ | 'residual' residual clamp load at the interface |
| $F_N$ | normal load |
| $F_p$ | load at a joint caused by pressure |
| $F_S$ | bolt load |
| $F_T$ | load at a joint caused by temperature |
| $F_V$ | preload force |
| $F_{Ver}$ | vertical load |
| f | elastic linear deformation due to a force F |
| $f_{FV}$ | shrinkage of the clamped parts due to $F_K$ |
| $f_{FB}$ | shrinkage of the clamped parts due to $F_A$ |
| $f_{SB}$ | elongation of the bolt due to $F_A$ |
| $f_{SV}$ | elongation of the bolt due to $F_K$ |
| h | heat transfer coefficient |

| | |
|---|---|
| $h_{FF}$ | height of the milling groove in the flange |
| $h_{min}$ | thickness of one of two clamped flanges |
| $I_{BT}$ | moment of gyration of the interface area |
| $k_{RI}$ | superelevation of the internal radius at the flange hight |
| $l_{DH}$ | height of the expansion sleeve |
| $l_{FL}$ | thickness of one of two clamped flanges with a reduction for position the expansion sleeve |
| $l_{SK}$ | height of the head of a bolt |
| M | moment, general |
| $M_B$ | working moment (bending moment) acting at the bolting point |
| $M_{KI}$ | resulting moment in the clamping area |
| $M_p$ | resulting moment in the clamping area caused by pressure |
| $M_T$ | resulting moment in the clamping area caused by temperature |
| $p_i$ | internal pressure |
| $p_{i, max}$ | maximum internal pressure |
| $q_{min}$ | minimum contact pressure |
| $R_A$ / $r_a$ | external radius |
| $R_{FA}$ | imaginary radius between internal radius and external radius |
| $R_I$ / $r_i$ | internal radius |
| $Ry_I$ | internal radius (y axis) |
| $Rz_I$ | internal radius (z axis) |
| $r_{GF}$ | round radius between external radius and flange |

| | |
|---|---|
| $S_{sym}$ | distance between the bolt axis and the axis of the imaginary laterally symmetrical deformation body |
| s | wall thickness at the thinnest point of the casing |
| T | temperature, general |
| T(r) | temperature dependent of wall thickness r |
| u | edge distance of the opening point U from the axis of the imaginary laterally symmetrical deformation body |
| v | distance of the edge bearing point V from the axis of the imaginary laterally symmetrical deformation body |
| $v_{RA}$ | offset of the external radius (z axis) |
| $v_{ver}$ | Internal round radius |
| x | constant |
| $\sigma_B$ | bending stress |
| $\sigma_M$ | membrane stress |
| $\sigma_v$ | von-Mises-stress |
| $\sigma_{xx}$, $\sigma_{yy}$, $\sigma_{zz}$ | normal stress |
| $\tau_{xy}$, $\tau_{xz}$, $\tau_{yz}$ | shear stress in |

Most of the designations are taken from [2].

# List of Abbreviations

| | |
|---|---|
| AD | Arbeitsgemeinschaft Druckbehälter (committee pressure tanks) |
| ASME | American Society of Mechanical Engineers |
| approx. | Approximately |
| CAD | Computer Aided Design |
| cf. | Confer |
| eq. | Equation |
| FEM | Finite elemente method |
| fig. | Figure |
| i.e. | Id est |
| MARC | Modular Arrangement Concept |
| MDT-HBG | MAN Diesel & Turbo located in Hamburg |
| Tab. | Table |
| TRD | Technische Regeln für Dampfkessel (technical guidelines for steam boiler) |
| VDI | Verein Deutscher Ingenieure (Association of German Engineers) |

# 1 Introduction

MAN Diesel & Turboe SE is a subsidiary of the MAN concern and is specialized on building turbomachinery and diesel engines. The location in Hamburg develops and produces steam turbines with a power range of 1 - 40 MW. Steam turbines are turbomachines which transduce highly heated steam (potential energy) at first into flow (kinetic energy) and afterwards into work (mechanical energy) or by using a gear box with connected generator into electric power (electric energy). Steam turbines are applicable for driving a generator in industry and biomass power plants as well as a drivetrain for pumps, ships or compressors.

The current casing of steam turbines usually consists of an upper and under casing, which is shaped cylindrical. These halves are connected by using bolted flanges. An essential value, which affects the tightness of the flange joint, is the distance between the bolt axis and the point where the resultant force – caused by pressure – is transferred via the cylindrical casing into the flange. The greater distance the more inconvenient is the lever arm for the sealing effect of the bolt. In the case of insufficient bolt force, the flanges will gape on the inner surface of the casing and cause a leakage.

Results from a previous bachelor thesis have shown that the current shape of the casing geometry has only a slightly positive influence on the lever arm and can be improved by modifications of the geometry.

The purpose of the present bachelor thesis is to reduce the distance between the point of origin of the resulting compression force and the bolt axis by improving the casing geometry. Due to this modification the leak tightness will be improved without reducing the bolt force. The mechanical and thermal highly stressed region of the turbine – called wheel chamber – is used representatively for the entire turbine.

The thesis is structured as follows. First of all there is part 2 which puts the problem into the overall context and specifies the evaluation criteria for the analysis. The subsequent chapter 3 is presenting the current geometry together with the investigated variations based on FE-calculation models. Part 4 shows the method for the analysis and the evaluation of the results. Lastly, this thesis is concluding with a perspective in chapter 5.

# 2 Theory and Technical Principles of Steam Turbines

To put the topic of this thesis into the overall context, this chapter will describe the general construction of a steam turbine. Because the focus will be on the correlation between casing geometry and joint leak tightness, fundamental details will be given in the following text. After this, the specific geometry of the wheel chamber will be considered. Figure 2-4 will serve as the basis for the carried out analysis.

## 2.1 General Structure of a Steam Turbine

This thesis will only deal with axial-flow steam turbine casings with a horizontal joint. Figure 2-1 shows the cross-section of a MDT steam turbine of the type MARC 4 (**M**odular **AR**rangement **C**oncept). This turbine has typically a power range of 10 to 28 MW and has a rated speed of 7 000 to 9 000 rpm.

Basically a steam turbine is built-up of a rotating turbine rotor (1) and a stationary turbine casing (2). The rotor bearing consists of two radial and one axial slide bearings (4/5) with respective bearing boxes (3). The axial bearing absorbs the steam-caused the axial thrust and holds the rotor in axial position. The rotor is surrounded by the casing. Live steam flows though the influx body (10) across the control valves (9) towards the nozzles (11) and impinges upon the control stage (12). The steam flows from the chamber behind the control stage (wheel chamber) though several reaction parts (7). This part consists of one static row of guide blades and one rotating row of rotor blades. The guide blades are fixed on an inner casing guide blade carrier (6). After the steam evolved the largest part of the usable energy it flows through the exhaust casing (14) via exhaust connections (15) into the condenser. By using different extraction nozzles (13) on the bottom of the casing it is possible to extract steam of particular states. A non-contact labyrinth seal (8) between rotor and turbine casing reduces the amount of steam which leaks the casing and prevents the ingress of air into the casing. At the end of the rotor there is a coupling flange (16), which connects the turbine rotor via a gearbox with the generator. [5, 6]]

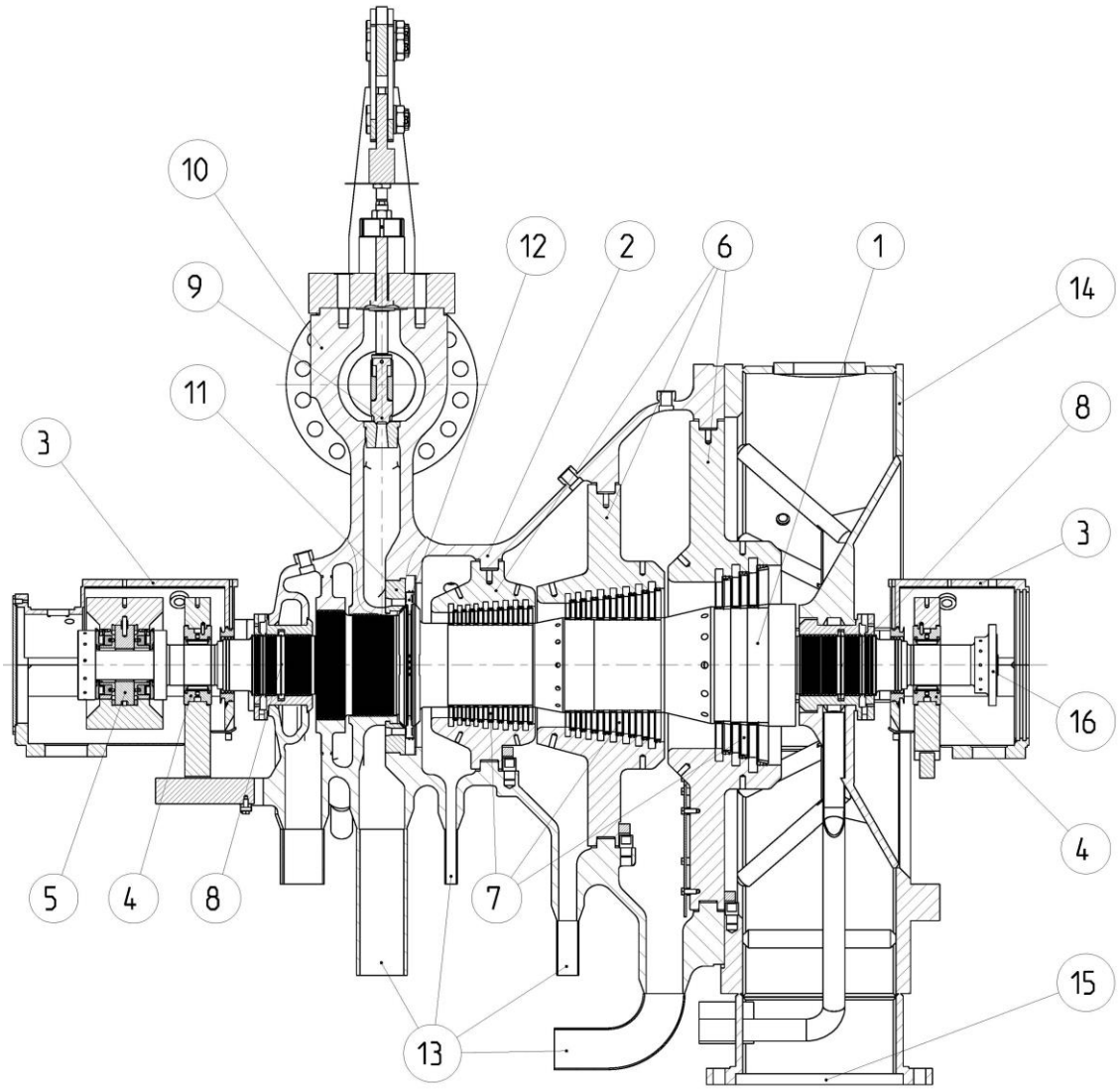


*Figure 2-1: Sectional drawing of a MARC steam turbine. Source: [6]*

## 2.2 Casing Geometry

Figure 2-2/3 is exemplary for a MDT steam turbine casing. Due to different demands, the casing design is partly adapted to the specifics of the order even so basic components will remain. In the following a representative example will describe the fundamental geometry characteristics.

The shown case parts are produced as steel casts. The mechanical reworked parts are marked green in these illustrations.

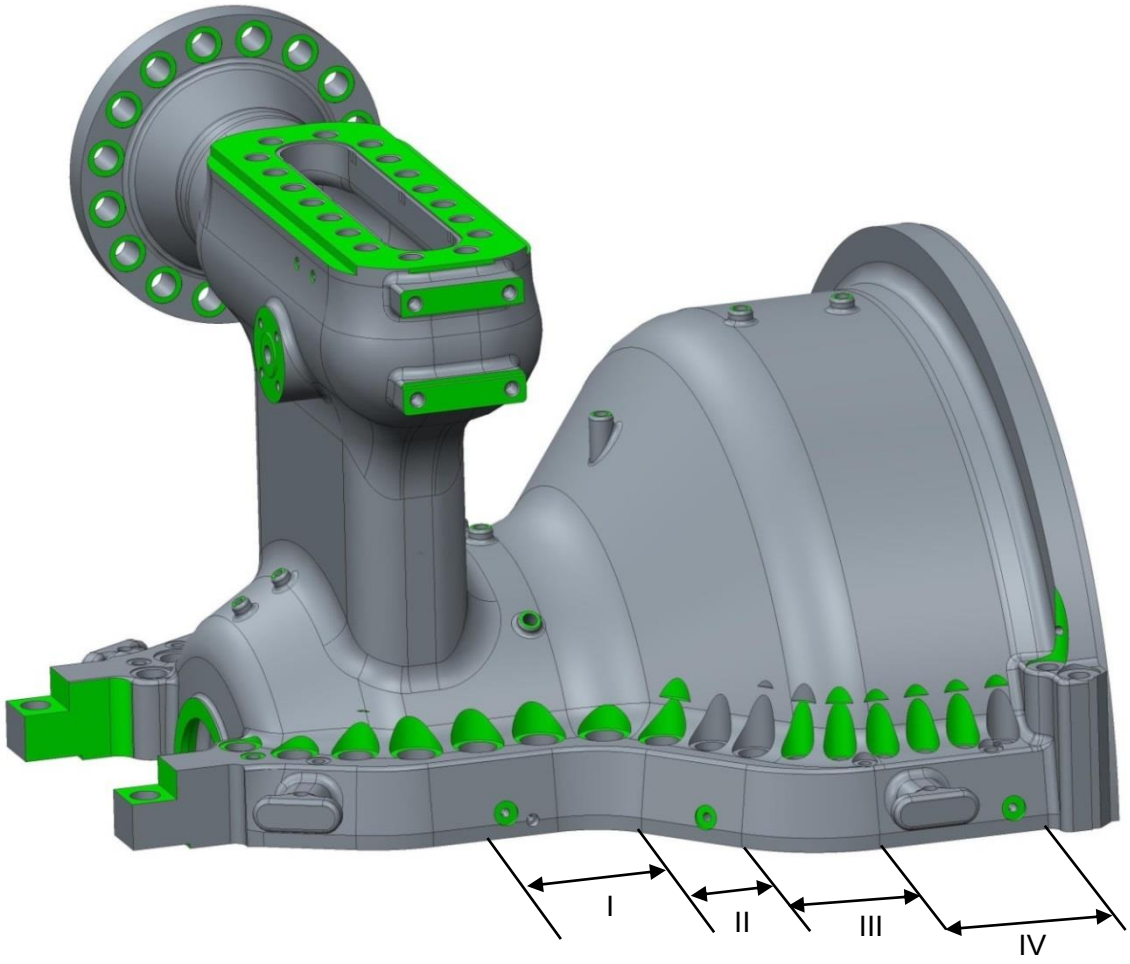


*Figure 2-2: Upper casing of a MARC steam turbine. Source: [8]*

Figure 2-2 and 2-3 show some in chapter 2.1 already mentioned components which will not be specified. The focus is set on components which are important for the following analysis.

The turbine casing is devided in four parts (I-IV). Starting with the cylindrical wheel chamber (I) the diameter of the following chambers (II-IV) are rising. At the end of the turbine the exhaust casing, which consists of a weldment is bolted with the cast casing by a vertical flange (1). The conical widening of the casing is correlated with the steam pressure, which is reduced by the onward going expansion in the blading in order to raise the volume. Another – besides the wheel chamber – emphasised component in this thesis is the horizontal flange (2). By use of this, the upper and under casing of the turbine are bolted. The on top of each other laying flange areas are called joint (3) and seal sheer metallic.

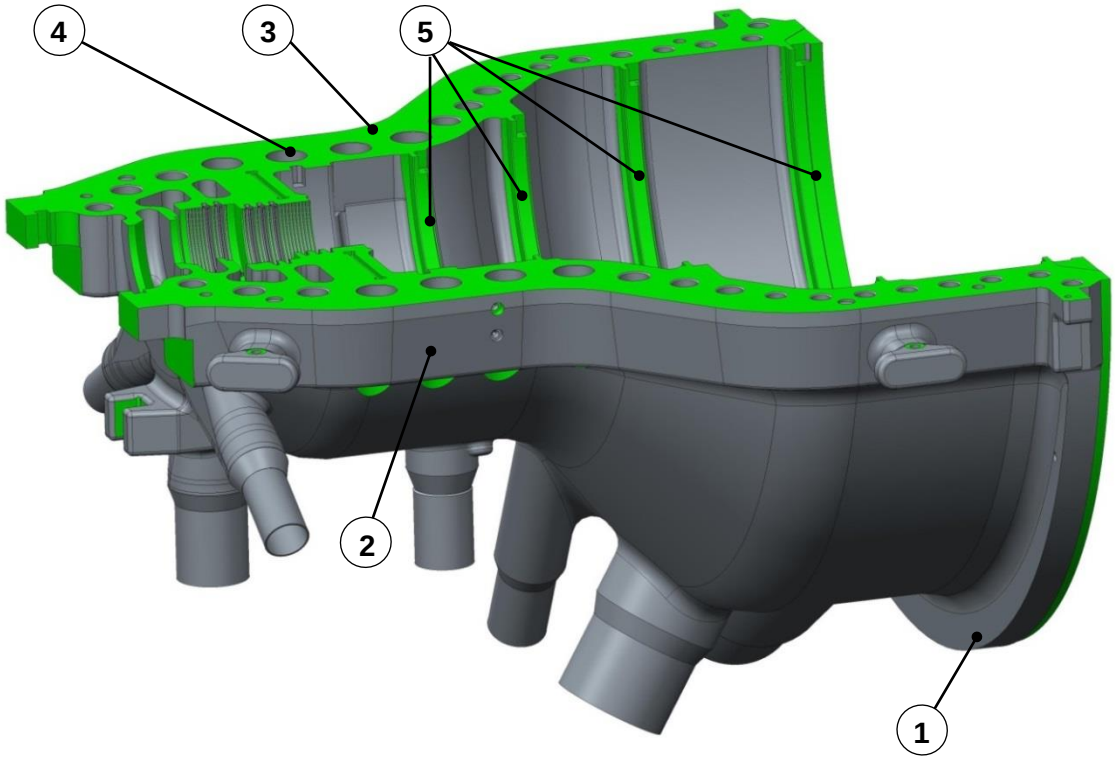


*Figure 2-3: Under-casing of a MARC steam turbine. Source: [8]*

The bore (4) for the bolted connection of the upper- and under-casing is located in the flange. Figure 2-3 shows also the location of the guide blades (5) which separates the particular chambers of the turbine.

As mentioned before, the following reflection and analysis use the wheel chamber exemplary for the whole turbine. This wheel chamber represents the thermally and mechanically highest loaded section of the casing joint.

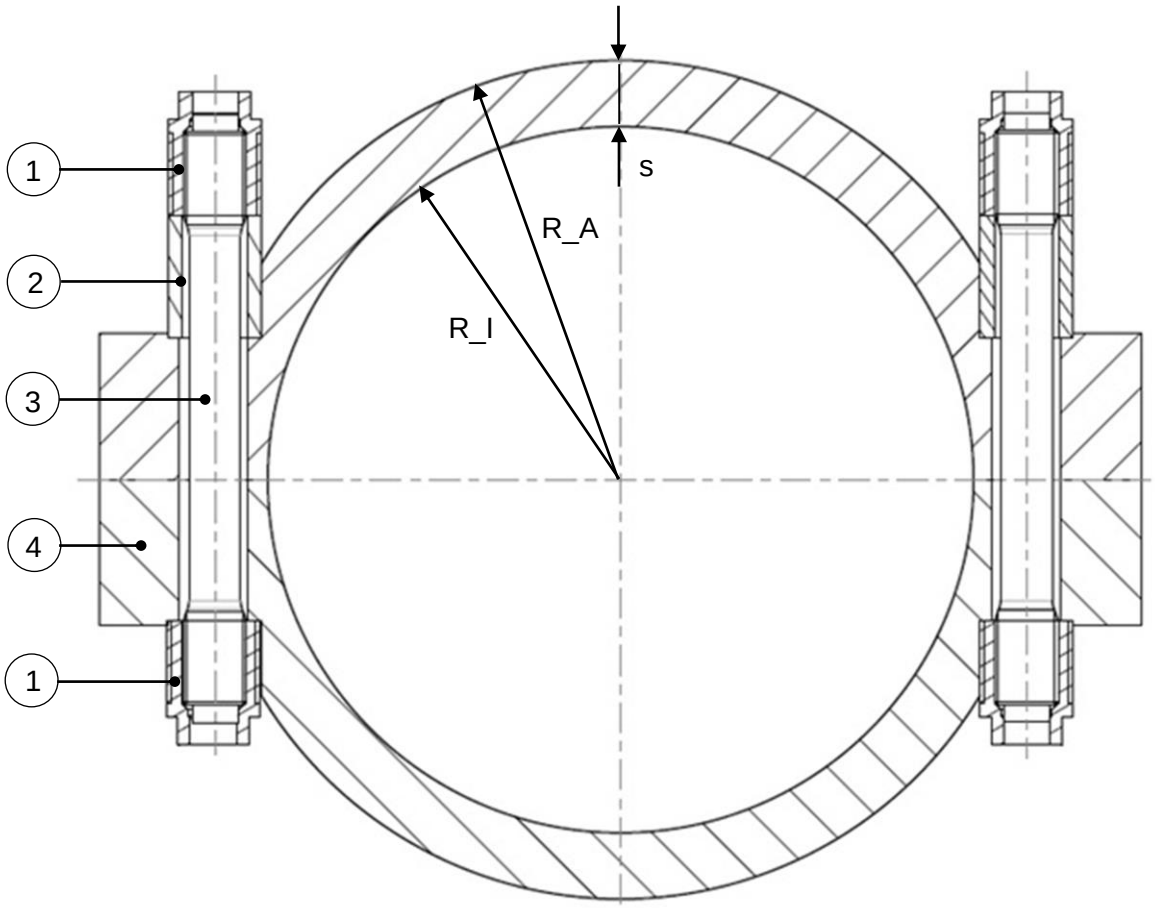


*Figure 2-4: Cross section model of a bolted cylindric wheel chamber.*

In the literature [7] used wheel chamber models assume a cylindrical constructed casing. Figure 2-4 shows that the internal radius (R_I) and external radius (R_A) has the same origin whereas the external radius is taller by the casing thickness (s). On the left and right side of the model the bolt connection of the flanges consisting of the bore (4), expension bolt (3), expension sleeve (2) and capped nuts (1) are pictured.

In the course of this thesis the model will be further simplified. In this way it becomes clearer and the later computational cost will considerably minimized. This fact facilitates the analysis of geometrical variations.

**Common geometrical variations**

The following text will describe common variations of the already presented cylindrical geometry and explain their effects.

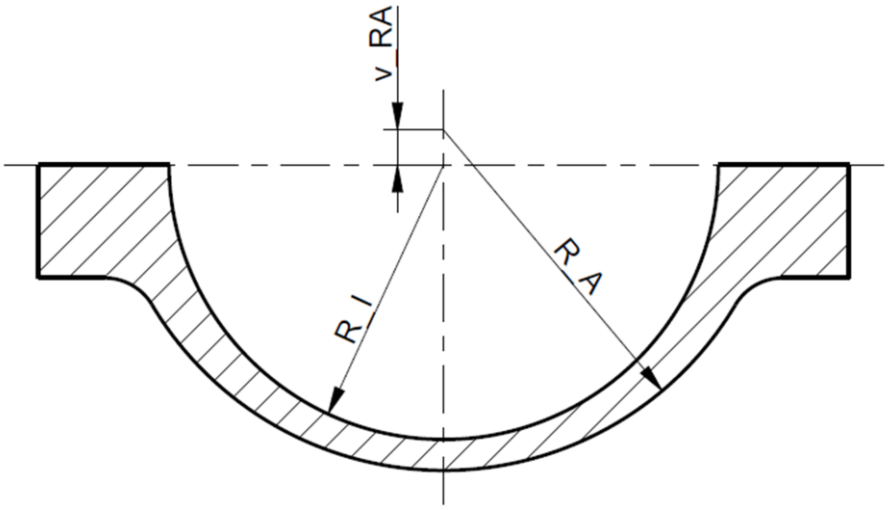


*Figure 2-5: Casing-half-shell with an eccentrically external radius.*

1. Figure 2-5 shows a casing-half-shell with an eccentrically exernal radius. Because of this variation the shell wall has the thinnest point at the bottom and enlarges in the direction to the flanges. This shape enables consequent benefits for the cast process as well as during operation. The upper and under shell of the casing are cast in the shown position. The molten steel is cast from above into the funnel-shaped negative mould of the casing and can solidify from the bottom up. The upwards increasing mass slows down the solidification process whereby formations of blowholes are reduced. Compared with the cylindrical casing shell, this variation has a thicker transition from the flange to the shell. This extra material at the transition can be used to relocate the bolt axis in the direction of the casing center. As a result there is a more favorable lever proportion for a better bolt connection with higher contact pressure and higher leak tightness at the inner joint surface.

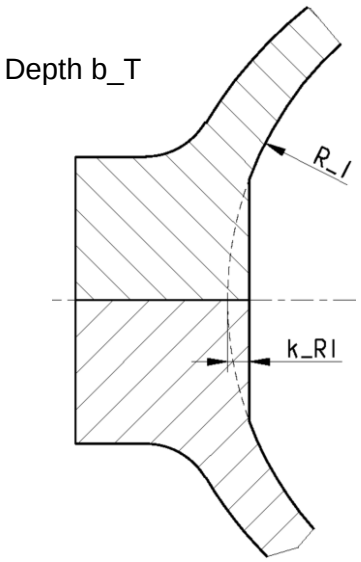


*Figure 2-6: Casing with superelevated flange. Source: [6]*

2. Another common variation of the initial geometry is a superelevated flange. This is constructively realized by adding some additional material on the inner casing at the level of the flange. Figure 2-6 shows this superelevated flange with the value k_RI. Beneficial is – as before – that the bolt axis can be relocated in the direction of the casing center. Hence, the bolt connection can be closer to the inner flange edge and deliver a higher contact pressure and higher leak tightness at the inner joint surface. A further advantage is a load relief of the bolt connection. Because of a shorter internal radius the pressurised surface (1) and the bolt connection effecting operating power (2) will decrease.

(1) $$A_p = (R_I - k_{RI}) \cdot b_T$$

(2) $$F_A = p_i \cdot (R_I - k_{RI}) \cdot b_T$$

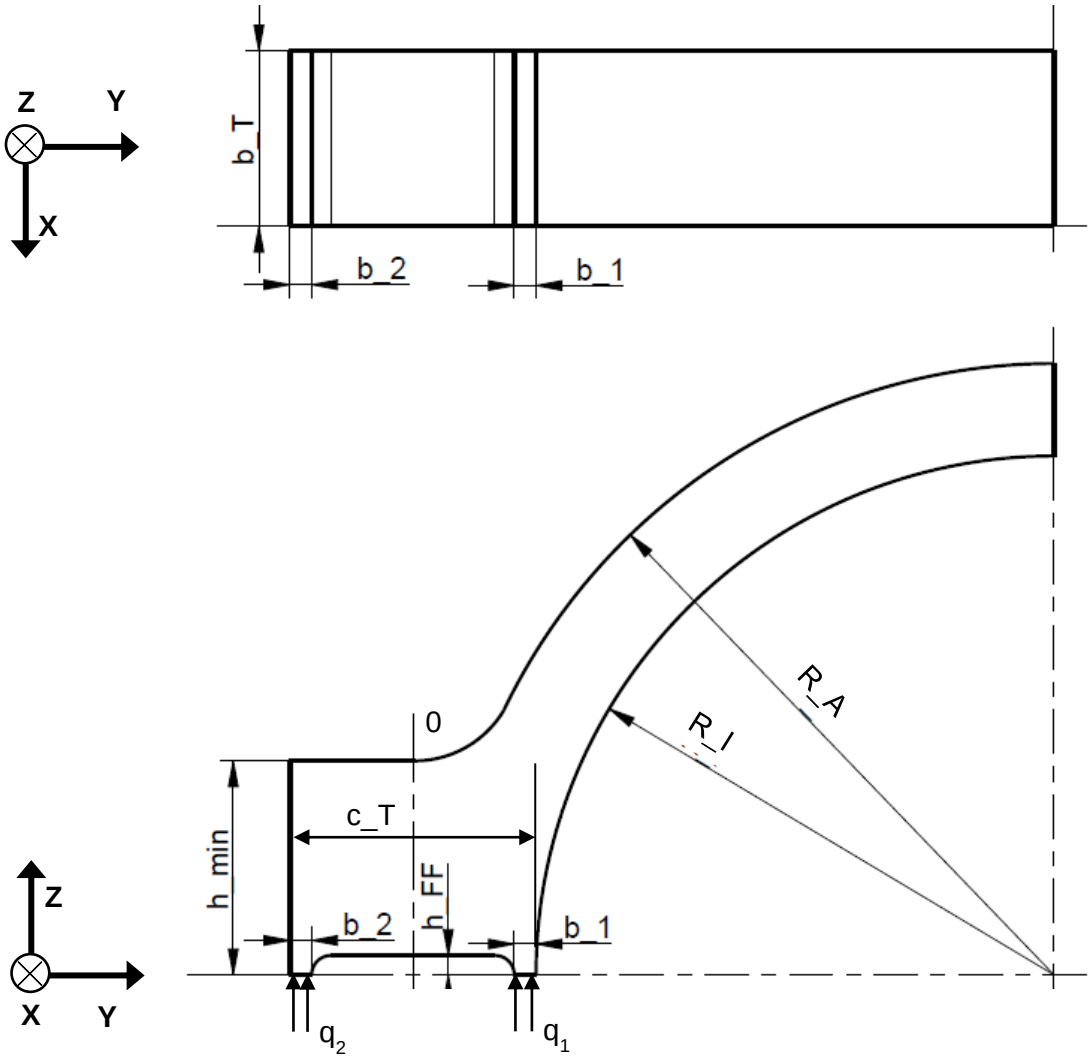


*Figure 2-7: Cylindric casing with milled groove inside the joint surface. Source: [6]*

3. The joint surface pressure is a measure for joint tightness. One constructive approach for increaseing the surface pressure is to reduce the contact surface by milling some part from the upper casing flange (constant operating power $F_A$) (cf. fig. 2-7). This sealing surface (3) is part of the joint surface and can become maximally this size.

(3) $A_D = b_T \cdot (b_1 + b_2)$ (cf. fig. 2-7)

In practice there is usually a combination of these three presented casing variations implemented.

## 2.3 The Flange-Bolt Connection

Joint bolt connections of the tubine casings at MDT-HBG are calculated based on VDI 2230 page 1. The following text will describe the relevant parameters concerning bolt connections, which are used for the analysis that will follow.

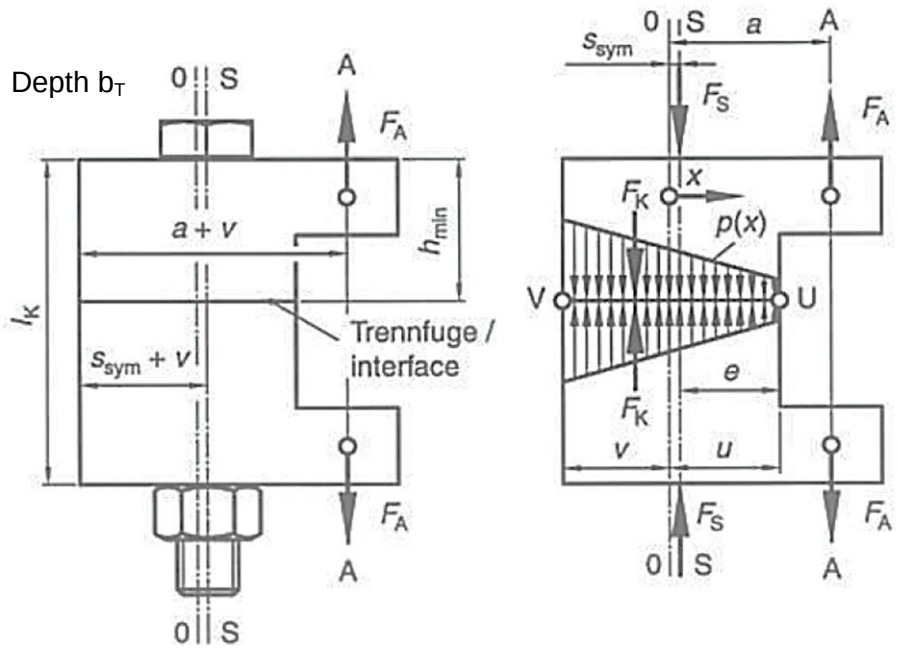


*Figure 2-8: Eccentric bracing and eccentric load of a bolt connection, dimensions and surface pressure in the joint. Source: [2]*

Figure 2-8 shows a bolt connection according to VDI 2230 page 1 which is absolutely comparable with the present case in this thesis. This involves an eccentric bracing (the axis of the imaginary laterally symmetrical deformation body (0) and the bolt axis (S) are moved by the amount of $S_{sym}$) as well as an eccentric load (the point of the operating force $F_A$ moved by the amount a from the axis of the imaginary laterally symmetrical deformation body (0)). The distances $S_{sym}$, $h_{min}$, $l_k$, e, u and v define the dimensions of the flange and the position of the bolt conncetion. The distance (a) and the loads ((working load ($F_A$), clamp force ($F_K$) and bolt force ($F_S$)) will be explained in more detail in the course of this chapter.

The left part of figure 2-8 shows the flanges as well as the bolt. In the right part the bolt is abstracted by the bolt force ($F_S$). The compressive stress inside the joint results from

the bolt preload force ($F_V$) and is assumed constant all over the contact surface. Assuming that the joint is permanently connected and symmetrically loaded, the working load ($F_A$) causes a bending stress, which is linearly distributed all over the flange. The result of this overlapping stresses is pictured in the right part of figure 2-8 as the joint pressure p(x). The lowest surface pressure and thus the critical part of the bolt connection is the steam-facing point U. The so-called clamp force ($F_K$) is connected with the surface pressure and thereby also a measure for the joint tightness.

By transfereing this general correlations of clamped components to the joint of a turbine casing, the pressure inside the wheel chamber ($p_{i,max}$) will cause the resulting work load ($F_A$). The force transmission point for the generally used cylindric casing is located at a middle radius ($R_{FA}$) (cf. fig. 2-9). The force ($F_A$) is working in the direction of the normal vector of the joint surface. This normal force is according to [2] called working load ($F_A$) and counteracts the bolt force ($F_S$). The result of the distance (a-$S_{sym}$) between the working load ($F_A$) and the bolt force ($F_S$) is a moment ($M_{Kl}$) inside the joint. This moment causes a reduction of the surface pressure at the inner part of the flange and a rising surface pressure at the outer part of the flange.

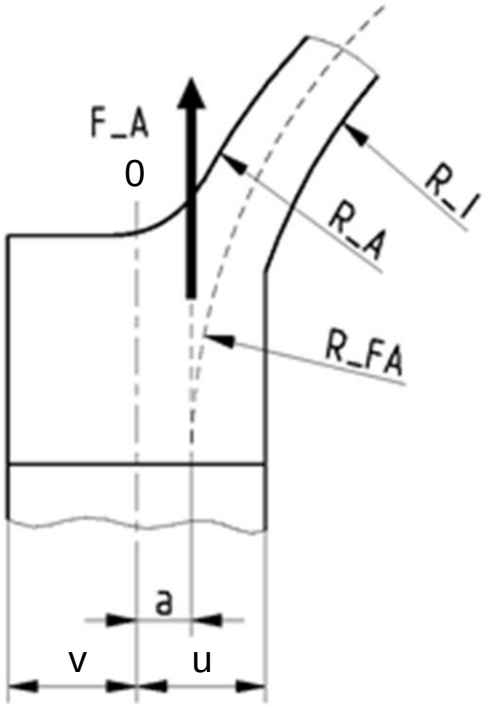


*Figure 2-9: Point of origin of the working load at a cylindric casing. Source: [6]*

**Relationships at an opening joint**

According to VDI 2230 page 1, one-sided opening means a reduction of the surface pressure inside the interface till zero. The focus in this thesis is the one-sided opening at the inner edge of the flange interface. In order to prevent a leak, there are specific requirements for the geometry and the clamp force (cf. [2]).

The minimum clamp force ($F_{Kerf}$) results from the requirements concerning the bolt connection. To ensure the joint leak tightness the minimum clamb force has to be greater or equal than the maximum of the shear force ($F_{KQ}$) or greater than the sum of clamb force against a medium plus clamp force before opening the interface ($F_{KP}+F_{Kab}$) (cf. eq. 4).

The clamp force, which is required for the leak tightness and prevention of the one-sided opening of the interface, is composed as follows:

(4) $$F_{Kerf} \geq max(F_{KQ};F_{KP}+F_{Kab})$$

1. Shear forces can be assumed to be negligible:

(5) $$F_{KQ}= 0$$

2. Minimum clamp force to ensure a sealing against a medium:

(6) $$F_{KP}= A_D \cdot p_{i,max}$$

with the sealing surface

(7) $$A_D=(u+v)\cdot b_T$$ (vgl. Abb.2-8)

3. Camp force before opening the interface:

(8) $$F_{Kab}=F_A \frac{a\cdot u\cdot A_D - s_{sym}\cdot u\cdot A_D}{I_{BT}+s_{sym}\cdot u\cdot A_D} + M_B \frac{u\cdot A_D}{I_{BT}+s_{sym}\cdot u\cdot A_D}$$

with the external operating moment

(9) $$M_B=0$$

with the moment of gyration of the interface area

(10) $$I_{BT}=\frac{b_T\cdot c_T^3}{12}$$

**Load-extension diagram**

Load-extenison diagrams are used to illustrate forces and extensions of the braced components. They serve as a basis for an analysis and computational dimensioning of a reliable bolt connection.

Figure 2-10 visualise the rigidity of a bolt material ($C_S$) (bolt + expansion sleeve) and the rigidity of a flange material ($C_F$) in the linear-elastic section in a diagram. Whether an element refers to the characteristic curve of the bolt or the flange depends on the behavior while it is loaded. For example the expansion sleeve refers to the characteristic curve of the bolt because it absorbs compressive loads during the preloads as well as during work loads. [2]

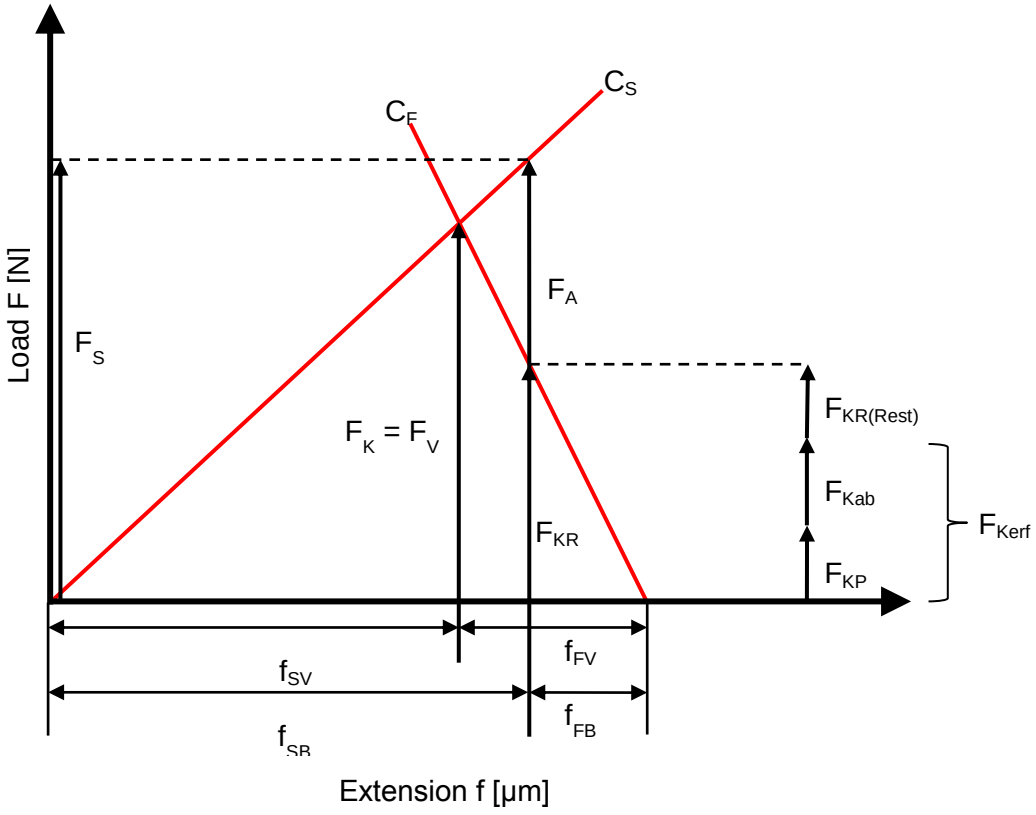


*Figure 2-10: Load-extension diagram for a bolt-flange conncetion.*

From tightening the bolt results a length variation ($f_{SV}$) of the bolt and expansion sleeve whereby the bolt gets extended and the expansion sleeve gets swaged. The flanges get swaged by the length of ($f_{FV}$). A preload/ mounting force ($F_V$) is effecting on the bolt connection. Additionally a constant static working load ($F_A$) is straining the bolt connection with tensile load. The bolt and expansion sleeve will expand ($f_{SB}$) whereas

the flanges will release ($f_{FB}$). The bolt force rises up to $F_S = F_A + F_{KR}$ whereas the original clamb force ($F_K$) is reduced to the residual clamp load ($F_{KR}$).

The required minimum clamp force ($F_{Kerf}$) consists of a clamb force to ensure a sealing against the inside pressure ($F_{KP}$) and a clamp force to ensure a non-opening of the interface. If the required clamp force ($F_{Kerf}$) is less than the the residual clamp force ($F_{KR}$) there will be an extra guarantee ($F_{KR(Rest)}$) for the sealing of the interface. If the required guarantee is exceeded it is possible to choose a smaller bolt size. However a closer analysis about a new bolt construction is not part of this thesis.

## 2.4 Load Cases

A turbine and thus the casing together with the bolt connection are exposed to different load cases. This thesis will analyse static-mechanical as well as static-thermal load cases. For the following analyses a representative and stationary load case was choosen. The stresses, which are caused by the loads will be evaluated by normal stress ($\sigma_{XX}$, $\sigma_{YY}$, $\sigma_{ZZ}$), shear stress ($\tau_{XY}$, $\tau_{XZ}$, $\tau_{YZ}$) and von Mises stress ($\sigma_V$). The so-called water pressure test deemed to be an extreme load case as well as the start-up and shutdown of the turbine.

### 2.4.1 Static-Mechanical

This static-mechanical load case contains a pure pressure load ($p_i$) from the inside of the turbine casing. During the assembly the seal tightness of the casing is proofed by this pressure test. Upper and under shell are bolted without a rotor and blades. The single chambers are separated and sealed by inserted plates.

Each chamber is filled up with water and is stationary loaded with 1.5 times of the maximum working pressure. The temperature during the pressure test equals room temperature and does not have any significant relevance in this contemplation. The wheel chamber of a steam turbine type MARC 4 has got a maximal internal pressure of 70 bar. After the delivery and installation the turbine runs in a turbine specific design point (e.g. 70 bar / 470 °C) where a static load is assumed.

### 2.4.2 Static-Thermal

The static-thermal load of the wheel chamber is induced by termal transfere of the incoming steam, which is up to 480 °C hot. Result of unevenly distributed temperature inside the casing wall is hightened stress inside the casing. Figure 2-11 shows a cylindrical casing with an exemplary temperature distribution T(r) caused by thermal conduction. [7, 8]

The start-up of a cold turbine is an extreme thermal load. To avoid inadmissible differences in temperature between the 'hot' inner surface of the casing and the 'cold' outer surface of the flange, the turbine will be heated up by a small amout of steam.

In this process maximal temperature differences (inner to outer surface) of 100 to 120 K are permissible. In a static mode of operation there will be a temperature difference about 40 K. [8]

### 2.4.3 Static-Mechanical and Static-Thermal

This chapter presents a combination of mechanical and thermal load which is representing the reality. The following figure 2-11 from [7] shows a cylindrical casing with an internal radius $r_i$, an external radius $r_a$ and a temperature distribution T(r). An internal pressure $p_i$ and an external pressure $p_a$ act on the casing. The external pressure is excluded in this contemplation. Normal stress and shear stress in this combinated load are the result from adding the single stresses of the invidual load cases. [7]

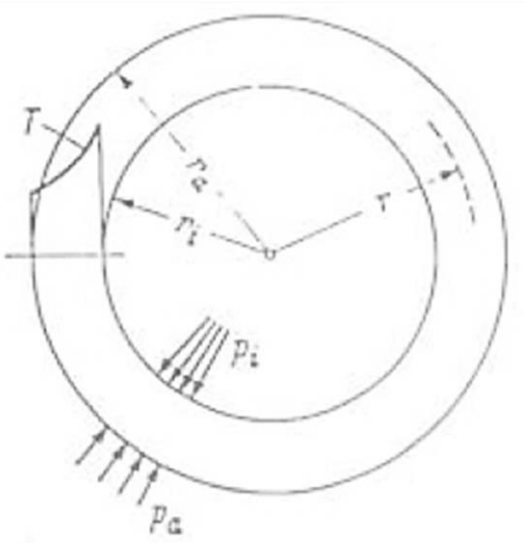


*Figure 2-11: Exemplary temperature and pressure load on a cylindrical casing. Source: [7]*

For the evaluation of stress, pressure as a static-mechanical load is more critical than the temperature. If components will fail because of too high internal pressure, this pressure would be present until the components are broken. Moreover, the stress would increase proportionally to the weakening component. In addition, too high temperature differences can increase the stress but would reduce themselves by the slow deformation (creep) of the components. Because of this correalation, the stress caused by static-mechanical loads compared to the stress caused by static-thermal loads has to be rated with a greater factor of safety.

## 2.5 Evaluation Criteria for the Assessment of Joint Leak Tightness

This chapter will present the selected evaluation criteria which are used to assess the bolt connection and the resulting joint leak tightness. Furthermore boundary conditions for the analysis are determined.

### 2.5.1 Point of Origin of the Working Load across the Flange

The quoted equation (8) in chapter 2.3 indicates the clamp load at the opening limit ($F_{Kab}$) at the inner edge of the joint surface. The analyses in this thesis assume that the turbine casing is loaded by a constant working load ($F_A$ = konstant) and no external moment ($M_B$ = 0). As a result the equation (8) for $F_{Kab}$ is simplified to:

(11) $$F_{Kab}=F_A \cdot (a - S_{sym}) \cdot \frac{u \cdot A_D}{I_{BT}+S_{sym} \cdot u \cdot A_D}$$

An assumption to use the point of origin (described by a) of the working load ($F_A$) as an evaluation criteria for the joint leak tightness is that the position of the flange and the bolt axis as well as their dimensions stay the same ([$A_D$, $I_{BT}$, u, $S_{sym}$] = constant) during this analysis.

Deduced from this condition:

(12) $$x=\frac{u \cdot A_D}{I_{BT}+S_{sym} \cdot u \cdot A_D} = \text{constant}$$

Equation (11) is simplified to:

(13) $$F_{Kab} = F_A \cdot (a - S_{sym}) \cdot x$$

This simplification conveys that the point of origin (described by a) of the working load ($F_A$) is the only variable in this equation which can effect on a gaping joint. The smaller the point of origin (a) the less the load ($F_K$) will be needed to prevent a gaping on the inner edge of the flange.

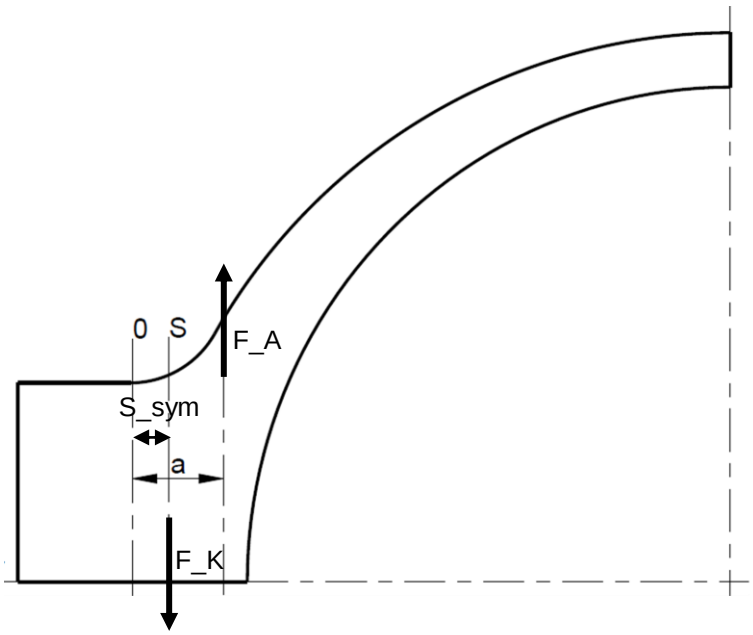


*Figure 2-12: Considered parameters concerning the flange.*

Figure 2-11 makes clear that the force transmission of F_A will be along the bolt axis if the distance between symmetry axis (0) and the bolt axis (S) and the distance between the symmetry axis (0) and the point of origin of F_A are the same (S_sym = a). Therefore the result of equation (13) is a required clamp force of $F_{Kab}$ = 0 N. In summary it can be said that an optimal lever arm (a) and a little bolt force prevents a gaping joint.

### 2.5.2 Membrane Stress and Bending Stress

In general there are unevenly distributed stresses in braced components. For an assessment and an interpretation of these stresses a highly loaded cross-section of the model is considered. The stresses are splited by so-called stress-linearisation into theoretical stress shares (membrane stress, bending stress and peak-stress). Technical standards such as DIN, AD-instructions, TRD or ASM-Code determine material specific limits as a function of stress causes (e.g. pressure and temperature) of each stress share. In this thesis the limit values for stresses are determined by a reference model. [8]

Figure 2-12 pictures the membrane stress, the bending stress as well as the overlapping stress on a bending beam. Furthermore the vertical, normal and resultant forces are shown.

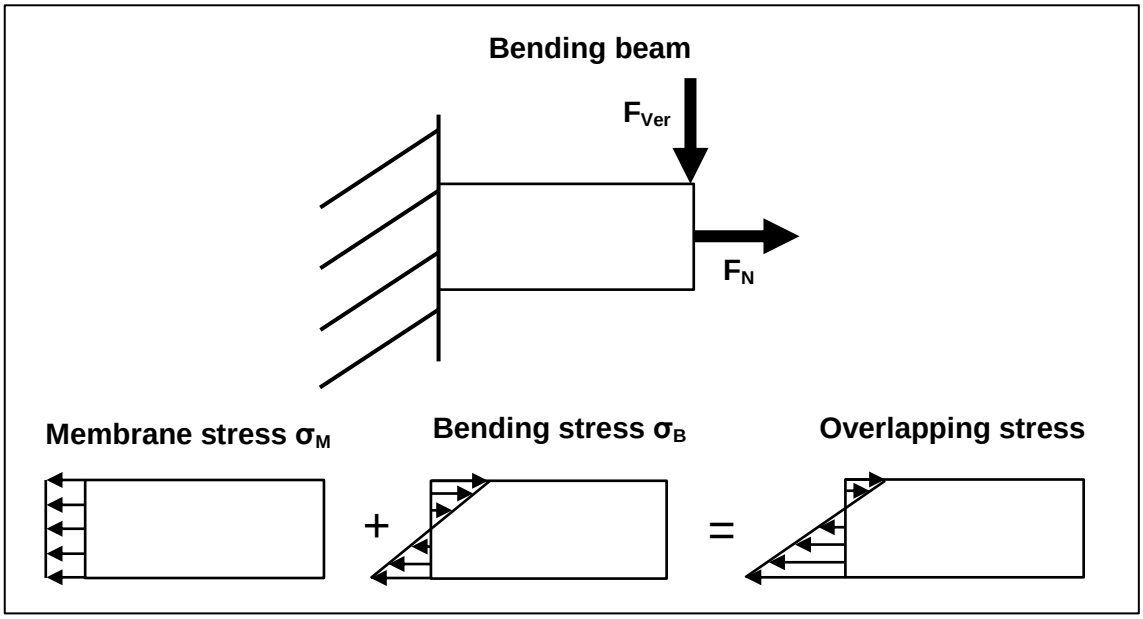


*Figure 2-13: Loads and stress shares at a bending beam.*

**Membrane stress**

The membrane stress is the averaged, constant stress share through the cross-section, which is caused by $F_N$.

**Bending stress**

The bending stress is the overlapping, linear stress share, which is caused by $F_{Ver}$. Bending stress occurs if a component is loaded by a bending moment.

**Peak stress**

The peak stress is the share which exists over the linear and constant share. Most often peak stress is caused by notches, edges or inhomogeneities. This stress will not be discussed in more detail.

### 2.5.3 Joint Surface Pressure

Figure 2-12 exemplary shows a linear distribution of a joint surface pressure at a cylindrical casing. The lowest surface pressure occurs on the inner edge of the flange.

Consequently this is the point which has to be analysed. To prevent a gaping the residual clamp load ($F_{KR}$) can not fall below the clamp load at the opening limit ($F_{Kab}$).

(14) $$F_{KR} \cdot A_D > F_{Kab} \cdot A_D = \bar{q}_{min}$$

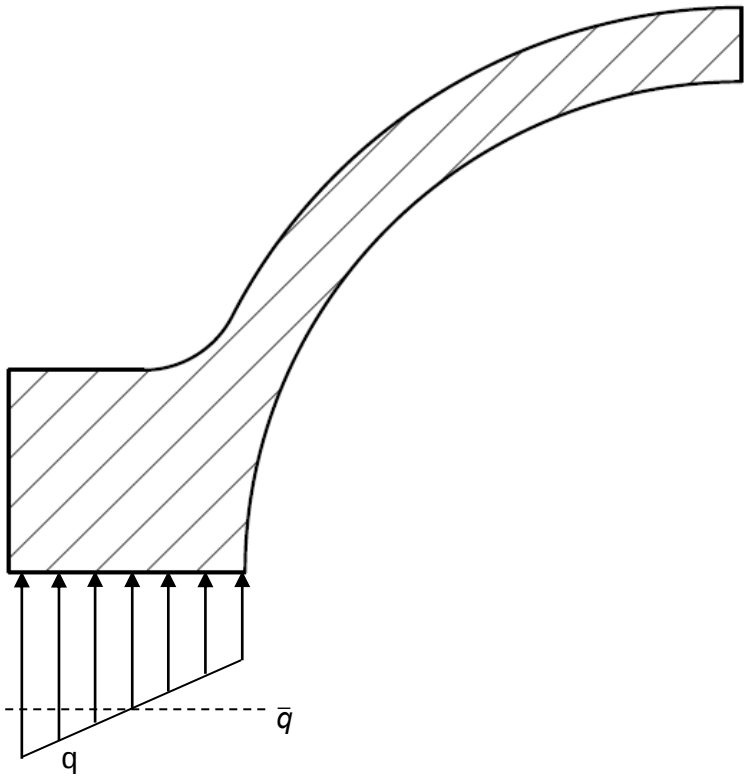


*Figure 2-14: Distribution of joint surface pressure at a cylindrical casing. Source: [9]*

For example start-ups and shut-downs result in large differences in pressure and temperature. These changes have an effect of the joit surface pressure. To ensure leak tightness all over the joint surface by taking these changes into account, it is the goal to have a constant surface pressure all over the joint.

It is valid until a material specific limit (yield point): The higher the surface pressure the better the leak tightness of the joint.

# 3 FEM Model Construction

The finite element method (FEM) is a method where complex geometries with unknown structural-mechanical behavior are sectioned into a finite number of simple geometric elements with known structural-mechanical behaviour. [1]

The following will show the construction and setup of the calculation models. Furthermore the stepwise approach of calculating the models will be described which is based on VDI 2230 page 2.

Symmetrically loads, boundary conditions and geometries are used to considerably simplify the model. Instead of the whole model it is sufficient to analyse only a quarter. Due to this, the model becomes clearer and the calculation effort will be reduced.

## 3.1 FEM Model Classes According to VDI

On the basis of FEM model classes, CAD-based 3-D models are created, boundary conditions set and the FE analyses performed.

The VDI 2230 page 2 differentiates between four FE model classes. A clear assignment to only one model class is usually not feasible in practice. FE-models can contain characteristics from several model classes. Also in this thesis one of the models has characteristics from model class I and II but is continuously titeled as model class II. With each model class the level of details, the accuracy and the calculation effort will increase. A too detailed analysis at this point would be unrewarding. Due to that this thesis will only deal with model class I and (II+III). Model class IV will be mentioned in the following for the sake of completeness.

**Model class I**

Neither the real bolt nor the joint is considered in this model class. The braced components are modeled as one piece. This model considers through the defined material properties and the omission of the bore, the compliableness of the components and the bolt. The goal of this consideration is to identify the stress results at the imaginary joint to use them for the bolt calculation based on VDI 2230 page 1. [3]

**Model class II**

In this model class the bolt is modeled as a line element (tension member, balk or spring element). The contact of the joint surfaces can be taken into account. The aim of this consideration is to determine the stress results inside the bolt. [3]

**Model class III**

The bolt is illustrated as a surrogate volumetric solid without thread. By adapting the bolt geometry and adjusting the material properties the real bolt properties are simulated. Beside the contact of the joint surfaces,it is possible to consider the contact of the surface between bolt and nut by defining adequate boundery conditions. [3]

**Model class IV**

This model class contains a detailed bolt. The threads as well as all contatct conditions are modeled. On the one hand, this class has the highest accuracy and the largest outcome, whereas on the other hand it takes the biggest effort for the FE-calculation. The goal of this consideration is to determine stress resultants and local stress preaks inside the bolt. [3]

**Overlapping model class characteristics**

Joint gaping is caused by a superposition of the bolt preload and the external load. In model class II-IV it is possible to allow this gaping by defining appropriate contact conditions. [3]

## 3.2 Model Class I

This chapter describes the principal procedure for modeling a FE model, based on model class I by using the program Creo Simulate.

### 3.2.1 General Construction Class I

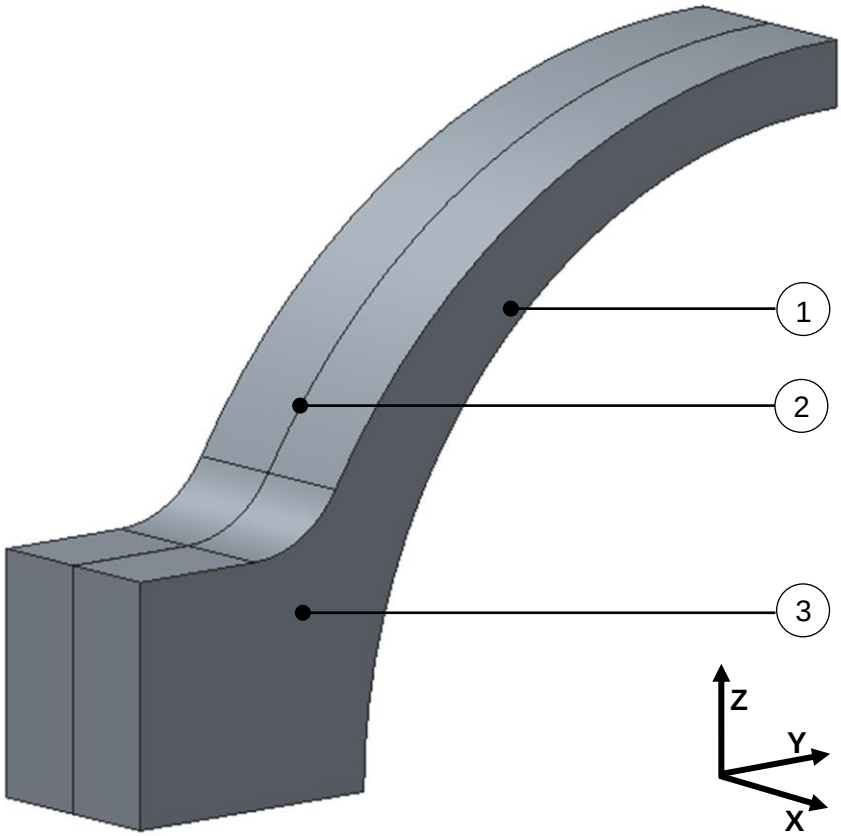


*Figure 3-1: Basic model according to model class I.*

The following presents the basic model accoring to model class I. The dimensions are taken from an actual turbine of MDT-HBG. To simply the basic model, the superelevation $k_{RI}$ from the original is excluded.

This model consists of a casing shell (1) and a flange (3), which is built-up by an eccentrical external arch and a centrical internal arch. Because of the eccentricity of the external arch the shell is becoming thicker in the direction to the flange. The transition between external arch and upper surface of the flange is blunted with a specific radius. The model is assembled by two similar components at a vertical interface (2).

Following this, boundary conditions are presented which apply for all models in model class I. Model 400 is consistently used as an example.

**Geometry**

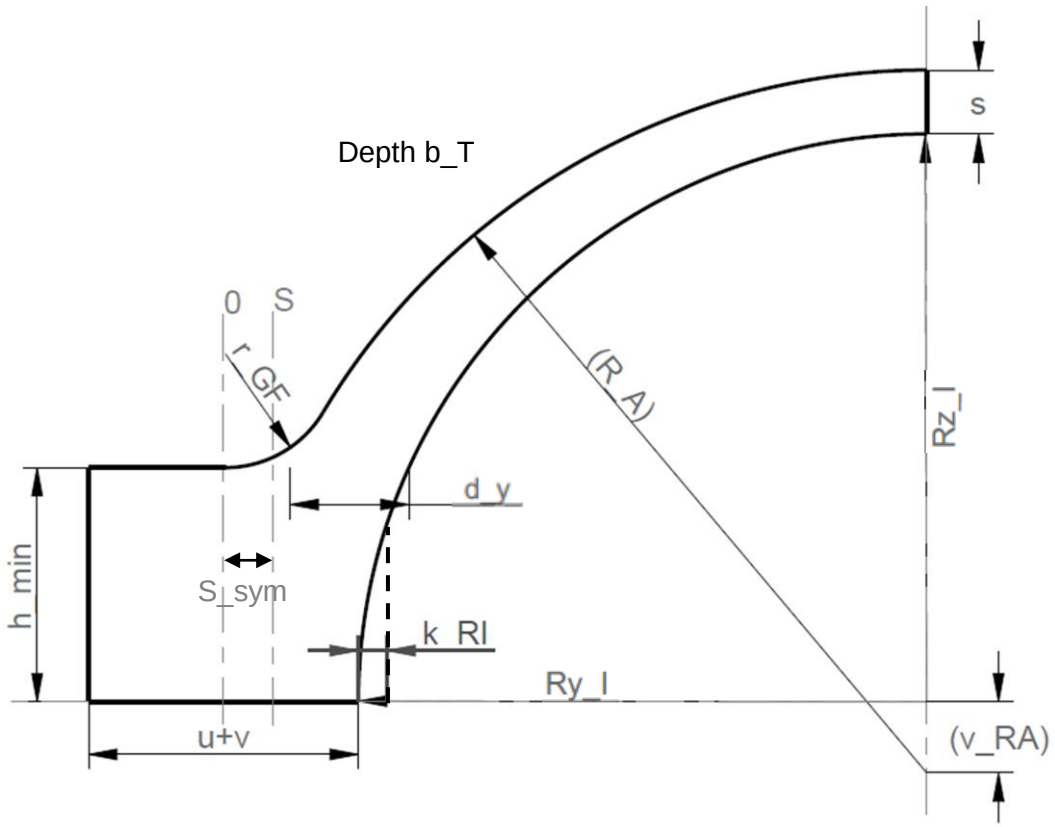


*Figure 3-2: Parameterised FEM-model concerning model class I.*

*Table 3-1: Fixed parameters for all FEM-models in model class I*

| Parameters | Symbol | Unit | Fixed values |
|---|---|---|---|
| Distance between bolt axis and symmetry axis | $S_{sym}$ | mm | 35 |
| Flange width | u+v | mm | 190 |
| Flange hight | $h_{min}$ | mm | 165 |
| Innternal radius in Y direction | $Ry_I$ | mm | 400 |
| Thinnest wall thickness | s | mm | 45 |
| Wall thickness at transition | $d_y$ | mm | 83.79 |
| Radius of the rounding | $r_{GF}$ | mm | 80 |
| Depth in X direction | b_T | mm | 135 |
| Superelevation of the flange | $k_{RI}$ | mm | 0 |

$Rz_I$ is changing during the analysis, $R_A$ and $v_{RA}$ are reference values. Their values are shown in table 3-2 and 3-3.

**Meshing**

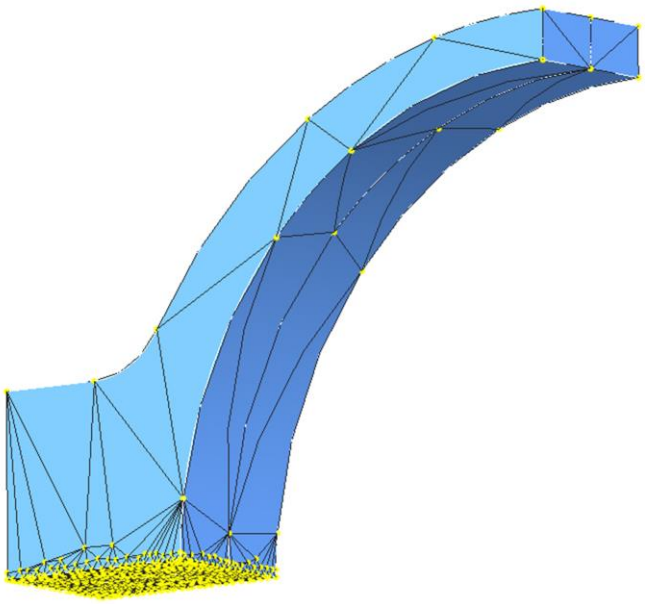

*Figure 3-3: Meshed model of model class I.*

The whole model is automatically meshed by using the function “AutoGEM” of the program Simulate. To get a more exact result at the joint surface the mesh is refined at this part to 10 mm.

**Material assignment**

Material properties of the cast steel material G17CrMoV5-10 is assigned to the whole model. The temperature-dependent material properties density, elastic modulus, Poisson´s ratio, specific heat capacity and heat conductivity are tabled in the program. These values are obtained from the material database of MDT.

**Loads**

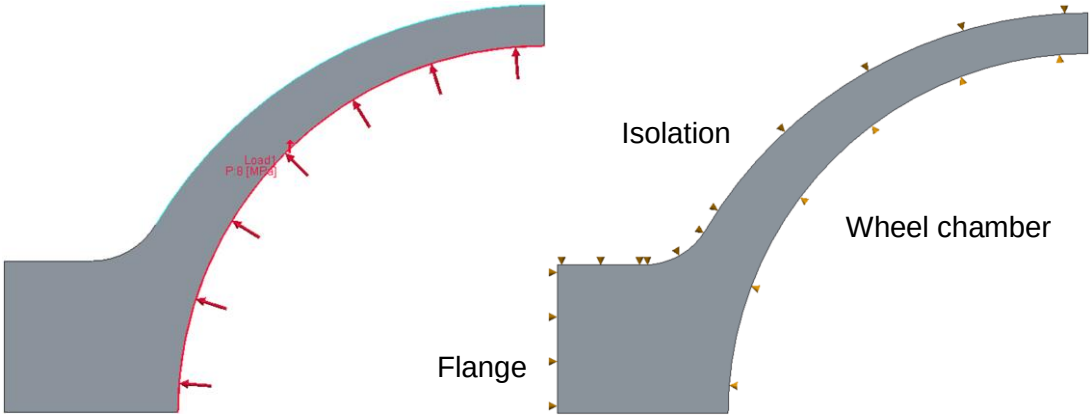


*Figure 3-4: Models with pressure load (left) and temperature load (right).*

| | | |
|---|---|---|
| Pressure load: | $p_i$ = 8.0 MPa | |
| Temperature load: | | |
| Isolation | h = 1.5 W/(m² K) | T = 20 °C |
| Flange | h = 10 W/(m² K) | T = 20 °C |
| Wheel chamber | h = 1000 W/(m² K) | T = 480 °C |

The static-mechanical load is imprinted on this model by a pressure load of $p_i$ = 8.0 MPa. The atmospheric pressure is excluded in this contemplation.

The temperature loads are set by using boundary conditions of convection on several surfaces. The isolation on the whole external casing surface is set to a temperature of T = 20 °C and a heat transfer coefficient of h = 1.5 W/(m²K). The temperature load on the internal surface of the wheel chamber is set to T = 480 °C and h = 1000 W/(m²K). Furthermore a temperature load of T = 20 °C und h = 15 W/(m²K)) is set on the external surface of the flange to generate a temperature difference of approx. 40 K between internal and external surface of the casing. [8]

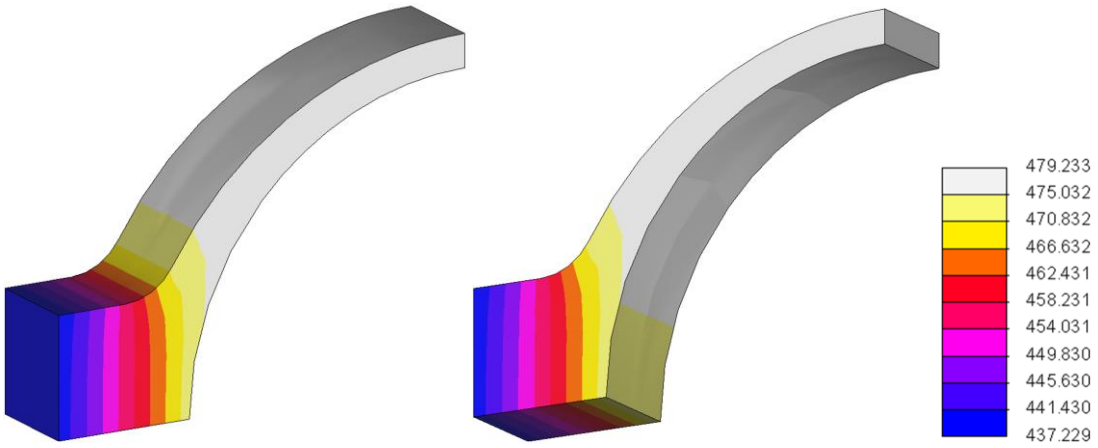


*Figure 3-5: Exemplary temperature distribution for model class I [°C].*

**Clamping**

The model is assembled through two similar components at a vertical interface to realize the clamping for the thermal-mechanical calculation and for an exact positioning of the measured variables.

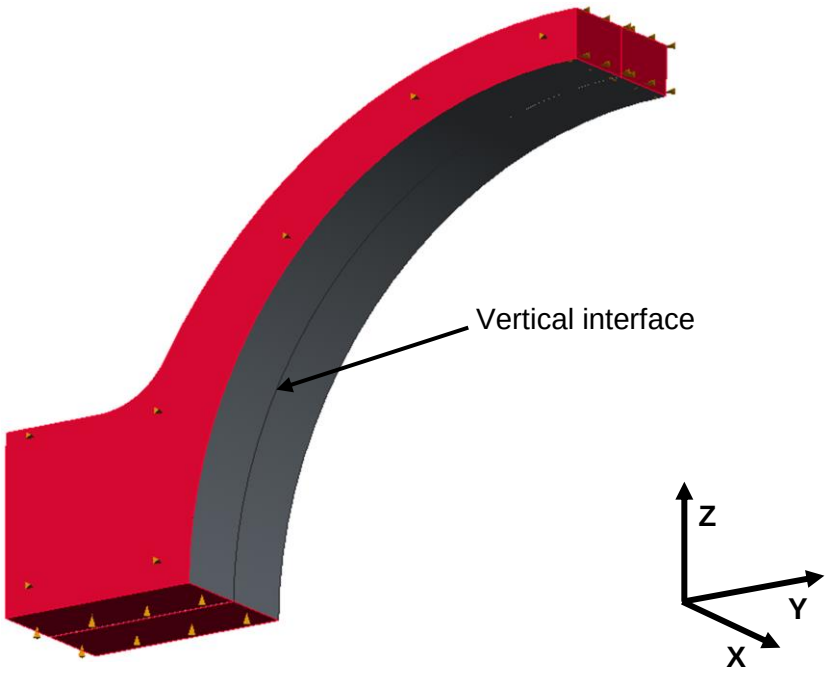


*Figure 3-6: Clamping of the model in model class I.*

The areas emphasised in red in figure 3-6 show the clamping for the static-mechanical load case. The arrows show in which direction the area is clamped. This model is clamped in X, Y and Z direction.

**Measured variables**

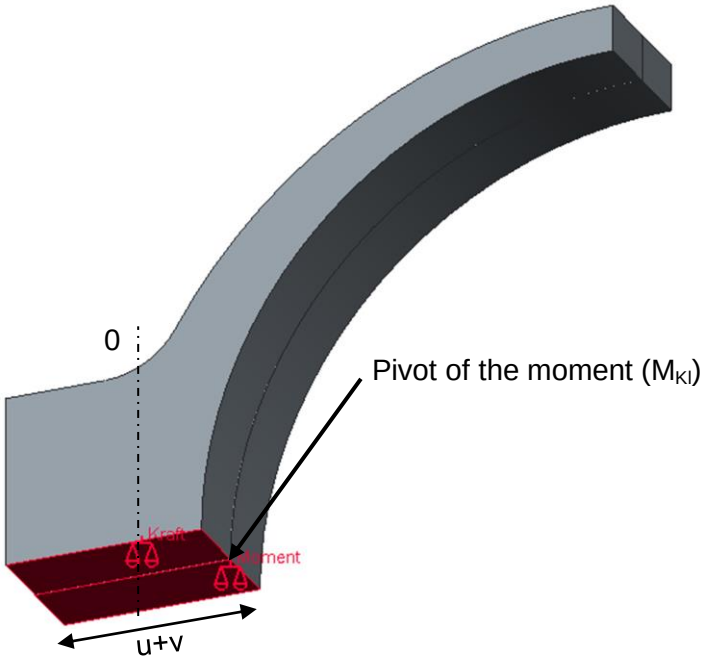


*Figure 3-7: Measured points on the FEM-model for model class I.*

Before the calculation starts the measurement values are defined as shown in figure 3-7 and afterwards selected from the FEM-calculation-protocol. The working load is definied location-independent through the area emphasised in red whereas the pivot of the moment is defined location-dependent in the middle of the inner edge of the flange (cf. figure 3-7). This point was picked for that measurement because it was easy to define. The result of the moment has to be recalculated to be in accordance with the VDI 2230 page 2, which is using the symmetry axis of the flange (0) as the pivot of the moment. Generally the lever arm (distance between working load axis and symmetry axis) can be calculated by force and moment (M = F a). To compare the lever arm (a) in this model with the one defined in VDI 2230 page 2 the quotient of the force and moment has to be deduced by the half flange width (cf. eq. 15).

$$a = \frac{(u+v)}{2} - \frac{M_{Kl}}{F_A} \tag{15}$$

By the use of the presented flange geometries in table 3-1 the optimal lever arm (a) is at 35 mm.

### 3.2.2 Basic Model Class I

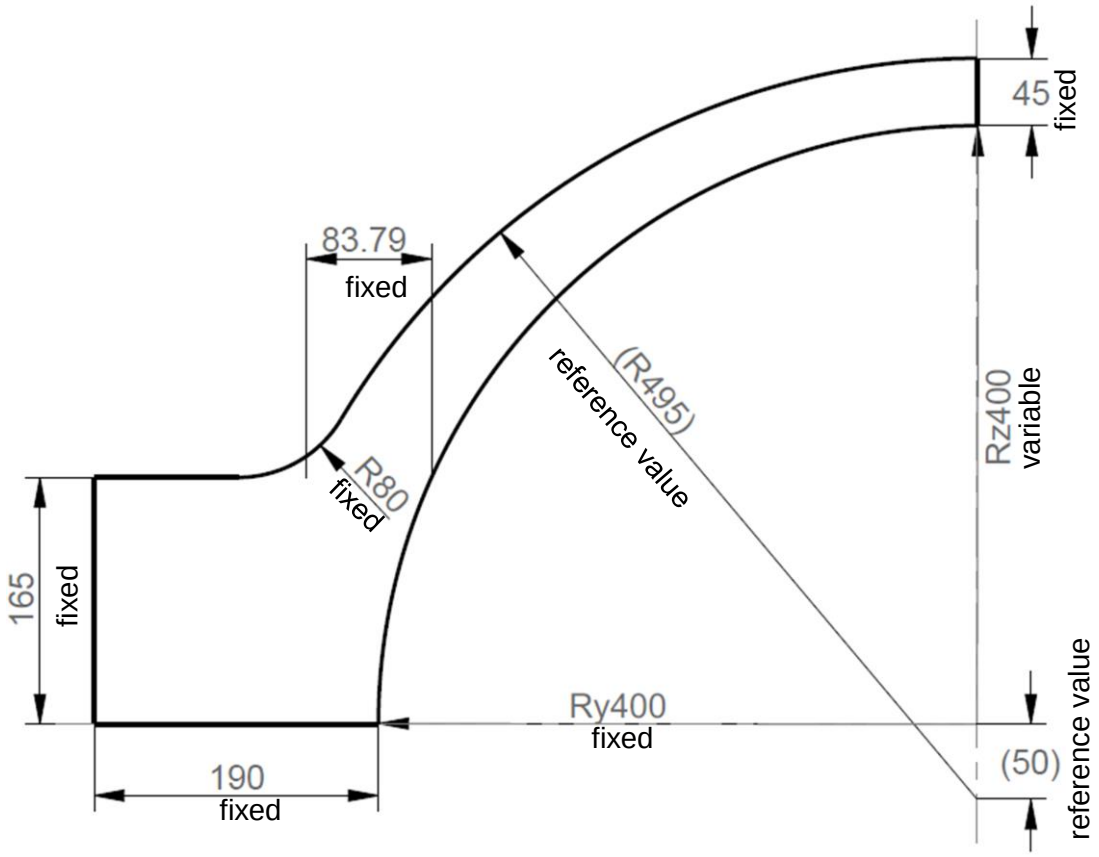


*Figure 3-8: Dimensioning of the basic model of model class I.*

Figure 3-8 shows the basic model of model class I with all necessary values for the following analyses. It is differenced between fixed, variable and reference values.

### 3.2.3 Variation of the Basic Model Class I

All the variations in this chapter are based on the basic model of model class I. The first step is to substitute the internal radus with an ellipse, which is defined by two radii ($Ry_I$ und $Rz_I$). To fix the flange in the same position the radius in the Y direction is constant ($Ry_I$ = 400 mm). Whereas the radius in the Z direction is scaled up from $Rz_I$ = 400 mm

in 10 mm steps to $Rz_I$ = 450. Each of these models are analysed in the same manner. Table 3-2 shows the varied geometries. As mentioned before the working load ($F_A$) and the moment ($M_{KI}$) are measured in the FEM-analyses and the lever arm (a) is calculated.

*Table 3-2: Variation of $Rz_I$ with appropriate reference values*

| Parameters | Symbols | Unit | Model 400 | Model 410 | Model 420 |
|---|---|---|---|---|---|
| Internal radius in Z direction | $Rz_I$ | mm | 400 | 410 | 420 |
| External radius | $R_A$ | mm | (495)* | (490.33) | (486.10) |
| Offset of the external radius | $v_{RA}$ | mm | (50)* | (35.33) | (20.10) |

| Parameters | Symbols | Unit | Model 430 | Model 440 | Model 450 |
|---|---|---|---|---|---|
| Internal radius in Z direction | $Rz_I$ | mm | 430 | 440 | 450 |
| External radius | $R_A$ | mm | (482.30) | (478.90) | (475.87) |
| Offset of the external radius | $v_{RA}$ | mm | (7.30) | (6.10) | (19.13) |

*() reference value, i.e this value is dependend on $Rz_I$

Based on these results a further model is designed. The following will present the geometry of this model (model 420_20).

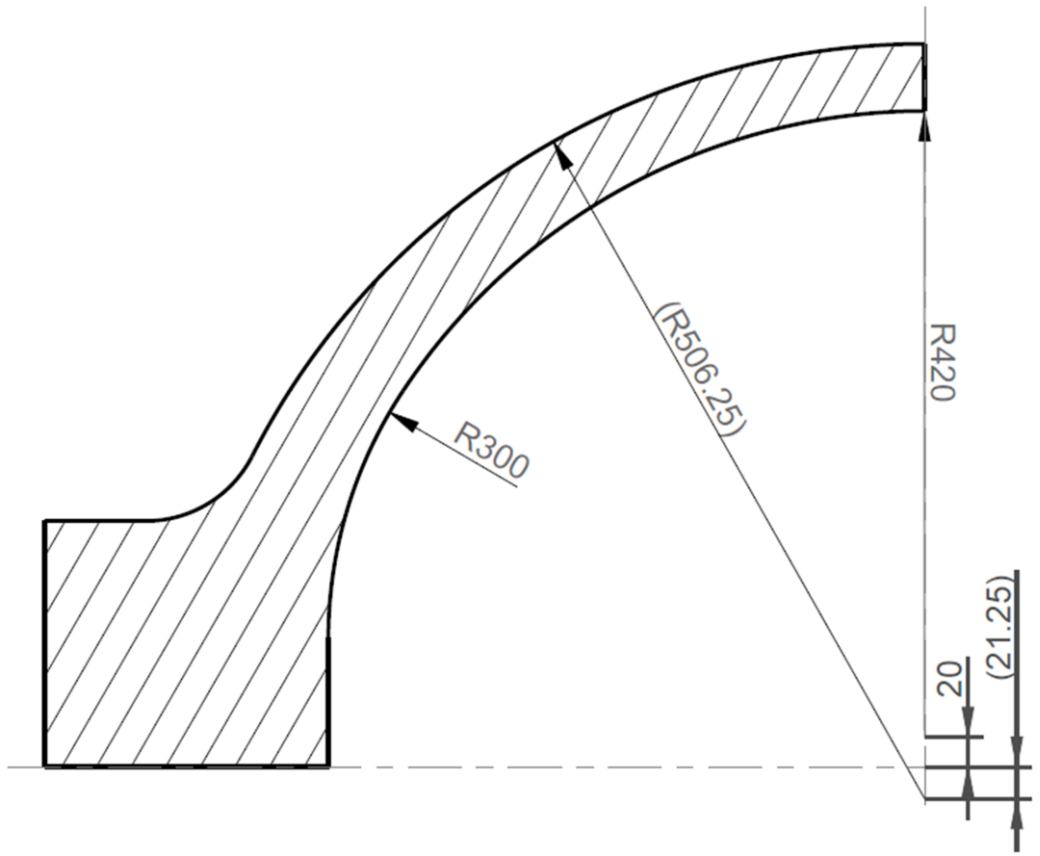


*Figure 3-9: Partial dimensioning of model 420_20 of model class I.*

Dimensions which are not mentioned here are the same as in the basic model (cf. figure 3-8).

*Table 3-3: Parameters of model 420_20 of model class I (cf. symbols with figure 3-2)*

| Parameters | Symbols | Unit | Model 420_20 |
|---|---|---|---|
| Internal radius in Z direction | $Rz_I$ | mm | 420 |
| External radius | $R_A$ | mm | (506,25) |
| Offset of the internal radius in Z direction | $v_{RI}$ | mm | 20 |
| Offset of the external radius in X direction | $v_{RA}$ | mm | (21,25) |
| Internal round radius | $ver_I$ | mm | 300 |

## 3.3 Model Class II

This chapter describes the principal procedure for modeling a FE-model based on model class II by using the program Creo-Simulate.

### 3.3.1 General Construction Class II

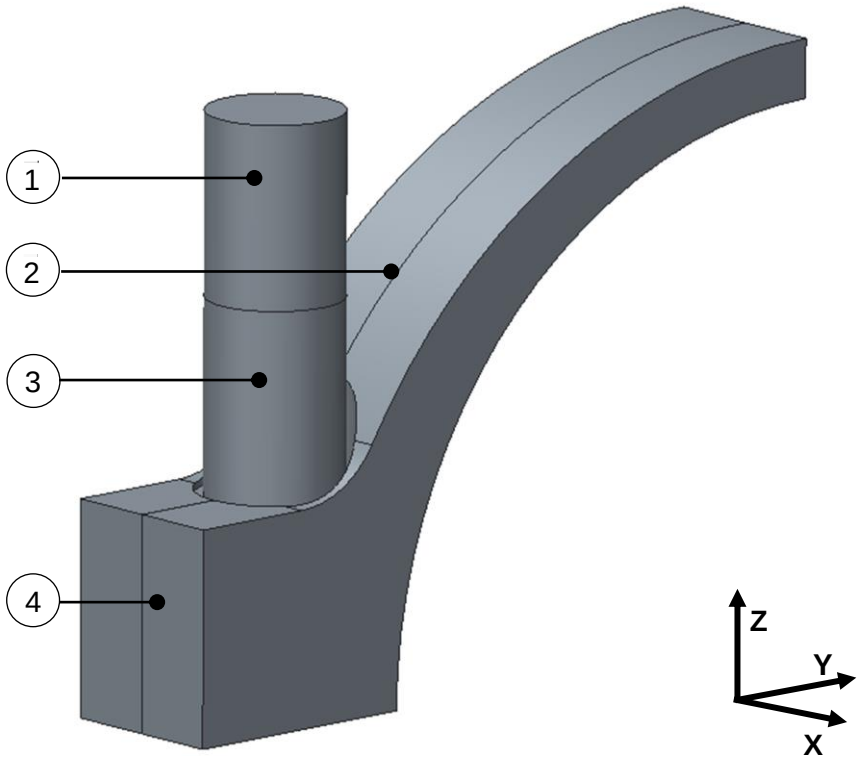


*Figure 3-10: Basic model according to model class II.*

Based on the basic model of model class I figure 3-10 shows the basic model according to model class II. In addition to the casing shell (4), a bore inside the flange, a bolt including a capped nut (1) and an expansion sleeve (3) are added. These components are designed as simple volumetric solids. The casing is assembled of two similar components at a vertical interface (2).

**Geometry**

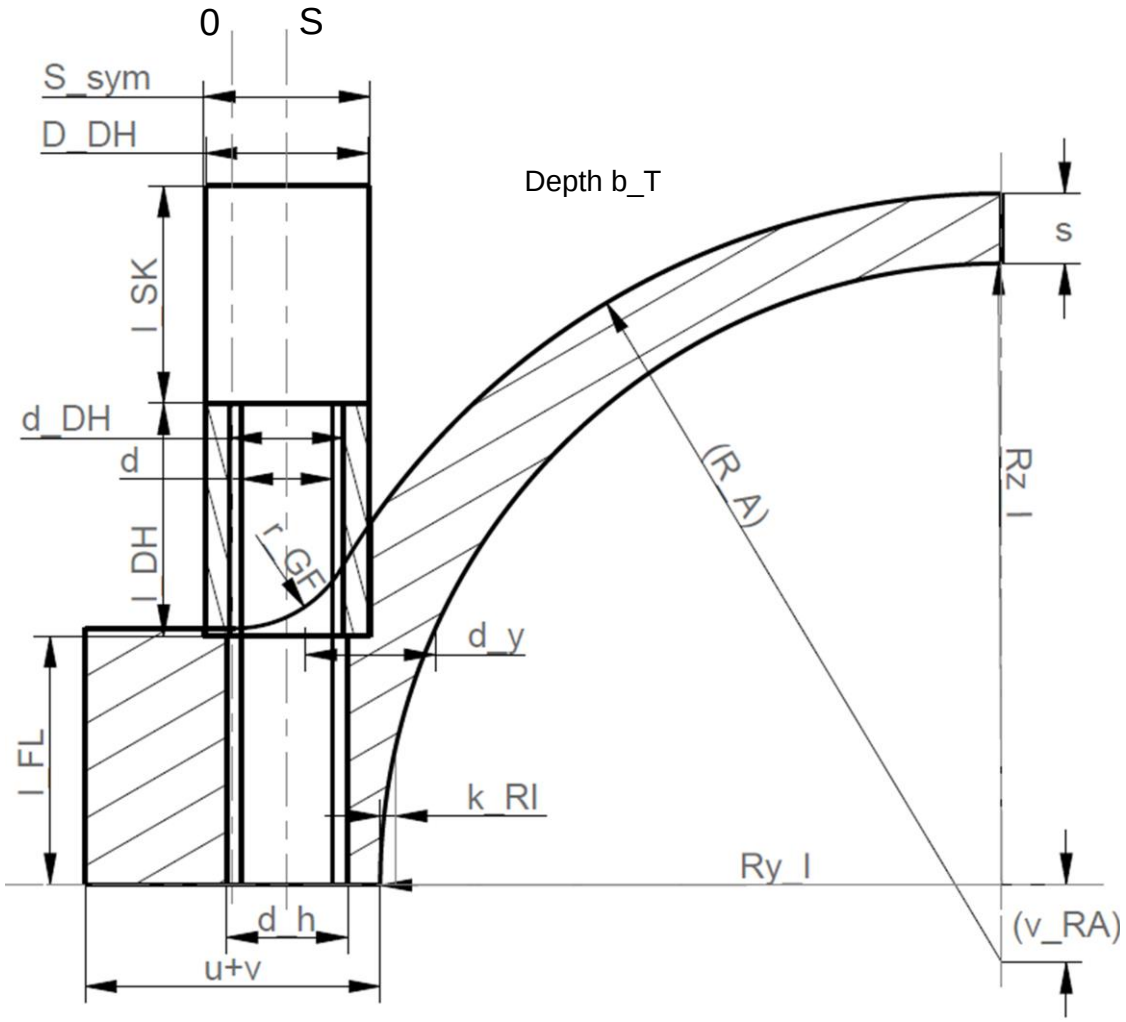


*Figure 3-11 Parameterised FEM-model concerning model class II.*

*Table 3-4: Fixed parameters of FEM-models 400-450 of model class II*

| Parameters | Symbols | Units | Fixed values |
|---|---|---|---|
| Distance between symmetry axis and bolt axis | $S_{sym}$ | mm | 35 |
| Flange width | u+v | mm | 190 |
| Internal radius in Y direction | $Ry_I$ | mm | 400 |
| Thinnest wall thickness | s | mm | 45 |
| Wall thickness at the transit | $d_y$ | mm | 83,79 |
| Radius of the rounding | $r_{GF}$ | mm | 80 |
| Depth in X direction | b_T | mm | 135 |

| | | | |
|---|---|---|---|
| Superelevation of the flange | $k_{RI}$ | mm | 0 |
| Bolt diameter | d | mm | 58,5 |
| Diameter of the reduction surface for position of the expansion sleeve | $d_{af}$ | mm | 107 |
| External diameter of the expansion sleeve | $D_{DH}$ | mm | 105 |
| Internal diameter of the expansion sleeve | $d_{DH}$ | mm | 73 |
| Bore diameter of the braced components | $d_h$ | mm | 78 |
| Length of the expansion sleeve | $l_{DH}$ | mm | 150 |
| Length of the braced part of the flange | $l_{FL}$ | mm | 160 |
| Length of the bolt head | $l_{SK}$ | mm | 140 |

The variable parameters $Rz_I$, ($R_A$) and ($v_{RA}$) behave equivalent to the variable parameters in model class I and can be found in table 3-2.

Figure 3-11 shows the parametrisation of the new models. The general geometry of the casing does not change. The new values are caused by bore, bolt and expansion sleeve. Table 3-4 shows the fixed values for model 400-450 of model class II.

**Meshing**

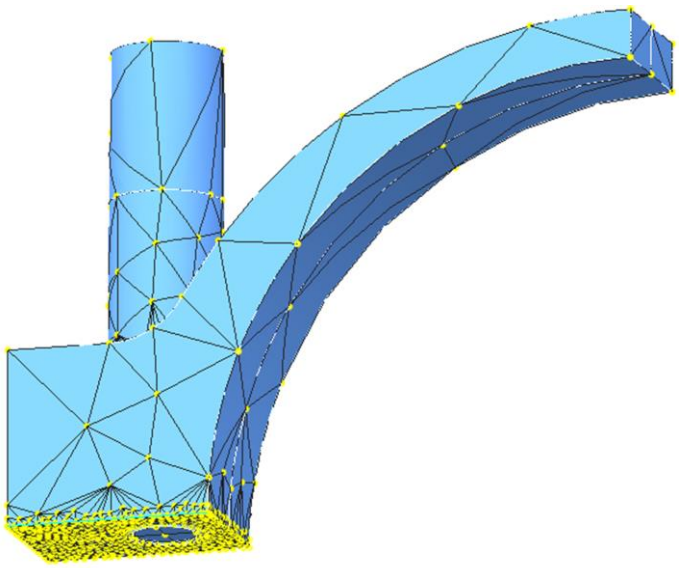

*Figure 3-12: Meshed model of model class II*

The whole model is automatically meshed – such as in model class I - by using the function “AutoGEM” of the program Simulate. To get a more exact result the joint surface mesh is refined to 10 mm and the mesh at the surface between expansion sleeve and upper flange surface is refined to 5 mm (cannot be seen in figure 3-12).

**Material assignments**

The material of each component of the analysed models is listed in table 3-5. The values are obtained from the material database of MDT.

*Table 3-5: Overview of used materials*

| Component | Material | Used values |
|---|---|---|
| Casing | G17CrMoV5-10 | Density<br>Elastic modulus<br>Poisson´s ratio<br>Specific heat capacity<br>Heat conductivity |
| Bolt<br>Expansion sleeve | 21CrMoV5-7 | |

**Loads**

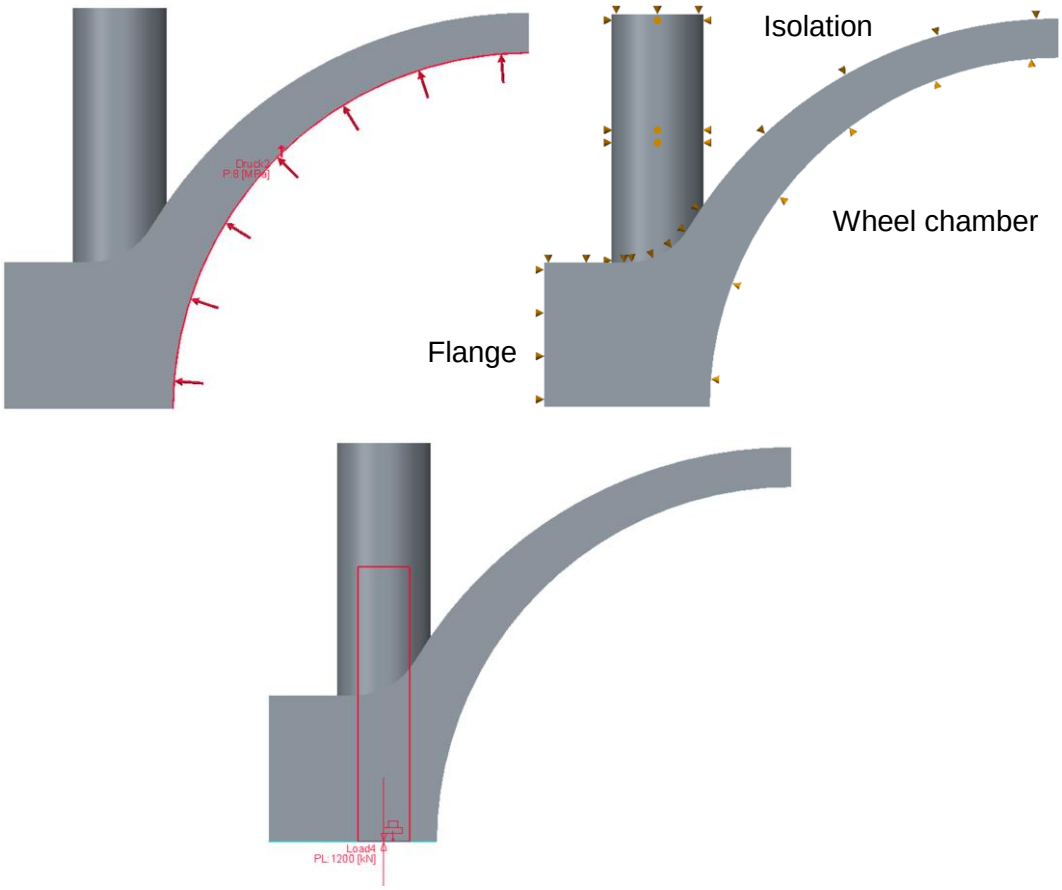


*Figure 3-13: Models with pressure load (left), temperature load (right) and bolt preload force (middle).*

In addition to the pressure load and temperature load in model class I, model class II includes also the bolt preload force. The isolation takes into account the added surface caused by the bolt head and expansion sleeve.

The preload is defined by a program function at the bolt shaft. Based on the know-how of MDT-HBG the preload for a M72 bolt with a temperature of approx. 400 °C should be about 800 kN. A control measurement of the reaction force at the clamped bolt shaft resulted in an approx. 30 % lower preload. To realize the aspired preload of 800 kN the initialised value was raised up to 1200 kN.

Pressure load: $p_i$ = 8.0 MPa

Temperature load:

| | | |
|---|---|---|
| Isolation: | h = 1.5 W/(m² K) | T = 20 °C |
| Flange: | h = 10 W(/m² K) | T = 20 °C |
| Wheel chamber: | h = 1000 W/(m² K) | T = 480 °C |
| Bolt preload force: | $F_S$ = 1200 kN (800 kN) | |

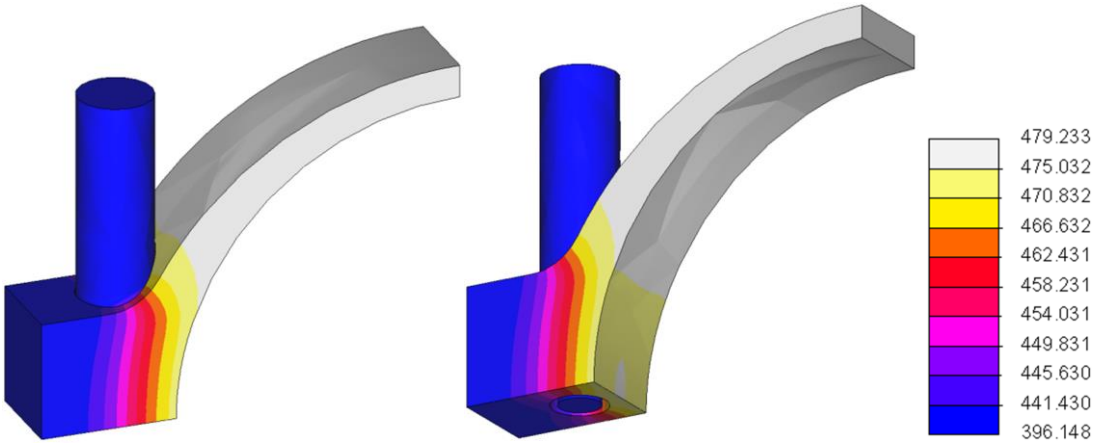


*Figure 3-14: Exemplary temperature distribution for model class II [°C].*

Figure 3-14 shows the exemplary temperature distribution for model class II. Caused by the bore and the bolt, there are some differences in the temperature distribution betweeen model class I and model class II. However, the important fact is that there is also in model class II a temperature difference between internal and external surface about 40 K.

**Clamping**

There are seperated calculations for the pressure load, temerpature load and the bolt preload force.

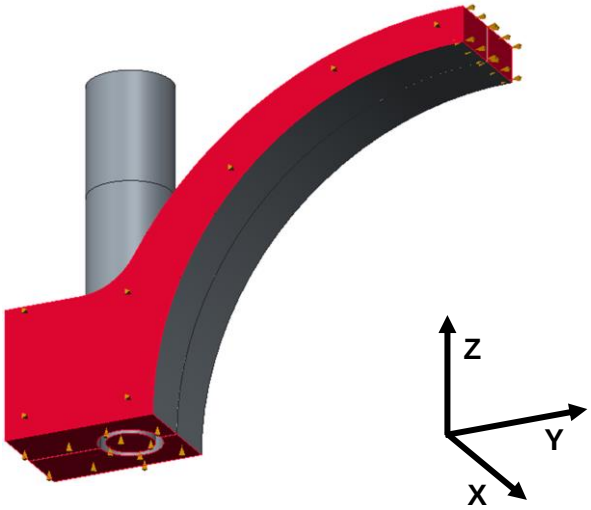


*Figure 3-15: Clamping for pressure load and bolt preload force.*

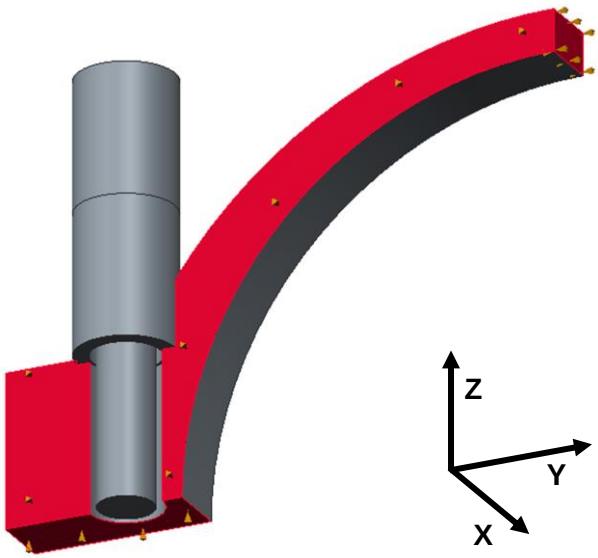


*Figure 3-16: Clamping for temperate load.*

The areas emphasised in red in figure 3-15 and 3-16 show the clampings for different load cases. The arrows show in which direction the area is clamped. The model is clamped differently for each case in X, Y and Z direction.

**Measured variables**

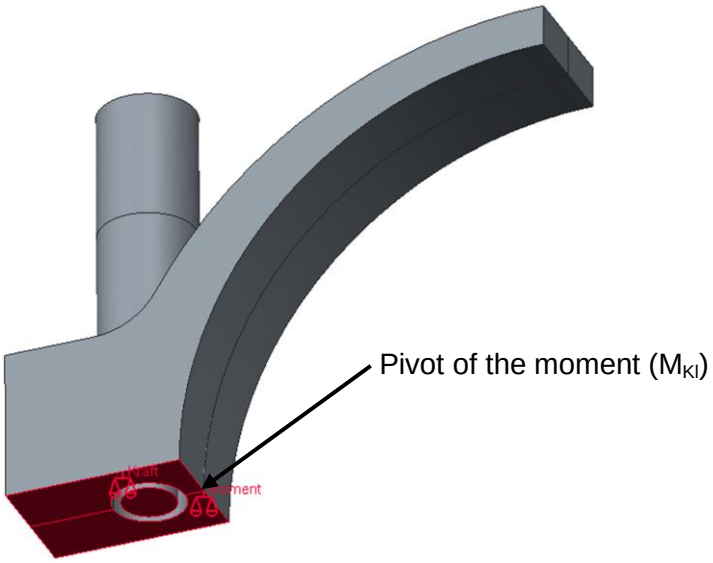


*Figure 3-17: Measured points on the FEM-model for model class II.*

The measured values are force and moment. The area to determine the working load consists of the joint surface and the bolt cross-section. The lever arm (a) is calculated by equation (8) as applied in model class I.

### 3.3.2 Basic Model Class II

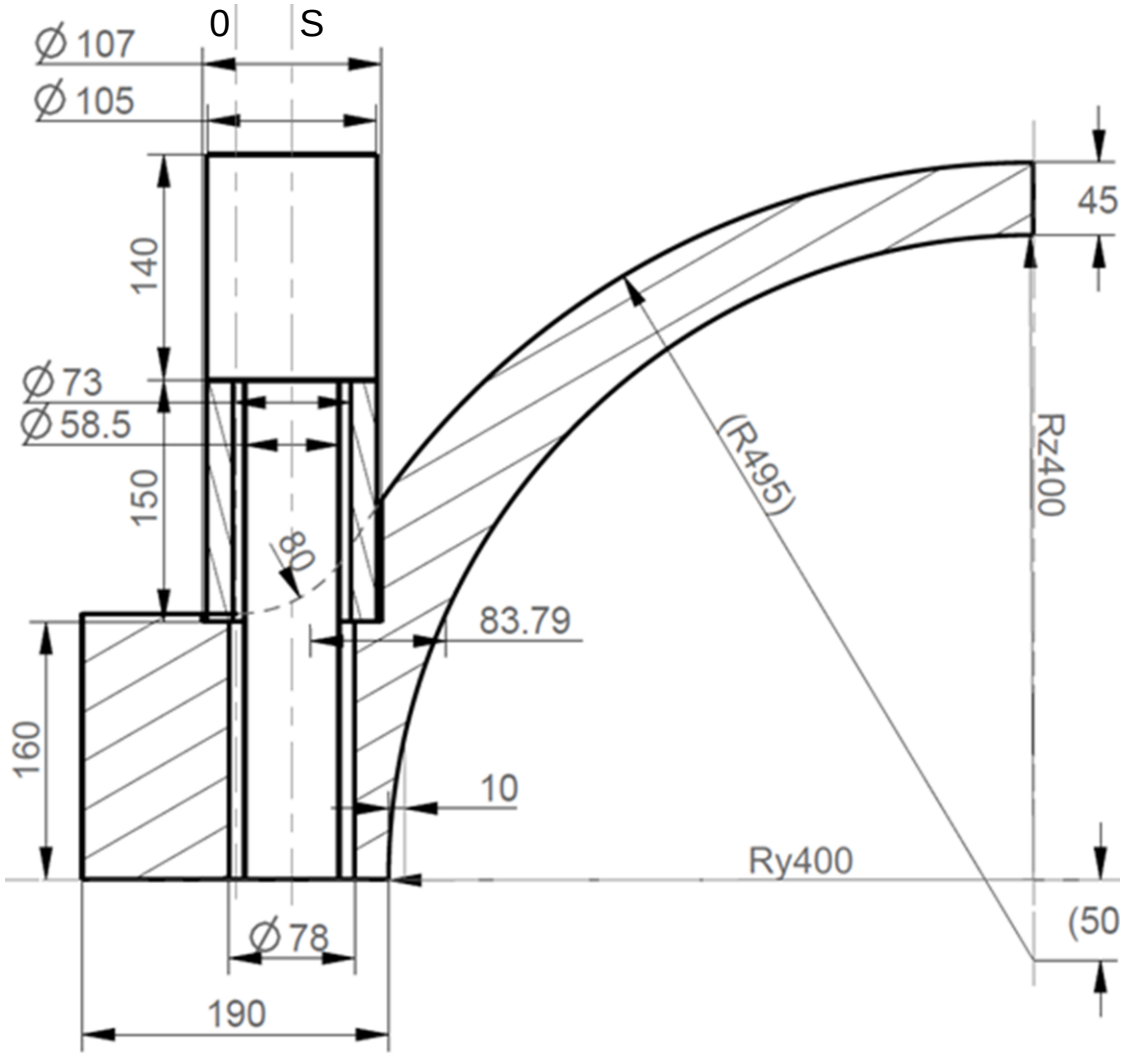


*Figure 3-18: Dimensioning of the basic model of model class II.*

Figure 3-18 shows exemplary the dimensioning of the basic model of model class II with all necessary values for the following analyses. Compared with model class I, only the dimensions for the bolt connection are added.

### 3.3.3 Variation of the Basic Model Class II

Compared with the variations of the basic model class I, either the general dimensions of the casing or the approach of analyzing changed. Only the dimensions for the new

components are added. The values for $Rz_I$, ($R_A$) and ($v_{RA}$) of the model 400-450 are the same as in model class I and can be looked up in table 3-2.

Also in model class II the model 420_20 is designed.

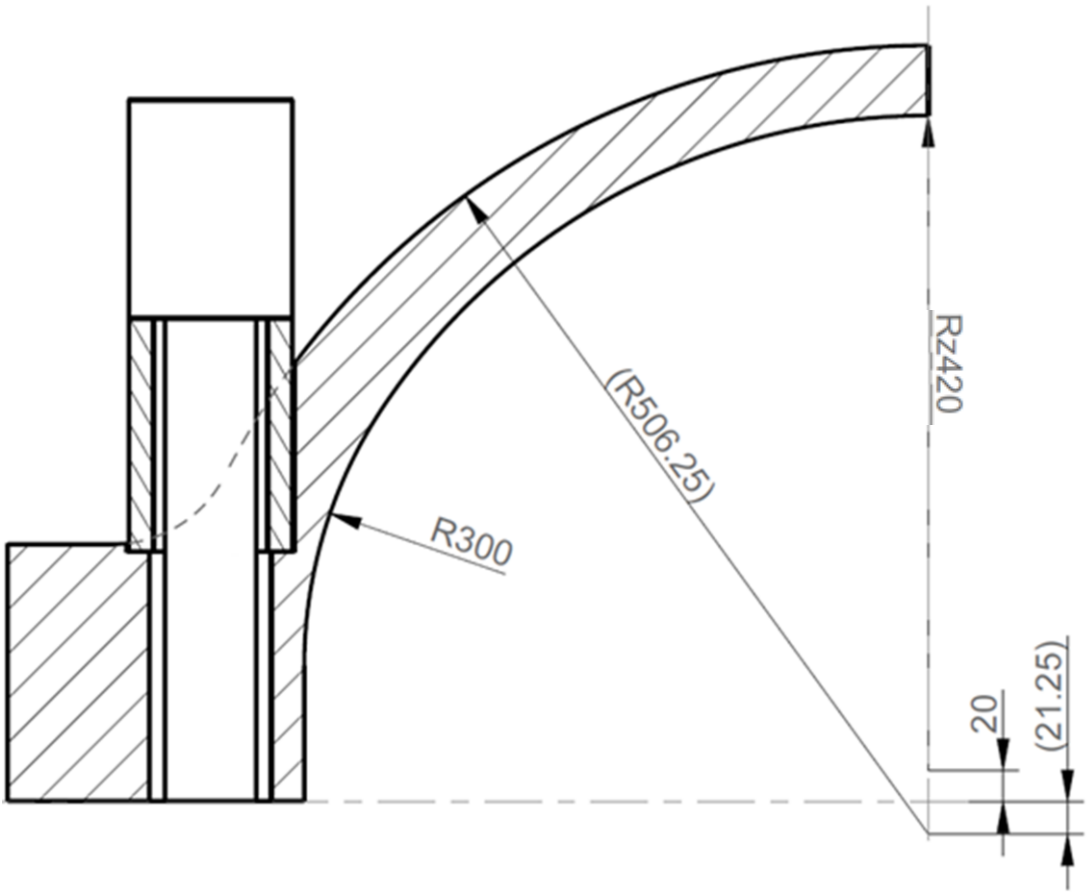


*Figure 3-19: Partial dimensioning of model 420_20 of model class II (cf. 3-11).*

A further variation based on model 420_20 is the model narrow-flange. The improvement of this model is that the flange width is reduced from 190 mm to 120 mm. Moreover the flange height is raised from 165 mm up to 210 mm. The bolt and the expansion sleeve are adjusted accordingly (cf. 3-20).

*Table 3-6: Parameters of the model narrow-flange (cf. figure 3-11)*

| Parameters | Symbols | Unit | Fixed values |
|---|---|---|---|
| Distance between symmetry axis and bolt axis | $S_{sym}$ | mm | 0 |
| Flange width | u+v | mm | 120 |

| | | | |
|---|---|---|---|
| Internal radius in Y direction | $Ry_I$ | mm | 400 |
| Thinnest wall thickness | s | mm | 45 |
| Rounding radius | $r_{GF}$ | mm | 80 |
| Depth in X direction | b_T | mm | 135 |
| Superelevation of the flange | $k_{RI}$ | mm | 0 |
| Bolt diameter | d | mm | 58.5 |
| Diameter of the reduction surface for position of the expansion sleeve | $d_{af}$ | mm | 107 |
| External diameter of the expansion sleeve | $D_{DH}$ | mm | 105 |
| Internal diameter of the expansion sleeve | $d_{DH}$ | mm | 73 |
| Bore diameter of the braced components | $d_h$ | mm | 78 |
| Length of the expansion sleeve | $l_{DH}$ | mm | 100 |
| Length of the braced part of the flange | $l_{FL}$ | mm | 210 |
| Length of the bolt head | $l_{SK}$ | mm | 140 |

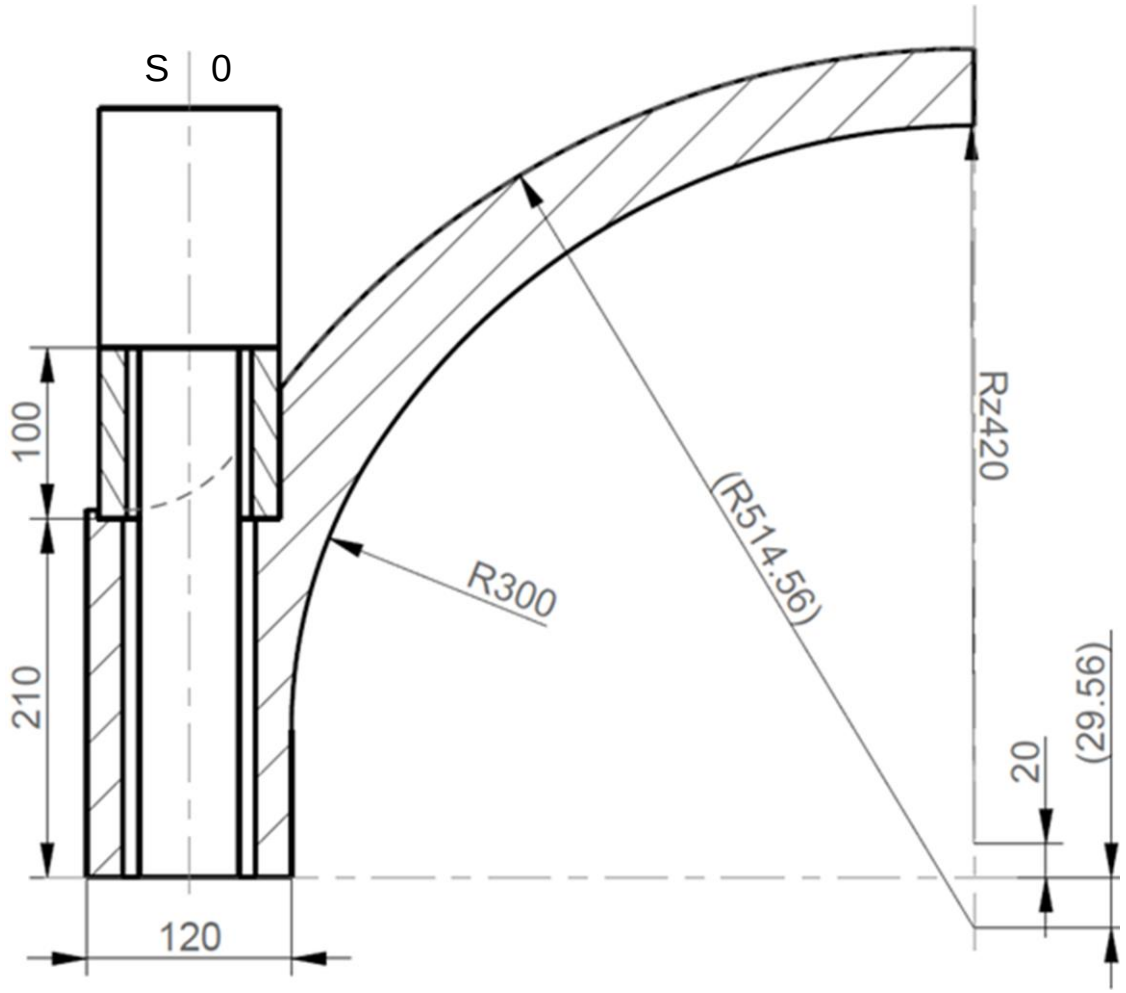


*Figure 3-20: Partial dimensioning of model narrow-flange of model class II.*

Dimensions which are not mentioned here are the same as in the basic model (cf. figure 3-18).

# 4 Analysis of the FEM Models Related to Joint Leak Tightness

This chapter presents the results as well as the order of the analyses. The evaluation uses mostly a consistent coulor scale as a key shown in figure 4-1, otherwise a different scale is quoted. The maximum value of this scale is determined by the basic model of model class I.

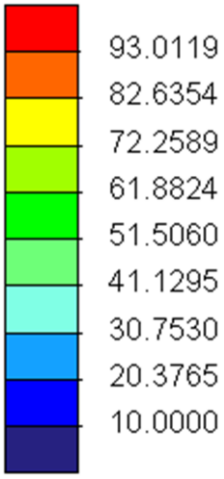


*Figure 4-1: Consistent colour scale for the stress distribution [N/mm²].*

During the FEM analysis stresses caused by the mechanical and thermal load can be figured as colour-scaled models. Due to the clamping of these simplified models a combination of these load cases is not possible. However, an alternative is to analyse the stress of each load case and to sum them up by using the superposition principle. Looking at figure 4-2 makes clear that the thermal load case compared with the mechanical load case has an influence < 1 % of the combined (mechanic-thermal) load case. Based on this fact the thermal load case is secondary and the mechanical load case can be used for representing the combined load case.

Furthermore it is mentioned that normal stresses are differentiated into positive stress (tensile stress) and negative stress (compressive stress) (cf. figure 4-2).

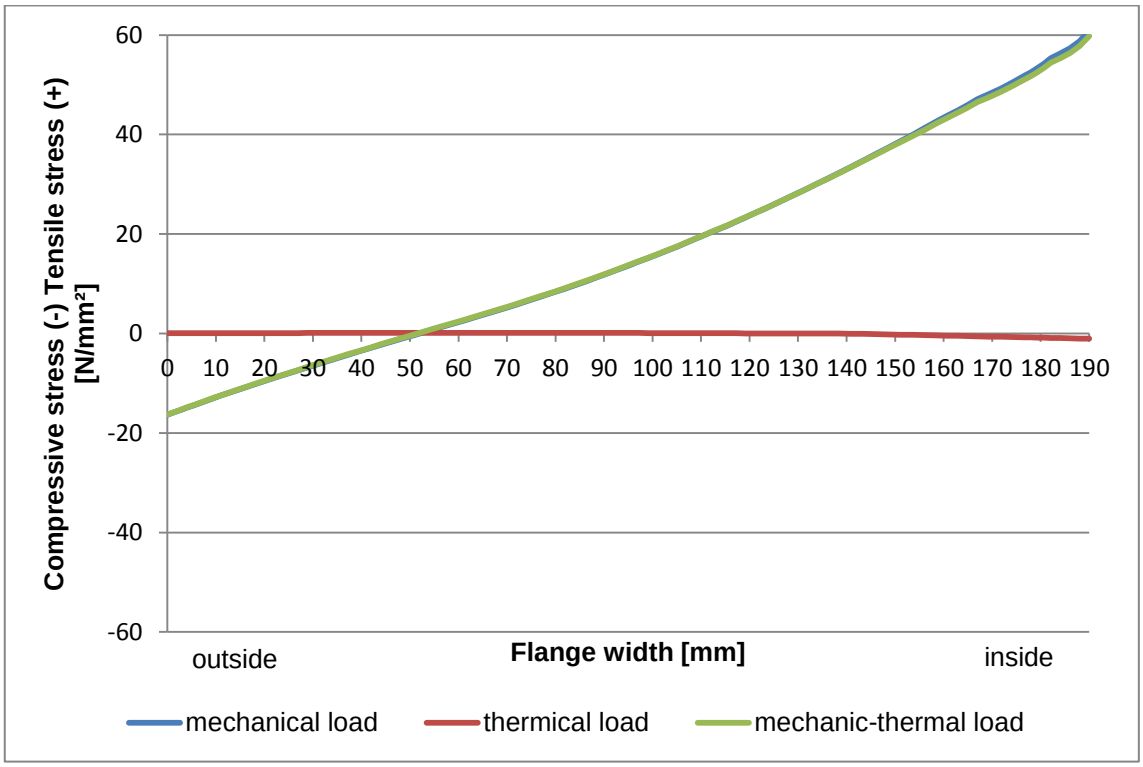


*Figure 4-2: Example (model 400 class I) – normal stress across the flange width with different load cases (pressure, temperature).*

## 4.1 Analysis – Model Class I

In this first step the models defined in chapter 3.2 are analysed by using the assessment criteria which are determined in chapter 2.5.

### 4.1.1 Variation of the Basic Geometry Class I

**Point of origin of the working load across the flange**

The following text presents the in chapter 3.2.1 described measurements. The values are calculated for each case by using the FE calculations program. They are summarised in table 4-1. The mechanic-thermical load case is put together by adding the mechanical and the thermical load case.

1) Mechanical load case (pressure): F_p M_p
2) Thermical load case (temperature): F_T = 0 M_T
3) Mechanic-thermical load case: F = F_p + F_T M = M_p + M_T

The lever arm (a) is calculated by equation (15):

$$a = \frac{u+v}{2} - \frac{M}{F} \qquad \text{with } u+v = 190 \text{ mm}$$

*Table 4-1: Measurements and calculated lever arm for model 400-450 of model class I*

| **Model class I** | | | | | | |
|---|---|---|---|---|---|---|
| **Model** | **400** | **410** | **420** | **430** | **440** | **450** |
| Determined values | | | | | | |
| **F_p [kN]** | 432 | 432 | 432 | 432 | 432 | 432 |
| **M_p [Nm]** | 11232 | 14836 | 18598 | 22361 | 26114 | 30272 |
| **F_T [kN]** | 0 | 0 | 0 | 0 | 0 | 0 |
| **M_T [Nm]** | 323 | 333 | 350 | 374 | 403 | 433 |
| Calculated values | | | | | | |
| **F [kN]** | 432 | 432 | 432 | 432 | 432 | 432 |
| **M [Nm]** | 11555 | 15169 | 18948 | 22735 | 26517 | 30705 |
| **a [mm]** | 68 | 60 | 51 | 42 | 34 | 24 |

Table 4-1 indicates that the pressure caused force (F_p) at the flange has a constant value of 432 kN during these variations. Compared to that the temperature caused force (F_T) has no influence (F_T = 0). Furthermore, it is noticeable that both moments caused by the pressure or temperature are constantly increasing. The moment (M_p) is up to 70 times bigger than the moment (M_T) and has consequently the major impact on the combined load case. The calculated value of the force (F) is in each model 432 kN. The difference between combined and mechanical load case is concerning the moments during these variations < 5 %. As mentioned before, the lever arm (a) is calculated by the force (F) and the moment (M) for the combined load case. The variation of the casing geometry obviously effects an improvement of the lever arm (a). The principle of the lever arm (chapter 2.5.1) and the geometry from table 3-1 the results in an optimal lever arm when the force (F_A) is working along the bolt axis (S) (a = S_sym). In other words, a lever arm of a = 35 mm is the optimum. Compared with table 4-1, model 440 (a = 34 mm) is the best variation concerning the lever arm.

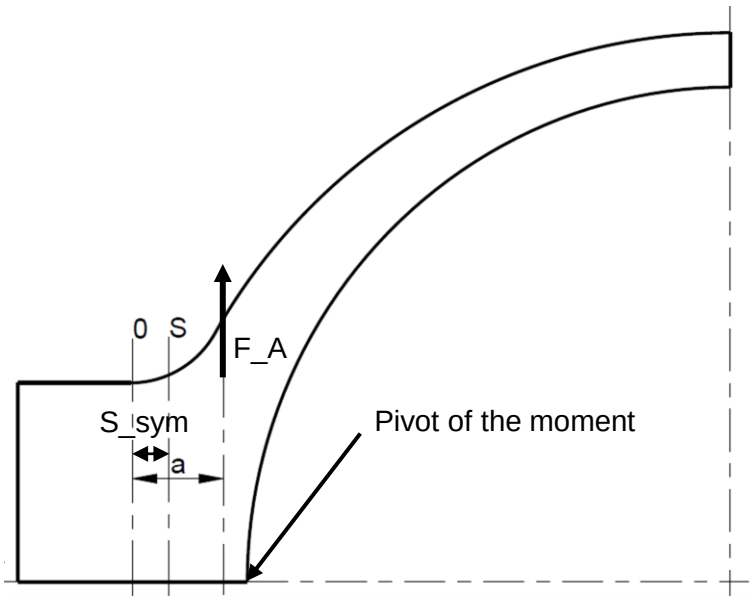


*Figure 4-3: Lever arm and working load across the flange for model class I.*

**Stresses inside the models**

Table 4-2 shows four of the six analysed models. They illustrate the trend of the von Mises stress depending on the geometric variation. Noticable is that the stress varies in particular points more than in others. These points and their maximal stress level are marked in each model.

Critical parts are the thinnest point of the casing as well as the transition from casing shell to the upper flange surface. Both parts develop varyingly strong stresses during the variation. The thinnest part of the shell contains stresses about 89-167 N/mm² with a maximal stress moving from the outside of the shell to the inside. The transition area contains stresses about 20-114 N/mm². The following analyses are using model 400 as the comparison model.

*Table 4-2: Von Mises stress trend of model (400/420/430/450) of model class I with maximal stresses*

| Model 400 | Model 420 | Model 430 | Model 450 |
|---|---|---|---|
| 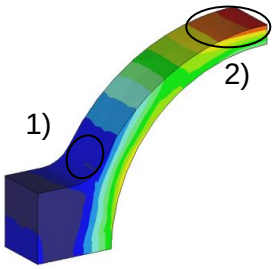 | 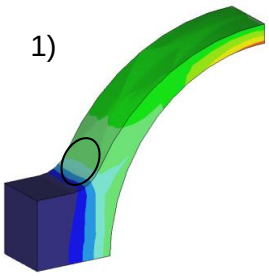 | 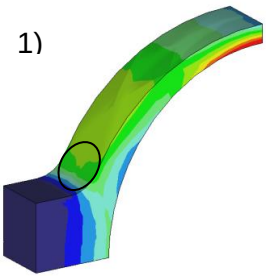 | 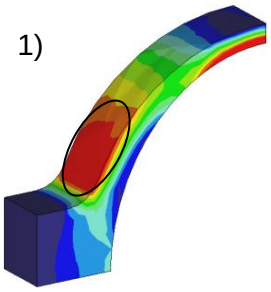 |
| 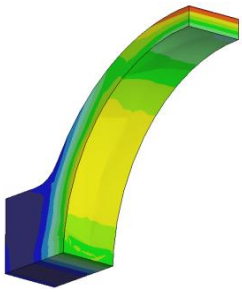 | 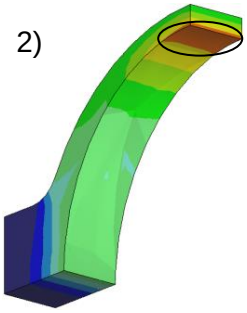 | 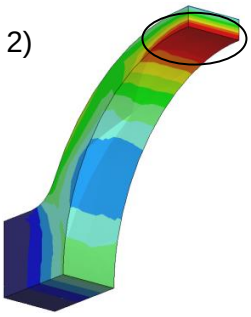 | 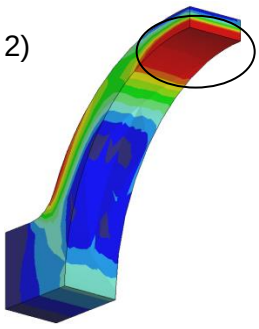 |
| 1) max. 20 N/mm²<br>2) max. 93 N/mm² | 1) max. 48 N/mm²<br>2) max. 89 N/mm² | 1) max. 65 N/mm²<br>2) max. 115 N/mm² | (1) max. 114 N/mm²<br>(2) max. 167 N/mm² |

The principally method to calculate the stresses of the combined (mechanic-thermical) load case is presented exemplary for the model 400 of model class I and can be transferred to all other models.

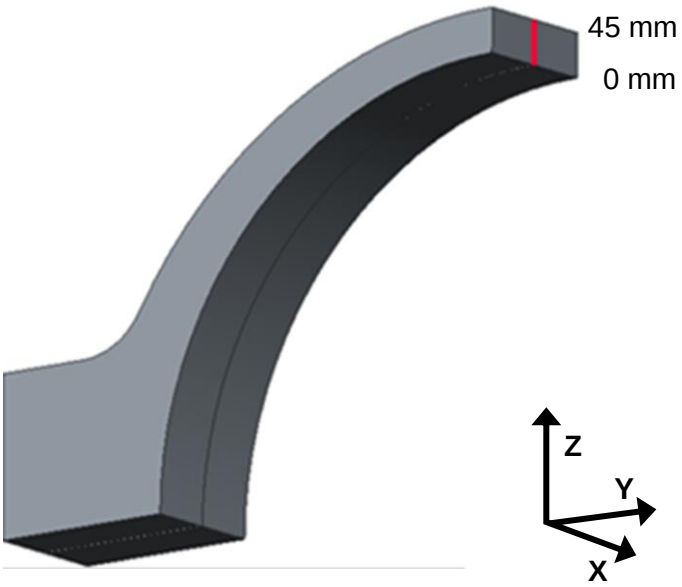


*Figure 4-4: Analysed distance for evaluation of the stress components in the thinnest point of the model of model class I.*

Figure 4-4 shows the analysed distance which is representative for the thinnest area of the model. By using the program Creo Simulate it is possible to extract the stress data for X, Y and Z direction of the selected distance.

The FEM calculation includes all stress components of the mechanical and thermal load case. The data are extracted to Excel and summed up in the following tables.

*Table 4-3: Stress components of the thinnest point of model 400 of model class I with mechanical load*

| **Length [mm]** | **Stress components [N/mm²]** | | | | | |
|---|---|---|---|---|---|---|
| | **XX** | **XY** | **XZ** | **YY** | **YZ** | **ZZ** |
| 0 | 8.013 | -0.061 | -0.039 | 37.124 | -0.484 | -8.508 |
| 11.25 | 13.569 | 0.099 | 0.07 | 54.287 | 0.997 | -5.088 |
| 22.5 | 18.885 | 0.062 | 0.069 | 71.12 | 0.977 | -3.156 |
| 33.75 | 24.022 | -0.03 | 0.011 | 87.551 | 0.683 | -1.644 |
| 45 | 29.042 | -0.035 | -0.054 | 103.512 | 1.338 | 0.52 |

*Table 4-4: Stress components of the thinnest point of model 400 of model class I with thermal load*

| Length [mm] | Stress components [N/mm²] | | | | | |
|---|---|---|---|---|---|---|
| | XX | XY | XZ | YY | YZ | ZZ |
| 0 | -0.209 | 0.002 | -0.008 | -7.675 | -0.006 | -0.055 |
| 11.25 | -0.055 | -0.001 | -0.007 | -3.826 | 0.033 | -0.07 |
| 22.5 | 0.026 | -0.003 | -0.006 | -0.16 | 0.029 | -0.119 |
| 33.75 | 0.074 | -0.007 | -0.003 | 3.335 | 0.018 | -0.115 |
| 45 | 0.132 | -0.011 | 0 | 6.669 | 0.042 | 0.026 |

The result of adding each stress component from table 4-3 (mechanical load) and 4-4 (thermal load) can be seen in table 4-5 (mechanic-thermal load). Using the calculated values, the von Mises stress for the combined load case can be calculated by equation (16). [4]

$$\sigma_v=\sqrt{\sigma_{xx}^2+\sigma_{yy}^2+\sigma_{zz}^2-\sigma_{xx}\sigma_{yy}-\sigma_{xx}\sigma_{zz}-\sigma_{yy}\sigma_{zz}+3(\tau_{xy}^2+\tau_{xz}^2+\tau_{yz}^2)} \quad (16)$$

*Table 4-5: Stress components and von Mises stress of the thinnest point of model 400 of model class I with mechanic-thermal load*

| Length [mm] | Von Mises stress [N/mm²] | Stress components [N/mm²] | | | | | |
|---|---|---|---|---|---|---|---|
| | | XX | XY | XZ | YY | YZ | ZZ |
| 0 | 33.037 | 7.804 | -0.059 | -0.048 | 29.449 | -0.49 | -8.563 |
| 11.25 | 49.059 | 13.515 | 0.098 | 0.062 | 50.461 | 1.03 | -5.158 |
| 22.5 | 66.024 | 18.91 | 0.059 | 0.064 | 70.96 | 1.006 | -3.275 |
| 33.75 | 82.812 | 24.096 | -0.036 | 0.008 | 90.886 | 0.701 | -1.759 |
| 45 | 98.521 | 29.174 | -0.046 | -0.054 | 110.181 | 1.379 | 0.546 |

It is noticeable in all three tables is that the stress component YY (normal stress) has the largest share of all analysed components in this part of the model. This normal stress is analysed for all six models and plotted in figure 4-5. The corresponding data can be found in appendix A.

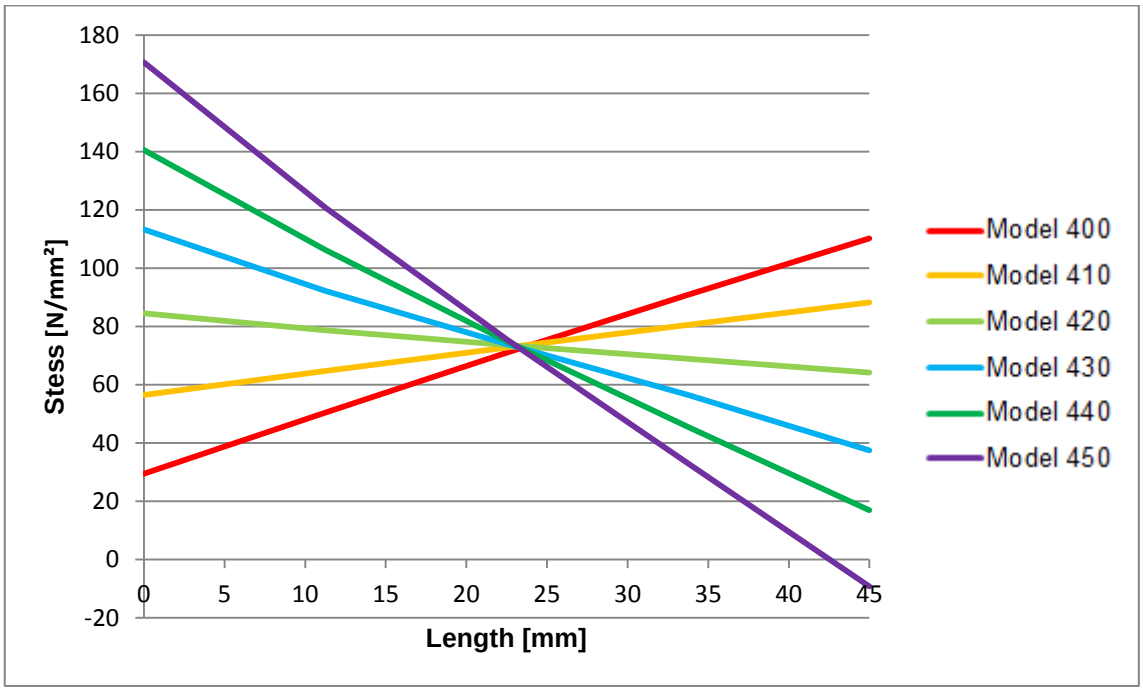


*Figure 4-5: Normal stress (YY) of the thinnest point of the model 400-450 of model class I for mechanic-thermal load.*

The stress is distributed approximately linear in each model. It is noticeable that the slopes of the graphs vary a lot. A steep graph indicates a big stress difference inside the casing shell. A constant stress distribution inside the shell should be targeted. Model 420 with a nearly constant stress distribution and an average stress of 70 N/mm² is rated as the best out of these six models.

**Surface pressure across the flange**

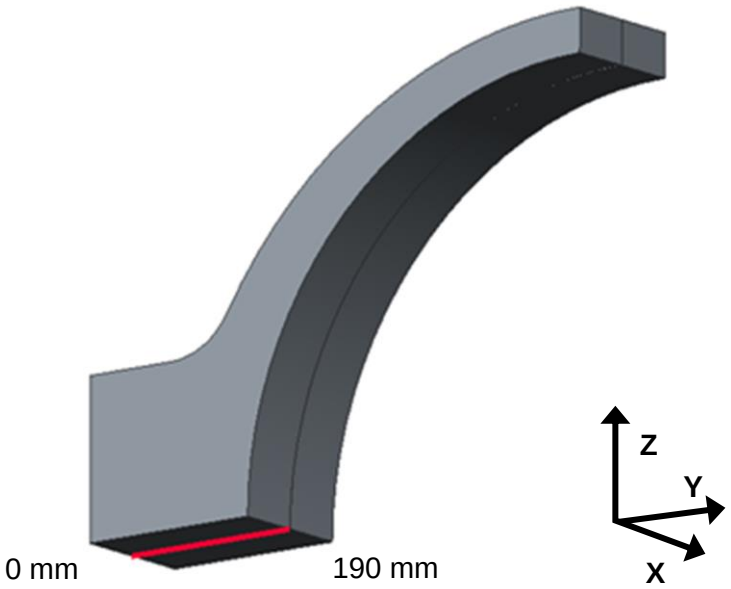


*Figure 4-6: Analysed distance for evaluation of the normal stress (ZZ) across the flange of model class I.*

Figure 4-6 shows the analysed distance which is representative for the whole joint surface. By using the program Creo Simulate it is possible to extract the stress data for X, Y and Z direction of the selected distance. The FEM calculation includes all stress components of the mechanical and thermal load case. The data are extracted to Excel and summed up in the following tables.

The following tables illustrate that the stress component ZZ (normal stress) has the largest share of all analysed components in this part of the model. Also, it is noticeable that the impact of the thermical load referring to the mechanic-thermical load is < 1 %. This normal stress (ZZ) is analysed for all six models and plotted in figure 4-7. The corresponding data can be found in appendix A.

*Table 4-6: Stress components across the flange of model 400 of model class I with mechanical load*

| Length [mm] | Stress components [N/mm²] | | | | | |
|---|---|---|---|---|---|---|
| | XX | XY | XZ | YY | YZ | ZZ |
| 0 | -4.551 | 0 | 0.001 | -0.002 | 0.001 | -16.323 |
| 47.5 | -0.126 | 0.015 | 0.001 | 0.997 | -0.002 | -1.396 |

| | | | | | | |
|---|---|---|---|---|---|---|
| 95 | 4.337 | -0.003 | 0 | 1.748 | -0.017 | 13.636 |
| 142.5 | 9.192 | -0.011 | 0.001 | -1.564 | 0 | 33.951 |
| 190 | 14.634 | -0.021 | 0.005 | -7.744 | -0.116 | 60.841 |

*Table 4-7: Stress components across the flange of model 400 of model class I with thermal load*

| **Length [mm]** | **Stress components [N/mm²]** | | | | | |
|---|---|---|---|---|---|---|
| | **XX** | **XY** | **XZ** | **YY** | **YZ** | **ZZ** |
| 0 | -0.108 | -0.045 | -0.01 | -0.078 | 0.093 | 0.035 |
| 47.5 | -0.01 | 0.061 | -0.032 | -0.005 | 0.018 | 0.133 |
| 95 | -0.114 | 0.14 | -0.111 | -0.085 | -0.071 | 0.101 |
| 142.5 | -0.2 | 0.135 | -0.141 | -0.116 | -0.088 | -0.048 |
| 190 | -0.806 | -0.005 | -0.019 | -0.653 | 0.046 | -1.054 |

*Table 4-8: All stress components and von Mises stress across the flange of model 400 of model class I with mechanic-thermal load*

| **Length [mm]** | **Von Mises stress [N/mm²]** | **Stress components [N/mm²]** | | | | | |
|---|---|---|---|---|---|---|---|
| | | **XX** | **XY** | **XZ** | **YY** | **YZ** | **ZZ** |
| 0 | 14.473 | -4.658 | -0.045 | -0.008 | -0.08 | 0.094 | -16.288 |
| 47.5 | 1.954 | -0.136 | 0.077 | -0.031 | 0.992 | 0.015 | -1.263 |
| 95 | 11.021 | 4.223 | 0.137 | -0.111 | 1.663 | -0.088 | 13.737 |
| 142.5 | 31.629 | 8.992 | 0.124 | -0.141 | -1.68 | -0.089 | 33.903 |
| 190 | 60.229 | 13.828 | -0.026 | -0.013 | -8.397 | -0.07 | 59.786 |

The result of adding each stress component from table 4-6 (mechanical load) and 4-7 (thermal load) is shown in table 4-8 (mechanic-thermal load). Using the calculated values of all the components, the von Mises stress for the combined load case can be calculated by equation (16).

Because of the homogeneity (cf. table 4-9) in X direction the stress across this distance conduces as the representative value for the whole area and is analogous to the

surface pressure. The goal of this analysis is to detect the model with the lowest tensile stresses and the highest expected surface pressure at the inner edge of the bolted flanges. For the sealing the joint MDT-HBG has the criterion of a minimum surface pressure at the inner edge of the flange of three-times the internal pressure. In the present case a minimum surface pressure of -24 N/mm² is needed to ensure joint leak tightness. The normal stress across the flange will gain in significance in model class II because the bolt force will be considered. This is mentioned here for the sake of completeness.

*Table 4-9: Trend of the normal stress (ZZ) across the flange for models (400/420/430/450) of model class I*

| Model 400 | Model 420 | Model 430 | Model 450 | Key |
|---|---|---|---|---|
| 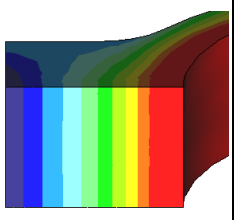 | 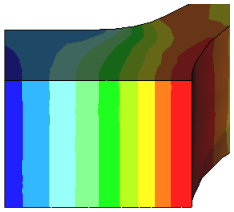 | 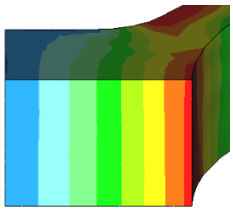 | 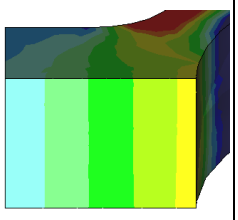 | 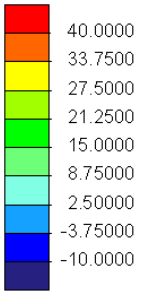  |

Table 4-9 shows the normal stress trend across the flange of different models with pressure load. The focus in these figures is the stress change as a function of geometry variation. It becomes clear that the tensile stresses at the inner edge of the flange decrease. Despite the missing bolt force this trend can be assessed as a positive effect for sealing. The lower tensile stress at the inner edge in model class entails higher compressive stresses at the inner edge in model class II. Moreover the variation shows an even stress distribution.

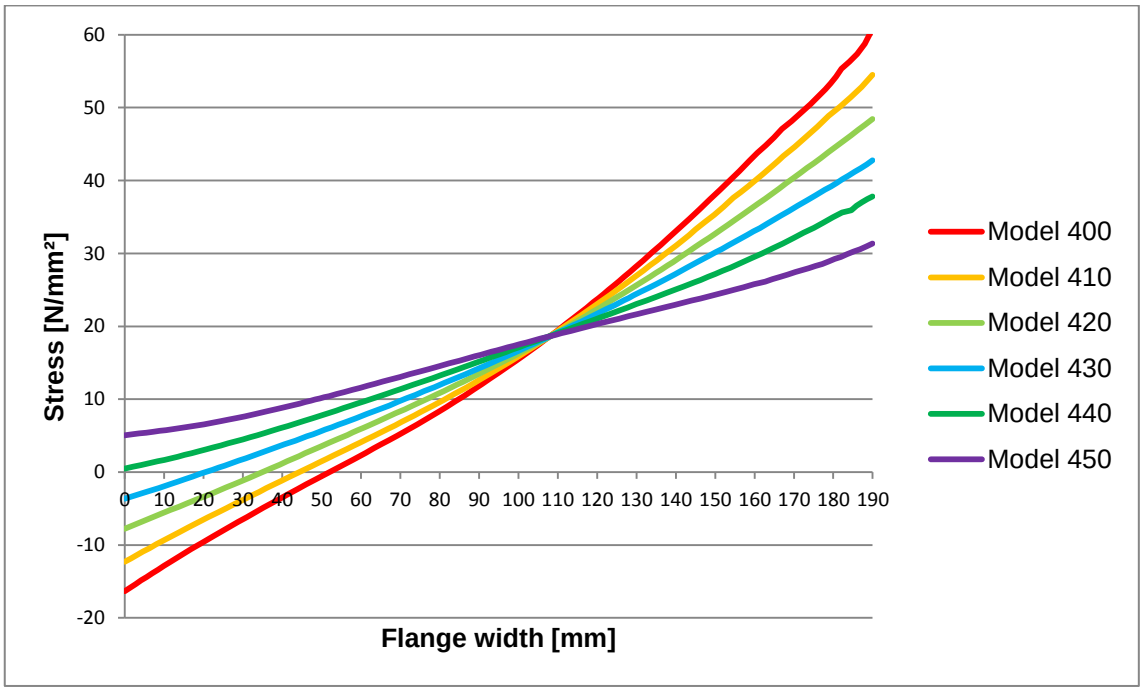


*Figure 4-7: Normal stress (ZZ) across the flange for model 400-450 of model class I with mechanical load.*

Figure 4-7 shows the normal stress (ZZ) across the flange for all models of model class I with mechanical load. Model 450 has the most evenly distributed stress as well as the lowest tensile stress at the inner edge of the flange.

### 4.1.2 First Geometry Optimisation Class I

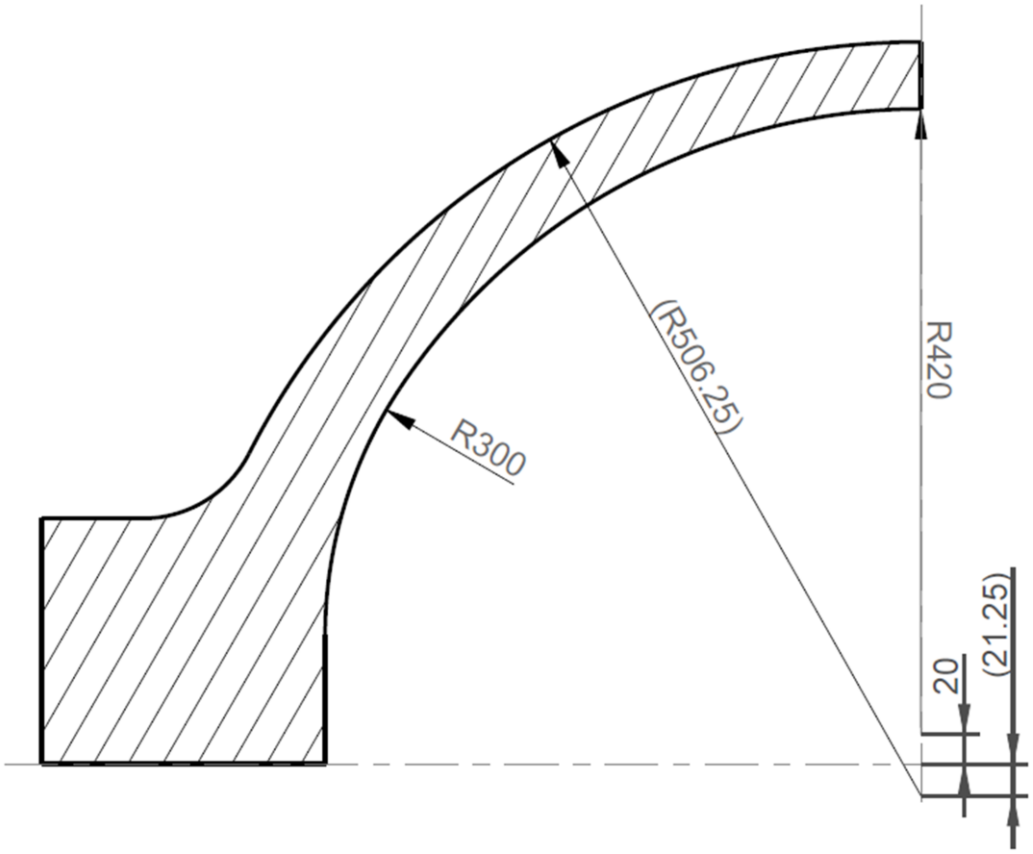


*Figure 4-8: Sectional drawing of model 420_20 with new values (model class I).*

The geometry of model 420_20 developed based on the results from the conclusions of the analysed variations. Because of the optimal lever arm (a) of model 440, which is documented in table 4-1, the vertical distance from the turbine center to the inner surface of model 420_20 is set to 440 mm. To counteract high stresses in model 440, the internal radius is set to 420 mm with a vertical offset of 20 mm (cf. figure 4-8). The goal is to combine the optimal lever arm of model 440 and the constantly distributed stress of model 420 (cf. figure 4-1 / table 4-2) in this new model. To retain the geometry and the position of the flange, a vertical line is set on the inner side of the flange. The point of intersection (circle (R420) and vertical line) is blunted by a radius of 300 mm (R300). In the next step the new model 420_20 is analysed such as conducted for the models before.

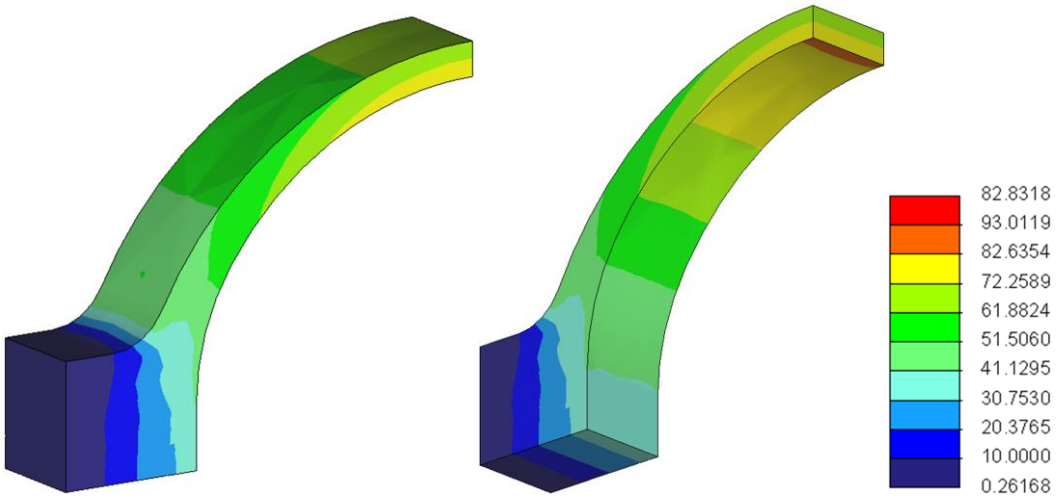


*Figure 4-9: Von Mises stress of model 420_20 of model class I.*

The inspection of von Mises stress shows an even contribution all over the shell. The highest stress is located in the thinnest part of the model with a value of 82.8 N/mm², which is still lower than the permissable value of 93.0 N/mm² (model 400).

*Table 4-10: Measured values and calculated lever arm for model 420_20 of model class I*

| **Model class I** | |
|---|---|
| **Model** | **420_20** |
| Determined values | |
| **F_p [kN]** | 432 |
| **M_p [Nm]** | 28524 |
| **F_T [kN]** | 0 |
| **M_T [Nm]** | 295 |
| Calculated values | |
| **F [kN]** | 432 |
| **M [Nm]** | 28819 |
| **a [mm]** | 28 |

The lever arm is calculated in the same manner as before. This variation brought a significant improvement of the lever arm from originally 68 mm (model 440) to 28 mm (model 420_20). The optimum of the lever arm is across the bolt axis with a value of 35 mm.

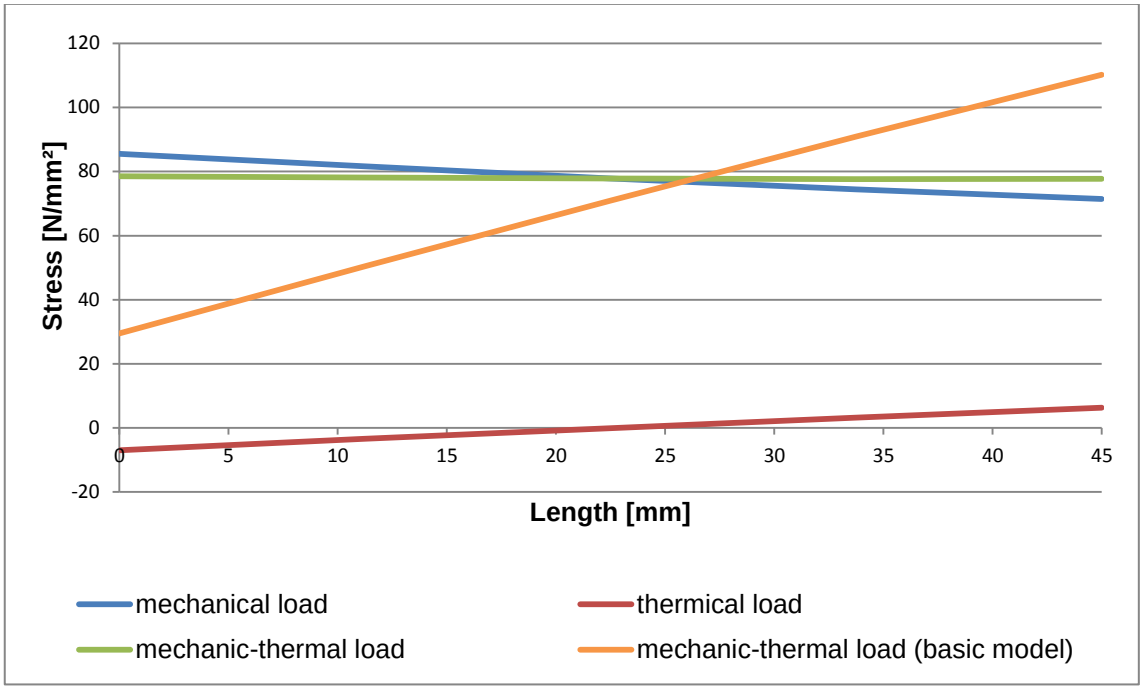


*Figure 4-10: Normal stress (YY) across the thinnest part of model 420_20 of model class I with different loads.*

Figure 4-10 and 4-11 show normal stresses in model 420_20. Unlike the analyses before, this figure contains all three load cases to get a more exact result. As mentioned before the impact of the thermical load case of the combined load case is < 1 %. The normal stress (YY) across the thinnest part of model 420_20 with mechanic-thermical load is averaged about 80 N/mm² and constantly distributed. This value corresponds to a similar niveau of the averaged normal stress (YY) of model 400 with a same load case. However, the deciding factor is that the normal stress (YY) of model 420_20 is much better distributed with an associated lower beding stress share compared to model 400.

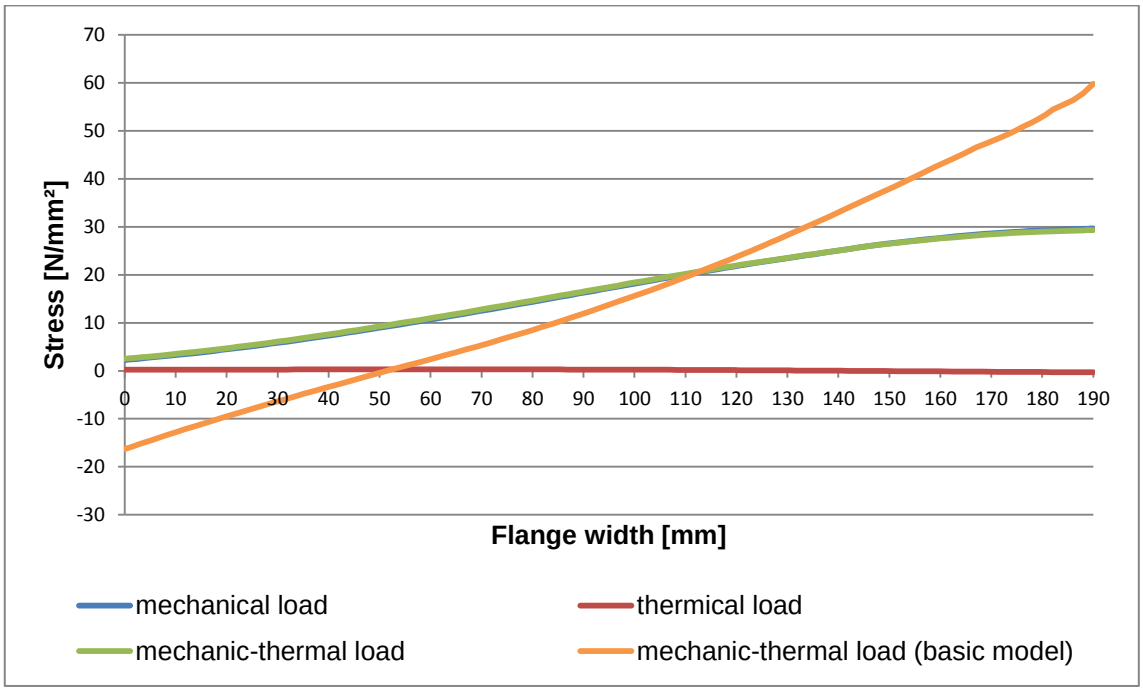


*Figure 4-11: Normal stress (ZZ) across the flange of model 420_20 of model class I with different loads.*

The normal stress (ZZ) in model 420_20 at the inner edge of the joint with mechanic-thermal load has a value of about 30 N/mm² which is almost 50 % lower than the normal stress (ZZ) of model 400. This will have a positive effect on the bolt preload force in model class II.

## 4.2 Analysis – Model Class II

Based on the first analysis this chapter presents further analysis, which includes the bolt connection.

### 4.2.1 Variation of the Basic Geometry Class II

**Point of origin of the working load across the flange**

The following text presents the in chapter 3.3.1 described measurements. The values are calculated for each case by using the FE calculations program. They are summarised in table 4-11. The mechanic-thermical load case is put together by adding the mechanical and the thermical load case.

| | | | |
|---|---|---|---|
| 1) | Mechanical load case (pressure): | F_p | M_p |
| 2) | Thermical load case (temperature): | F_T = 0 | M_T |
| 3) | Bolt force: | F_s | M_s |
| 4) | Combined load case | F = F_p + F_T + F_s | |
| | | M = M_p + M_T + M_s | |

The lever arm (a) is calculated by equation (15):

$$a = \frac{u+v}{2} - \frac{M}{F} \qquad \text{with u+v = 190 mm}$$

*Table 4-11: Measurements and calculated lever arm for model 400-450 of model class II*

| **Model class II** | | | | | | |
|---|---|---|---|---|---|---|
| **Model** | **400** | **410** | **420** | **430** | **440** | **450** |
| Determined values | | | | | | |
| **F_p [kN]** | 432 | 432 | 432 | 432 | 432 | 432 |
| **M_p [Nm]** | 11126 | 14568 | 18078 | 21664 | 25454 | 29130 |
| **F_T [kN]** | 0 | 0 | 0 | 0 | 0 | 0 |
| **M_T [Nm]** | 440 | 445 | 450 | 456 | 462 | 469 |
| **F_s [kN]** | 0 | 0 | 0 | 0 | 0 | 0 |
| **M_s [Nm]** | 107 | 102 | 96 | 91 | 84 | 80 |
| Calculated values | | | | | | |
| **F [kN]** | 432 | 432 | 432 | 432 | 432 | 432 |
| **M [Nm]** | 11673 | 15115 | 18624 | 22211 | 26000 | 29679 |
| **a [mm]** | 68 | 60 | 52 | 44 | 35 | 26 |

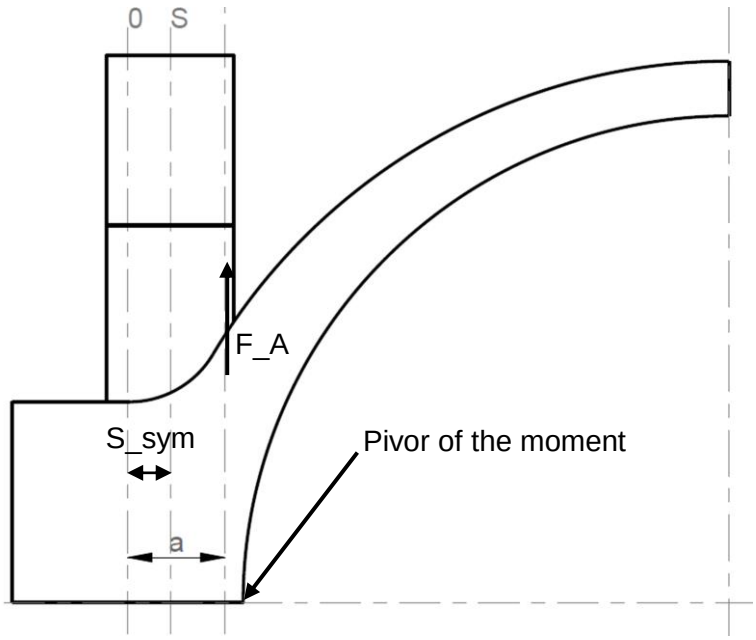


*Figure 4-12: Lever arm and working load across the flange for model class II.*

*Table 4-12: Lever arm (a) of model 400-450 for model class I and II*

| **Model** | | **400** | **410** | **420** | **430** | **440** | **450** |
|---|---|---|---|---|---|---|---|
| Model class I | a [mm] | 68 | 60 | 51 | 42 | 34 | 24 |
| Model class II | | 68 | 60 | 52 | 44 | 35 | 26 |

The comparison of model class I and II regarding the lever arm (a) shows a maximal difference of 2 mm. This shows that the model classes can be considered as comparable regarding the lever arm (a).

**Stresses inside the models**

The stresses within the bolt and expansion sleeve are not subject of this thesis and will not be explained in more detail.

*Table 4-13: Von Mises stress trend of model (400/420/430/450) of model class II with maximal stresses*

| Model 400 | Model 420 | Model 430 | Model 450 |
|---|---|---|---|
| 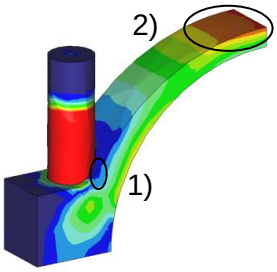  | 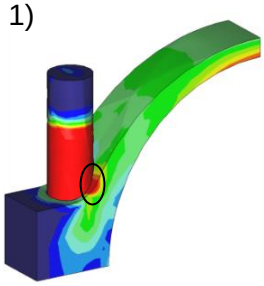  | 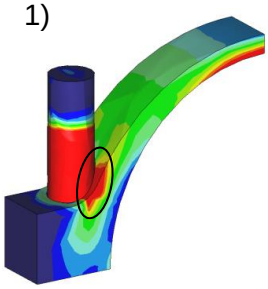  | 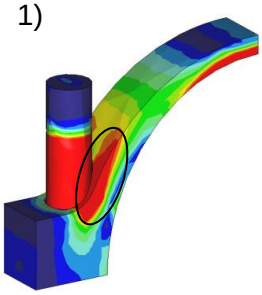  |
| 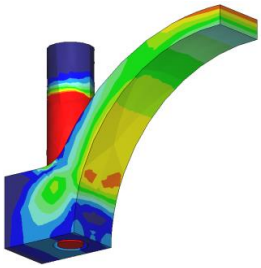 | 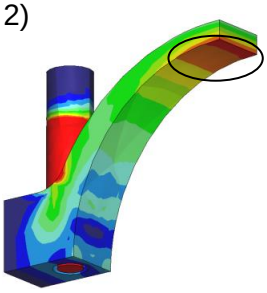  | 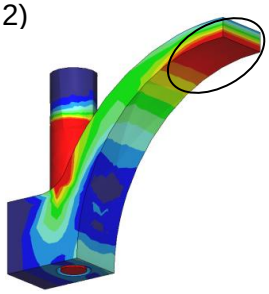  | 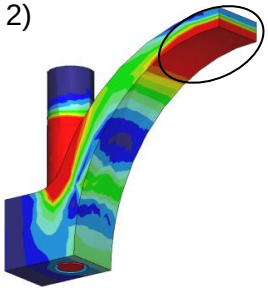  |
| 1) max. 31 N/mm²<br>2) max. 94 N/mm² | 1) max. 123 N/mm²<br>2) max. 96 N/mm² | 1) max. 184 N/mm²<br>2) max. 126 N/mm² | 1) max. 319 N/mm²<br>2) max. 189 N/mm² |

As in model class I, the thinnest part of the model and the transition from the outer shell to the flange are locations with high stress. Table 4-13 shows these locations and the maximum stresses are marked. Comparing table 4-2 and 4-13 makes clear that the trend of the von Mises stress in model class I and II is changing similarly. In both model classes the tensile stress across the thinnest part of the model is moving during the geometry variation from the outside to the inside of the shell. Also the tensile stresses at the flange transition increase during both variations. Considering the bolt force in model class II the stress level is much higher than in model class I. The von Mises stress in model class II for model 400 - 450 at the thinnest part is about 94 - 189 N/mm² and in model class I about 93 - 167 N/mm². Because of the bolt location surface some material is missing. This material is needed to transfer the working load. As a consequence of the missing material, stress is concentrating at the transition of the outer shell and flange. In model class I this stress is between 20 - 114 N/mm² and in model class II between 31 - 319 N/mm².

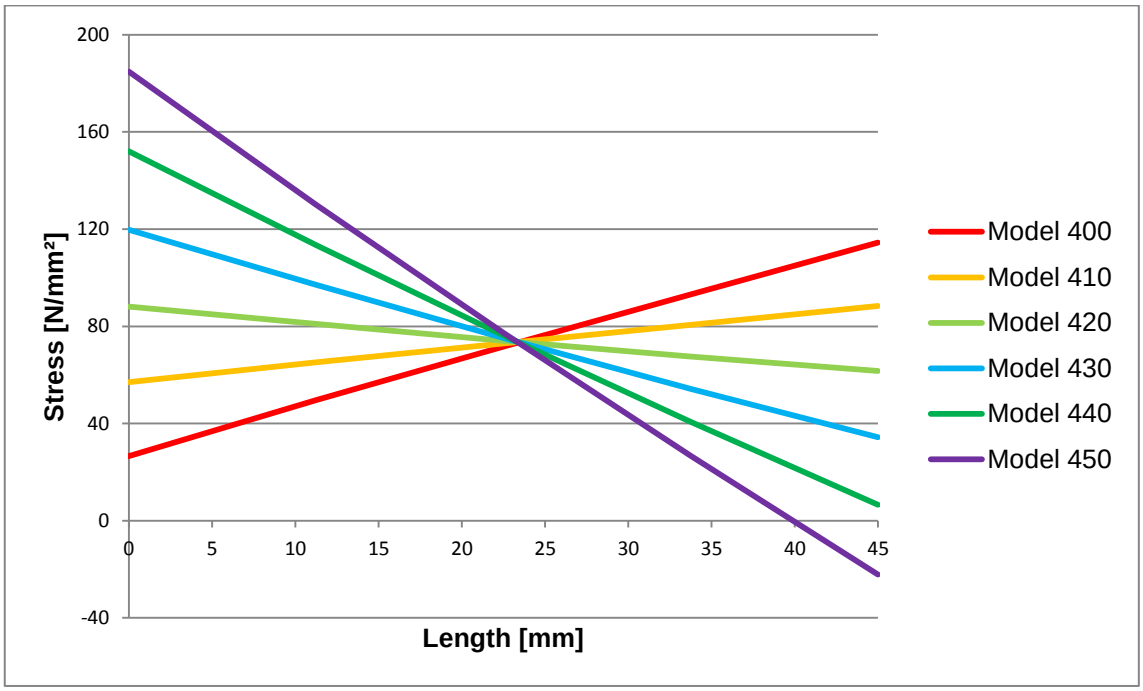


*Figure 4-13: Normal stress (YY) of the thinnest point of the model 400-450 of model class II for mechanic-thermal load.*

Figure 4-5 and 4-13 are used to compare the model classes regarding the normal stress (YY) across the thinnest part of the model with mechanic-thermal load. No significant changes are noticeable. In both model classes the model 440 has an approximately constant stress distribution of averaged 70 N/mm² and is rated as the best of these six models. Consequently it can be said that both model classes are equivalent regarding the normal stress (YY) at the thinnest point.

**Surface pressure across the flange**

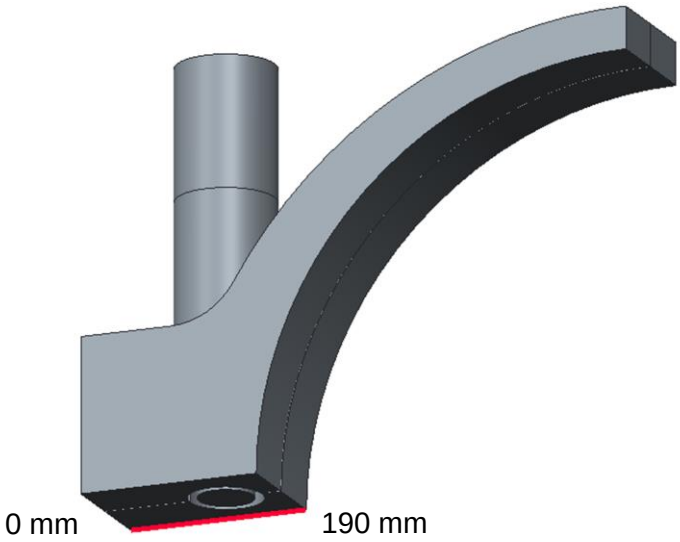


*Figure 4-14: Analysed distance for evaluation of the normal stress (ZZ) across the flange of model class II.*

The model class II has no continuous and centered line across the joint surface, like in model class I, caused by the bore. Instead of this, the marked line in figure 4-14 is used for evaluation of the normal stress (ZZ) across the flange.

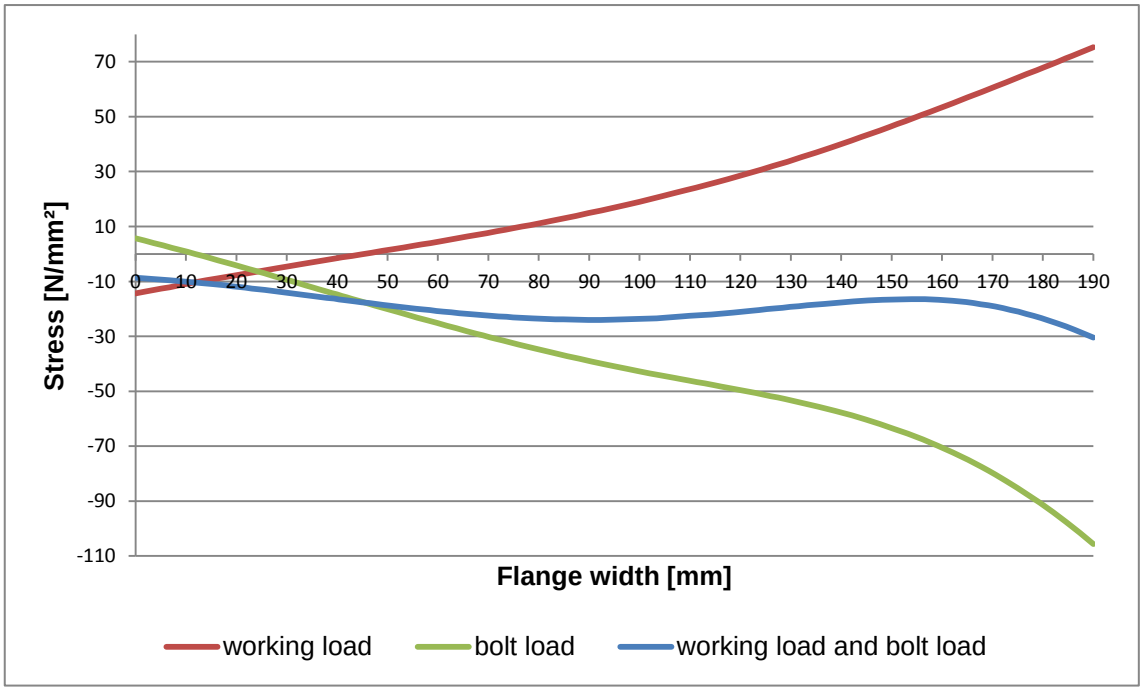


*Figure 4-15: Influence of working load and bolt load on the normal stress (ZZ) across the flange of model 400 of model class II.*

The slope of the graphs in figure 4-15 makes clear that the bolt force counteracts the working load. The working load causes a tensile stress (plus sign) and the bolt force causes a compressive stress (minus sign) at the inner edge of the flange. If a high enough bolt force is selected the resulting stress is a compressive stress, which affects a sealing at the inner edge.

*Table 4-14: Trend of the normal stress (ZZ) across the flange for models (400/420/430/450) of model class II*

| Model 400 | Model 420 | Model 430 | Model 450 | Key |
|---|---|---|---|---|
| 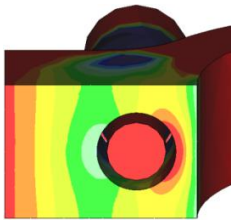 | 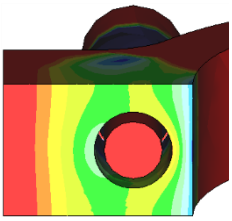 | 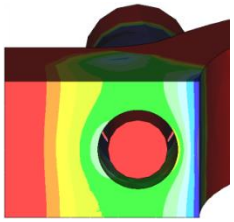 | 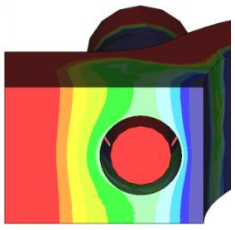 | 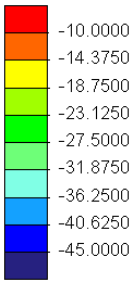  |

The four models in table 4-14 show exemplary the trend of the normal stress (ZZ) across the flange with parallel pressure load and bolt force. There are noteable differences between model class I and II by comparing table 4-9 and 4-14.

Figure 4-16 makes clear that during the geometry variation the compressive stress at the inner flange area (160-190mm) raises. Because of the bolt force the tensile stress in model class I, caused by the pressure load, is moving into the negative area of the diagram and changes in this way to compressive stress. As mentioned before, model 450 with the lowest tensile stress in model class I has the highest compressive stress in model class II. Futhermore the dashed line in figure 4-16 describes the sealing criterion. It is illustrated that the sealing of the inner joint surface gets better from model 400 to 450. On the outer joint surface the surface pressure is clearly decreasing. This part only makes a small contribution for the joint sealing. This issue prompts the question if it would be usefull to change not only the casing geometry but also reduce the flange width. One possible variation is shortly analysed under the designation 'narrow-flange' in chapter 4.2.3.

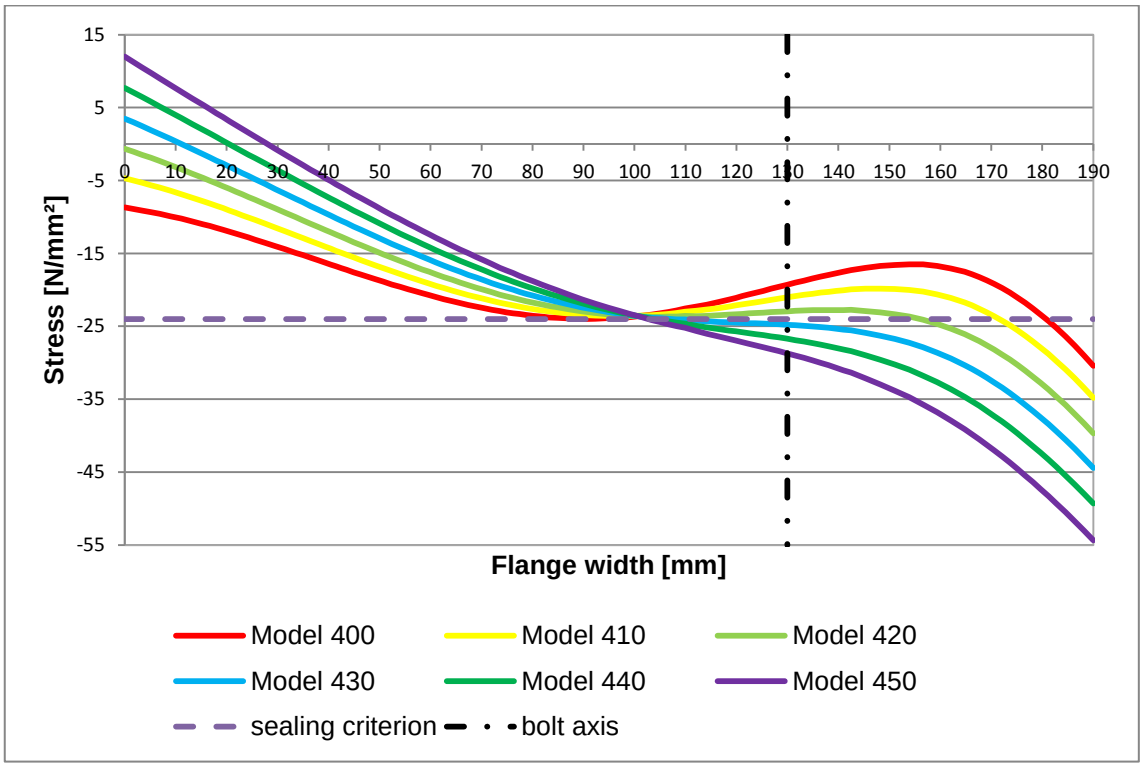


*Figure 4-16: Normal stress (ZZ) across the flange for model 400-450 of model class II with mechanical load.*

### 4.2.2 First Geometry Optimisation Class II

After the analyses of the six geometry variations the model 420_20 is analysed. The following figure 4-17 shows the geometry of model 420_20 of model class II. The bolt connection is the only geometric change compared with model 420_20 of model class I. The prior analyses revealed that the models of model class I and II are comparable. In this analysis, model 400 of model class II is used as the basic model.

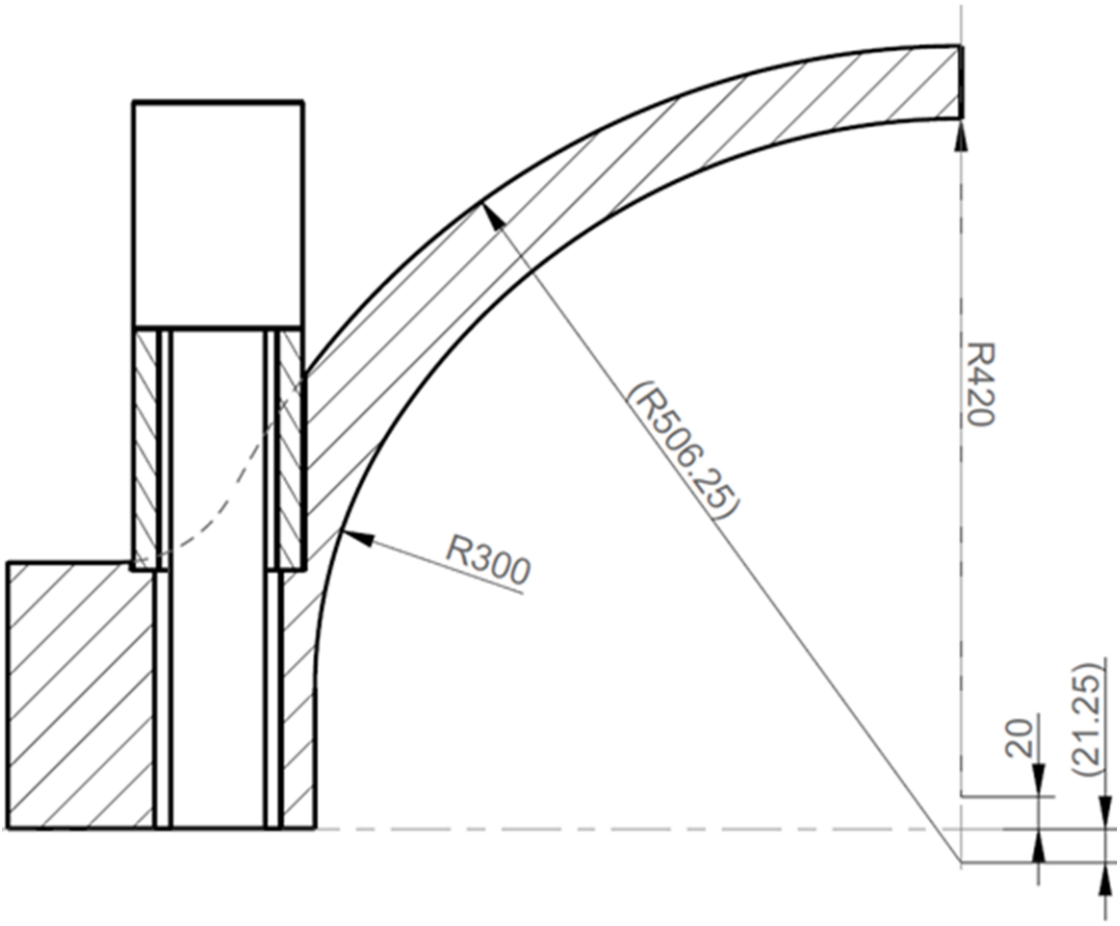


*Figure 4-17: Partial dimensioning of model 420_20 of model class II (cf. 3-11).*

The undimensioned geometries are quoted in figure 3-11.

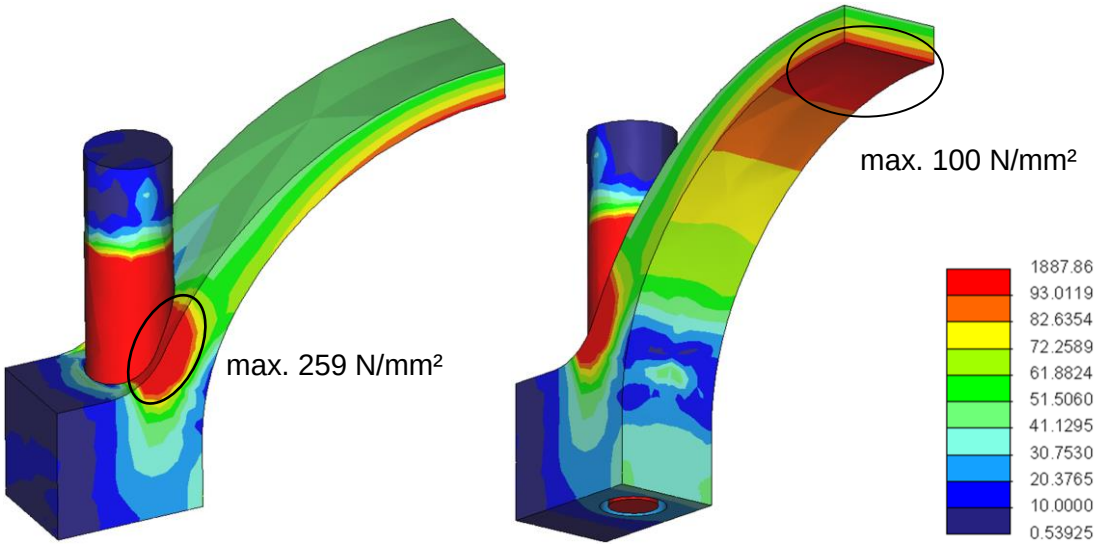


*Figure 4-18: Von Mises stress of model 420_20 of model class II.*

The highest von Mises stress at the thinnest part of the model 420_20 with pressure load is about 100 N/mm², which is 6 % higher compared to the basic model (94 N/mm²). One reason is that model 420_20 has a vertical distance of R420 + 20 mm, which is 10 % more compared to model 400 (R400 mm). This causes a 10 % larger pressure loaded surface. The second analysed stress peak at the transition from casing shell to the flange is in the basic model unincisive with a value of about 31 N/mm², whereas the value in model 420_20 is already about 259 N/mm². As a consequent the next step of geometric variation is about minimising the stress peak at the transition.

*Table 4-15: Calculation of the lever arm for model 420_20 of model class II*

| **Model class II** | |
|---|---|
| **Model** | **420_20** |
| Determined values | |
| **F_p [kN]** | 432 |
| **M_p [Nm]** | 27363 |
| **F_T [kN]** | 0 |
| **M_T [Nm]** | 377 |
| **F_s [kN]** | 0 |
| **M_s [Nm]** | 31 |

| Calculated values | |
|---|---|
| **F [kN]** | 432 |
| **M [Nm]** | 27771 |
| **a [mm]** | 31 |

The lever arm of model 420_20 (31 mm) compared with model 400 (68 mm) is more than two times shorter and is close to the optimum (35 mm).

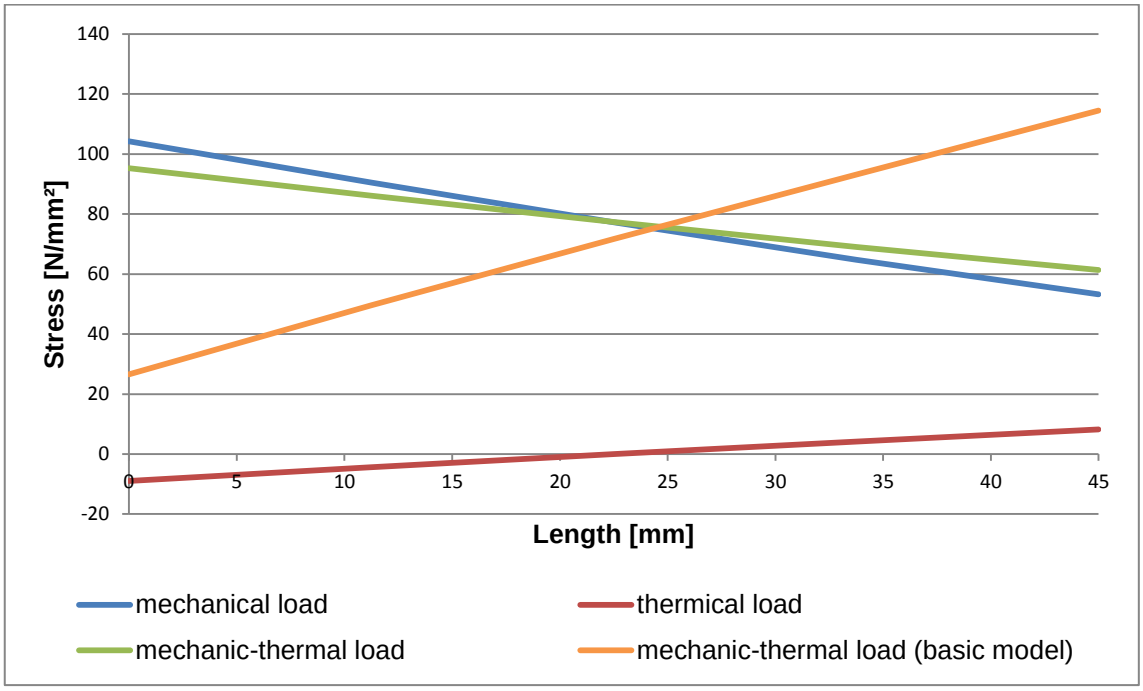


*Figure 4-19: Comparison of normal stress (YY) in the thinnest point of model 420_20 and model 400 of model class II with different loads.*

Figure 4-19 shows that model 420_20 has an advantage over the basic model concerning the normal stress (YY) distribution at the thinnest point of the model. The maximum stress of model 420_20 is about 95 N/mm² compared to 115 N/mm² of the basic model and is thus about 17 % lower. These facts make clear that the geometry variation has a positive effect on the level of the normal stress (YY) as well as the distribution referring the thinnest point of the model.

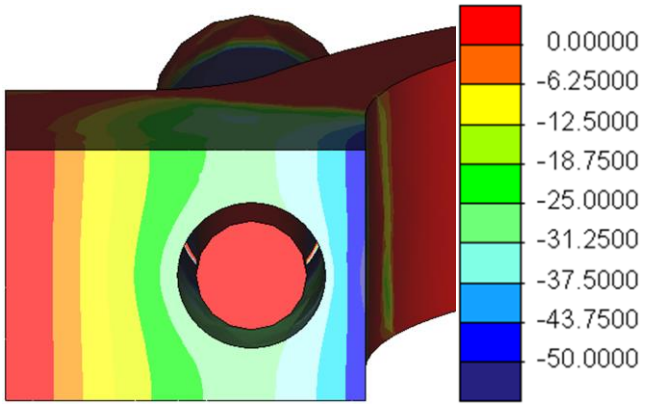


*Figure 4-20: Normal stress (ZZ) across the flange of model 420_20 of model class II.*

Figure 4-20 illustrates the normal stress (ZZ) across the flange in model 420_20. It is recognisable that a high compression stress is located on the inner part of the joint surface. The inner edge of the flange with about -50 N/mm² is obviously sealed (sealing criterion -24 N/mm²).

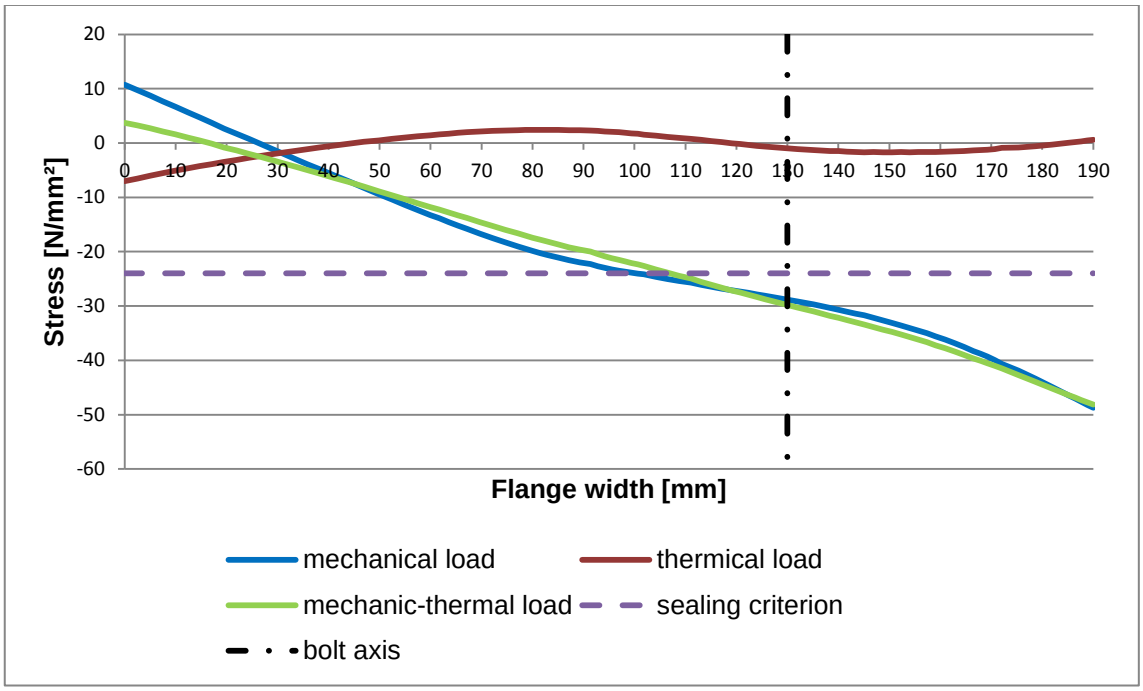


*Figure 4-21: Normal stress (ZZ) across the flange of model 420_20 of model class II with different loads.*

To sum up the analysis for model 420_20 of model class II, it can be said that this model has a good lever arm as well as acceptable stress in the thinnest part of the model. Also the sealing criterion for the joint surface is fulfilled. Nevertheless, there is

an excessive level of stress at the transition from casing shell to the flange. To reduce this peak stress a further geometry variation is following.

### 4.2.3 Second Geometry Optimisation Class II

The model narrow-flange is generally based on the geometry of model 420_20. Considering figure 4-18, it shows that a big part of the outer flange is loaded with a von Mises stress < 20 N/mm². It seems as if this part of the flange has a minor influence of the sealing and the solidity of the whole model. Figure 4-21 shows also a stress reversal from compressive stress to tensile stress. Thus, the outer part of the flange surface is loaded by tensile stress which should be avoided. For a better distribution of the stress and for the prevention of tensile stress, the flange is narrowed and heightened. Figure 4-22 shows the cross section of the model narrow-flange with the corresponding determinations of the flange. The external radius and the offset changed as well.

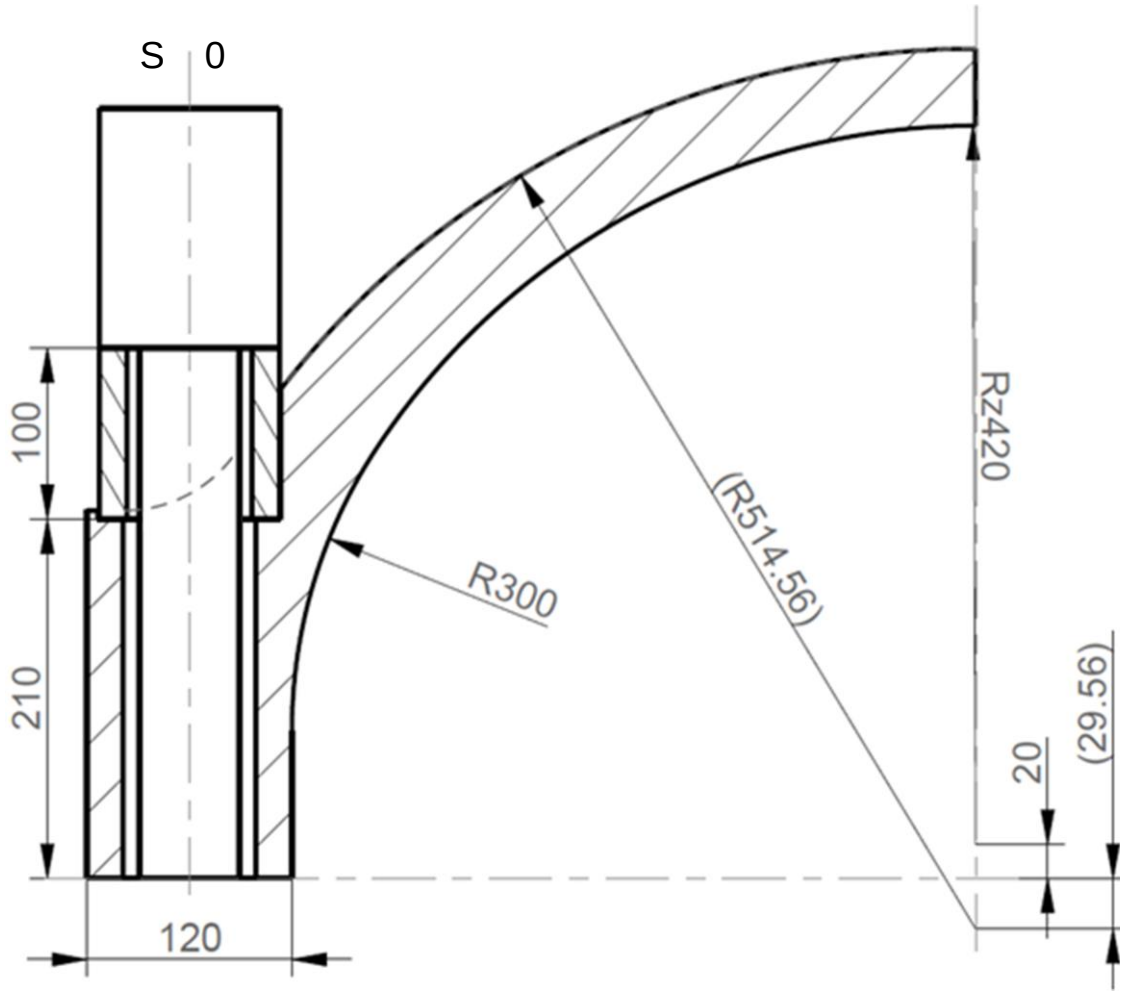


*Figure 4-22: Cross section of model narrow-flange of model class II (cf. 3-18).*

The undimensioned geometries are quoted in figure 3-11.

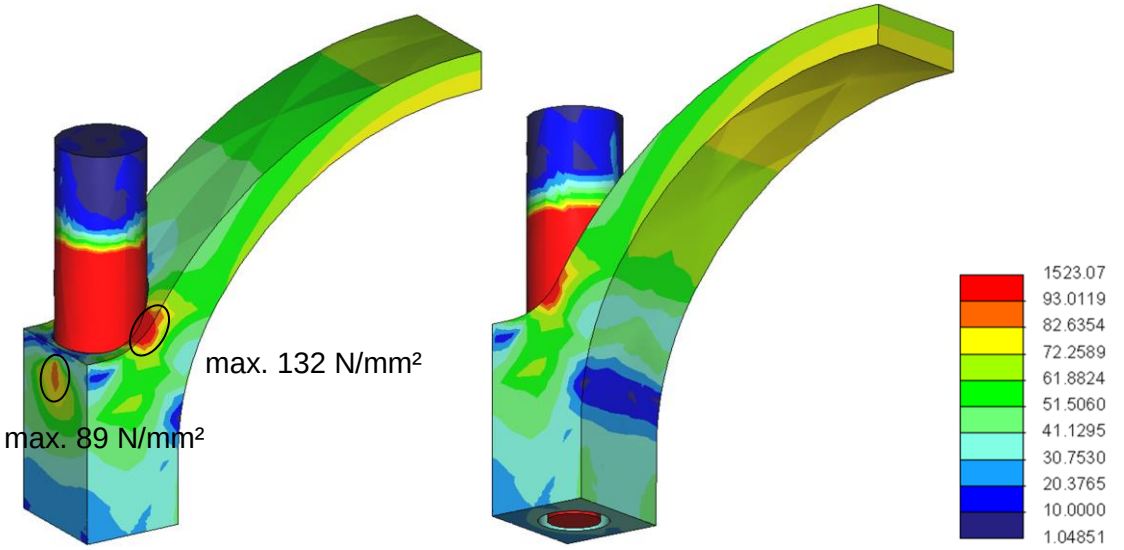


*Figure 4-23: Von Mises stress of model narrow-flange of model class II.*

In figure 4-23 is an all over the model evenly distributed von Mises stress shown with a value between 45-55 N/mm². Compared to model 420_20, this can be considered as a significant improvement. The peak stress at the transition decreases about 50 % from model 420_20 (289 N/mm²) to model narrow-flange (132 N/mm²). Even so the transition is still the point of the highest stress.

*Table 4-16: Calculation of the lever arm of model narrow-flange*

| **Model class II** | |
|---|---|
| **Model** | **Narrow-flange** |
| Determined values | |
| **F_p [kN]** | 432 |
| **M_p [Nm]** | 27979 |
| **F_T [kN]** | 0 |
| **M_T [Nm]** | 497 |
| **F_s [kN]** | 0 |
| **M_s [Nm]** | 216 |
| Calculated values | |
| **F [kN]** | 432 |
| **M [Nm]** | 28692 |

| **a [mm]** | -6 |
|---|---|

Because of the variation of the flange width to 120 mm, the bolt axis and the symmetry axis correspond. This causes a relocation of the optimal lever arm from 35 mm to 0 mm. With a lever arm of -6 mm, the point of origin of the working load is located to the left of the bolt/symmetry axis (cf. figure 4-22). Because of equation (13), the clamp load at the opening limit ($F_{Kab}$) becomes negative. As the orientation of the moment inverts, the critical point for opening moves from the inner edge of the flange to the outer edge of the flange. To keep using the opening criterion of equation (13), a case differentiation has to be launched:

$$F_{Kab} = F_A \cdot (a - S_{sym}) \cdot x \qquad \text{für } a \geq S_{sym} \tag{17}$$

$$F_{Kab} = F_A \cdot (S_{sym} - a) \cdot x \qquad \text{für } a < S_{sym} \tag{18}$$

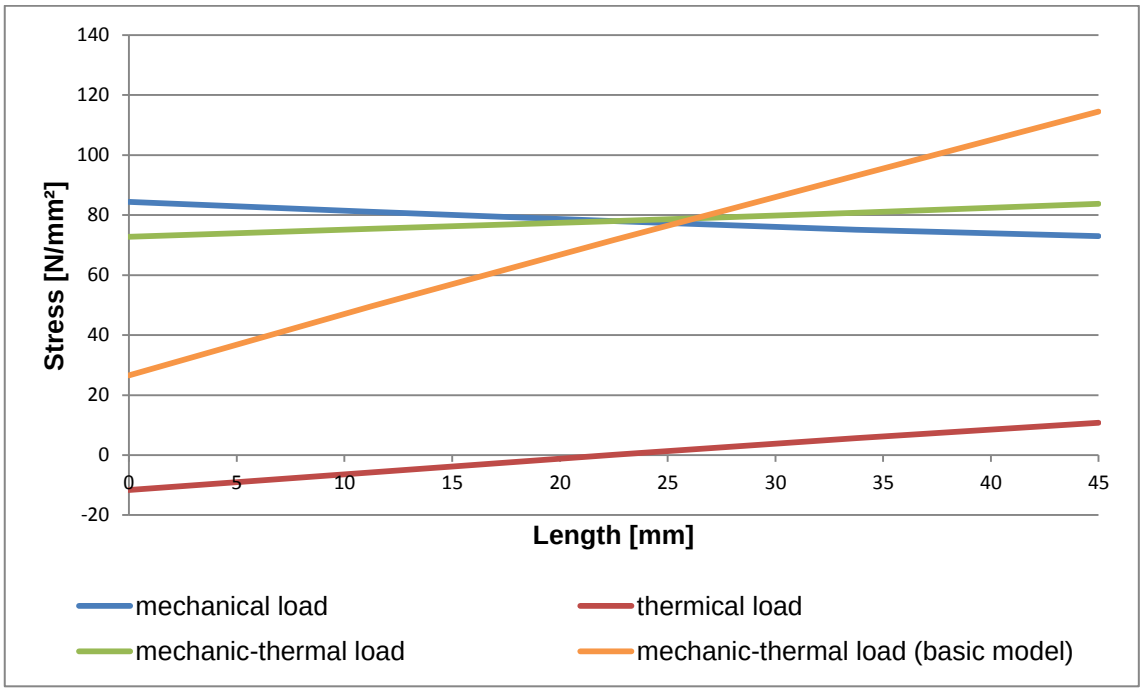


*Figure 4-24: Normal stress (YY) at the thinnest point of model narrow-flange with different loads.*

In figure 4-24 is a constantly distributed normal stress (YY) at the thinnest point of the model narrow-flange for the mechanic-thermal load case shown which has a value of about 80 N/mm². Compared with model 420_20, the stress is more constantly distributed and the averaged level stays the same.

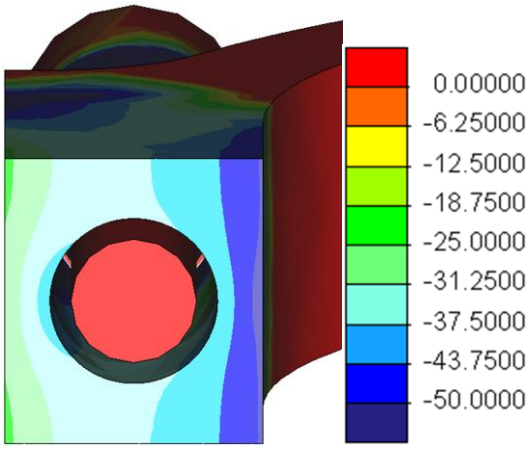


*Figure 4-25: Normal stress (ZZ) across the flange of model narrow-flange.*

Figure 4-25 illustrates that the model narrow-flange compared with model 420_20 has a continuously higher surface pressure. Furthermore, figure 4-26 shows that the sealing criterion (24 N/mm²) of the mechanic-thermal load case is fulfilled all over the flange width. Also the tendential distribution of low compressive stress at the outer edge to higher compressive stress at the inner edge is generally positive because a sealed inner edge prevents a contact between steam and bolt.

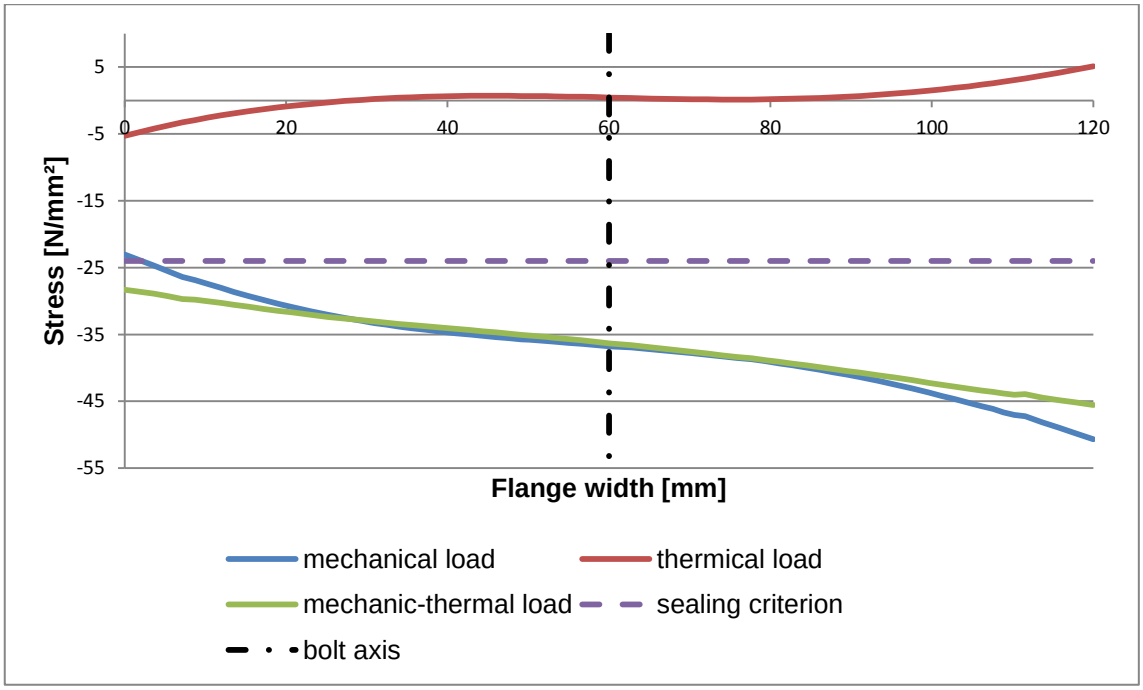


*Figure 4-26: Normal stress (ZZ) across the flange of model narrow-flange with different loads.*

# 5 Outlook

There is still a need for action concerning the improvement of joint leak tightness by varying the casing geometry. The following text shows which steps are needed to complete the present issue. These points are ordered by the expected effort.

For a continuing analysis, the designed one-bolt-model should be expanded to a multi-bolt model with contact conditions between the joint surfaces. Therefore, the simplified quarter model has to be expanded to a half model and afterwards expanded in axial direction. Afterwards, the upper and under casing have to be bolted by 5 - 7 bolts with a predefined bolt spacing. To get the model closer to a real pressure chamber, both openings have to be axial closed. Finally, the model should be equipped with adequate boundary conditions and analysed such as the present case. These results should give some indications about the transferability of one-bolt connections to mulit-bolt connection and about the differences between normal stresses by clamp connections compared with contact pressure connections.

Due to the fact that this thesis primarily deals with the geometry of the casing shell and to a lesser extent with the flange geometry, only one variation of flange dimensions were analysed. The influence of the flange geometry (height, width) concerning the joint leak tightness should be also analysed by a stepwise variation to get an optimal flange geometry.

The behaviour of the new designed casing geometry based on the preposed points should be analysed taking thermical loads with heightened temperature gradients such as it happens during cold starts. These situations are extreme loads for flange and bolt.

The last and most important point is the analysis of the constructive implementation regarding the position of the guide blade carrier inside the turbine. This effect is caused by the change from a circular inner contour to an elliptical inner contour. Furthermore, the axial and radial temperature distribution right before and behind the guide blade carrier should be analysed in reference to the joint leak tightness. These locations have the particularity that they separate chambers with temperature differences up to 200 K.

If these rudiments are followed up, a realisation of a new casing geometry can be achieved.

# 6 Summary

The present bachelor thesis deals with joint leak tightness of steam turbines. The goal is an improvement of joint leak tightness by a stepwise variation of the casing geometry.

First of all a theoretical chapter puts the problem into the overall context and transfers the relevant principles of steam turbines. It starts with the general composition of steam turbines, continues with the flange bolting and ends with the relevant values for the evaluation of joint leak tightness. Next, the thesis describes the procedure of how to construct FE models concerning the analysed casing part (wheel chamber). Concluding this analysis, the results are presented and evaluated.

The results are analysed by basing it on the predefined evaluation criteria (distance between bolt axis and working load axis; normal stress across the joint surface; maximal stress level) concerning joint leak tightness. For the first analysis, a basic model concerning model class I is designed and parameterised. Through stepwise variation of one geometric value, five additional and comparable models are created. The first result of this analysis reveals a model with good values for the distance between bolt axis and working load axis (lever arm) but undue values for the maximal stress level. In consequence of this, a further geometric variation is conducted. This second model compared with the basic model of model class I has an obvious improvement concerning the lever arm and the normal stress across the joint surface. The maximal stress level shows only a slight improvement.

The next step of these analyses is to expand the model from model class I to model class II, bringing with it a higher level of detail. The models of model class II are analysed by the same criteria and the same procedure as before in model class I. Both model classes show the same behaviour so they are basically comparable. However, one substantial difference is that the optimised model of model class II can not fulfil the criterion of the maximal stress level that is caused by an extra bolt force.

To fulfill all the criteria a last geometric variation at the flange (height, width) is conducted. The result of this analysis shows a model of model class II, which has better joint leak tightness and a reduced maximal stress level compared with the basic model.

These analyses illustrate, that a variation of the casing geometry can influences the joint leak tightness of steam turbines significantly. It becomes evident, that the present example has a great potential for an improvement of joint leak tightness. This issue should be pursued with all aspects from the outlook to gain a strong base for subsequent implementation.

# List of References

[1] VGB PowerTech e.V., “Richtlinie für Schrauben im Bereich hoher Temperaturen (VGB-R 505 M),” Essen, 2004.

[2] Verein Deutscher Ingenieure, Systematic calculation of highly stressed bolted joints - Joints with one cylindrical bolt, Draft ed., vol. VDI 2230 page 1, Düsseldorf: Beuth Verlag, 2003.

[3] Verein Deutscher Ingenieure, “Systematic calculation of highly stressed bolted joints - Multi bolted joints,” Draft ed., vol. VDI 2230 page 2, Düsseldorf, Beuth Verlag, 2011.

[4] H. Dubbel, Taschenbuch für den Maschinenbau, vol. 20, W. Beitz and K. H. Grote, Eds., Springer, 2001.

[5] U. Gloy, E. Höxtermann and J. Pasch, Kraftwerksschule e.V Lehrhefte für die Ausbildung zum Kraftwerker (Heft 9 Turbinen), Essen: Verlag technischer-wissenschaftlicher Schriften, 1987.

[6] D. Melcher, Bachelorarbeit - Anwendung und Verifikation des Ersatzmodells nach VDI 2230 Blatt 1 für die analytische Berechnung der Verschraubung der Gehäuseteilfuge von Dampfturbinen, Hamburg, 2013.

[7] W. Traupel, Thermische Turbomaschinen, vol. 2, Berlin: Springer Verlag, 2001, pp. 299-305.

[8] MDT-HBG, internal sources / personal information.

[9] F. Dietzel, Dampfturbinen: Berechnung, Konstruktion, Teillast- und Betriebsverhalten, Kondensation, 3., fully revised ed., München [i.a.]: Hanser Verlag, 1980.

# Appendices

### Appendix A for chapter 4.1

*Table A 1: Stress components of the thinnest point of model 400 of model class I with diffenrent loads*

| Mechanical load case | | | | | | | |
|---|---|---|---|---|---|---|---|
| Length [mm] | Von Mises stress [N/mm²] | Stress components [N/mm²] | | | | | |
| | | XX | XY | XZ | YY | YZ | ZZ |
| 0 | 40.026 | 37.124 | -0.061 | -0.484 | 8.013 | -0.039 | -8.508 |
| 11.25 | 52.619 | 54.287 | 0.099 | 0.997 | 13.569 | 0.07 | -5.088 |
| 22.5 | 66.095 | 71.12 | 0.062 | 0.977 | 18.885 | 0.069 | -3.156 |
| 33.75 | 79.54 | 87.551 | -0.03 | 0.683 | 24.022 | 0.011 | -1.644 |
| 45 | 92.134 | 103.512 | -0.035 | 1.338 | 29.042 | -0.054 | 0.52 |
| **Thermical load case** | | | | | | | |
| Length [mm] | Von Mises stress [N/mm²] | Stress components [N/mm²] | | | | | |
| | | XX | XY | XZ | YY | YZ | ZZ |
| 0 | 7.544 | -7.675 | 0.002 | -0.006 | -0.209 | -0.008 | -0.055 |
| 11.25 | 3.764 | -3.826 | -0.001 | 0.033 | -0.055 | -0.007 | -0.07 |
| 22.5 | 0.176 | -0.16 | -0.003 | 0.029 | 0.026 | -0.006 | -0.119 |
| 33.75 | 3.36 | 3.335 | -0.007 | 0.018 | 0.074 | -0.003 | -0.115 |
| 45 | 6.591 | 6.669 | -0.011 | 0.042 | 0.132 | 0 | 0.026 |
| **Mechanic-thermal load case** | | | | | | | |
| Length [mm] | Von Mises stress [N/mm²] | Stress components [N/mm²] | | | | | |
| | | XX | XY | XZ | YY | YZ | ZZ |
| 0 | 33.037 | 29.449 | -0.059 | -0.49 | 7.804 | -0.048 | -8.563 |
| 11.25 | 49.059 | 50.461 | 0.098 | 1.03 | 13.515 | 0.062 | -5.158 |
| 22.5 | 66.024 | 70.96 | 0.059 | 1.006 | 18.91 | 0.064 | -3.275 |
| 33.75 | 82.812 | 90.886 | -0.036 | 0.701 | 24.096 | 0.008 | -1.759 |
| 45 | 98.521 | 110.181 | -0.046 | 1.379 | 29.174 | -0.054 | 0.546 |

*Table A 2: Stress components of the thinnest part of the model 410 of model class I with different loads*

| Mechanical load case | | | | | | | |
|---|---|---|---|---|---|---|---|
| Length [mm] | Von Mises stress [N/mm²] | Stress components [N/mm²] | | | | | |
| | | XX | XY | XZ | YY | YZ | ZZ |
| 0 | 64.186 | 64.309 | -0.045 | -0.041 | 15.623 | -0.02 | -8.429 |
| 11.25 | 65.627 | 68.644 | -0.034 | 0.451 | 17.625 | 0.001 | -5.384 |
| 22.5 | 67.765 | 72.902 | -0.023 | 0.466 | 19.407 | -0.01 | -3.294 |
| 33.75 | 70.223 | 77.16 | -0.02 | 0.337 | 21.101 | -0.034 | -1.603 |
| 45 | 72.644 | 81.495 | -0.031 | 0.402 | 22.843 | -0.053 | 0.241 |
| **Thermical load case** | | | | | | | |
| Length [mm] | Von Mises stress | Stress components [N/mm²] | | | | | |

| | [N/mm²] | XX | XY | XZ | YY | YZ | ZZ |
|---|---|---|---|---|---|---|---|
| 0 | 7.689 | -7.816 | 0.001 | -0.006 | -0.215 | -0.009 | -0.042 |
| 11.25 | 3.836 | -3.898 | -0.001 | 0.037 | -0.058 | -0.007 | -0.067 |
| 22.5 | 0.182 | -0.165 | -0.004 | 0.031 | 0.027 | -0.005 | -0.119 |
| 33.75 | 3.416 | 3.394 | -0.007 | 0.02 | 0.082 | -0.003 | -0.115 |
| 45 | 6.704 | 6.787 | -0.012 | 0.044 | 0.145 | 0 | 0.024 |
| **Mechanic-thermal load case** | | | | | | | |
| **Length [mm]** | **Von Mises Stress [N/mm²]** | **Stress components [N/mm²]** | | | | | |
| | | **XX** | **XY** | **XZ** | **YY** | **YZ** | **ZZ** |
| 0 | 56.914 | 56.493 | -0.044 | -0.046 | 15.408 | -0.028 | -8.471 |
| 11.25 | 61.987 | 64.745 | -0.035 | 0.488 | 17.567 | -0.006 | -5.451 |
| 22.5 | 67.689 | 72.738 | -0.027 | 0.497 | 19.434 | -0.016 | -3.412 |
| 33.75 | 73.55 | 80.555 | -0.027 | 0.357 | 21.183 | -0.037 | -1.719 |
| 45 | 79.146 | 88.283 | -0.043 | 0.446 | 22.988 | -0.053 | 0.265 |

*Table A 3: Stress components of the thinnest part of the model 420 of model class I with different loads*

| **Mechanical load case** | | | | | | | |
|---|---|---|---|---|---|---|---|
| **Length [mm]** | **Von Mises Stress [N/mm²]** | **Stress components [N/mm²]** | | | | | |
| | | **XX** | **XY** | **XZ** | **YY** | **YZ** | **ZZ** |
| 0 | 88.659 | 92.428 | -0.117 | 0.134 | 23.76 | 0.022 | -7.661 |
| 11.25 | 78.226 | 82.607 | -0.015 | -0.073 | 21.546 | 0.041 | -5.568 |
| 22.5 | 68.509 | 73.754 | -0.058 | 0.031 | 19.721 | 0.064 | -3.301 |
| 33.75 | 59.529 | 65.457 | 0.006 | -0.043 | 17.973 | 0.06 | -1.327 |
| 45 | 51.321 | 57.305 | 0.43 | -0.783 | 15.991 | 0.002 | -0.114 |
| **Thermical load case** | | | | | | | |
| **Length [mm]** | **Von Mises Stress [N/mm²]** | **Stress components [N/mm²]** | | | | | |
| | | **XX** | **XY** | **XZ** | **YY** | **YZ** | **ZZ** |
| 0 | 7.84 | -7.963 | 0.001 | -0.006 | -0.222 | -0.009 | -0.028 |
| 11.25 | 3.912 | -3.974 | -0.002 | 0.041 | -0.063 | -0.007 | -0.064 |
| 22.5 | 0.188 | -0.169 | -0.004 | 0.034 | 0.029 | -0.005 | -0.118 |
| 33.75 | 3.475 | 3.457 | -0.008 | 0.021 | 0.09 | -0.003 | -0.115 |
| 45 | 6.823 | 6.912 | -0.013 | 0.047 | 0.158 | 0 | 0.022 |
| **Mechanic-thermal load case** | | | | | | | |
| **Length [mm]** | **Von Mises stress [N/mm²]** | **Stress components [N/mm²]** | | | | | |
| | | **XX** | **XY** | **XZ** | **YY** | **YZ** | **ZZ** |
| 0 | 81.178 | 84.465 | -0.117 | 0.128 | 23.538 | 0.013 | -7.689 |
| 11.25 | 74.505 | 78.633 | -0.016 | -0.032 | 21.483 | 0.034 | -5.632 |
| 22.5 | 68.428 | 73.585 | -0.062 | 0.065 | 19.75 | 0.059 | -3.419 |
| 33.75 | 62.914 | 68.915 | -0.002 | -0.022 | 18.063 | 0.058 | -1.442 |
| 45 | 57.94 | 64.216 | 0.418 | -0.736 | 16.149 | 0.001 | -0.092 |

*Table A 4: Stress components of the thinnest part of the model 430 of model class I with different loads*

| **Mechanical load case** | | | | | | | |
|---|---|---|---|---|---|---|---|
| **Length [mm]** | **Von Mises stress [N/mm²]** | **Stress components [N/mm²]** | | | | | |
| | | **XX** | **XY** | **XZ** | **YY** | **YZ** | **ZZ** |
| 0 | 114.689 | 121.375 | -0.355 | 0.566 | 31.917 | 0.142 | -7.912 |
| 11.25 | 90.275 | 96.246 | 0.027 | -0.425 | 25.4 | 0.197 | -5.393 |
| 22.5 | 68.357 | 74.151 | -0.213 | 0 | 20.05 | 0.352 | -2.668 |
| 33.75 | 48.151 | 52.947 | -0.092 | 0.007 | 14.628 | 0.363 | -1.096 |
| 45 | 29.223 | 30.487 | 1.369 | -2.236 | 7.896 | -0.015 | -2.036 |
| **Thermical load case** | | | | | | | |
| **Length [mm]** | **Von Mises stress [N/mm²]** | **Stress components [N/mm²]** | | | | | |
| | | **XX** | **XY** | **XZ** | **YY** | **YZ** | **ZZ** |
| 0 | 7.998 | -8.116 | 0 | -0.007 | -0.229 | -0.009 | -0.013 |
| 11.25 | 3.99 | -4.053 | -0.002 | 0.044 | -0.068 | -0.007 | -0.061 |
| 22.5 | 0.194 | -0.174 | -0.005 | 0.037 | 0.03 | -0.005 | -0.118 |
| 33.75 | 3.537 | 3.524 | -0.009 | 0.022 | 0.098 | -0.003 | -0.115 |
| 45 | 6.949 | 7.043 | -0.014 | 0.049 | 0.172 | 0 | 0.019 |
| **Mechanic-thermal load case** | | | | | | | |
| **Length [mm]** | **Von Mises stress [N/mm²]** | **Stress components [N/mm²]** | | | | | |
| | | **XX** | **XY** | **XZ** | **YY** | **YZ** | **ZZ** |
| 0 | 107.031 | 113.259 | -0.355 | 0.559 | 31.688 | 0.133 | -7.925 |
| 11.25 | 86.469 | 92.193 | 0.025 | -0.38 | 25.333 | 0.189 | -5.454 |
| 22.5 | 68.269 | 73.977 | -0.218 | 0.037 | 20.08 | 0.347 | -2.786 |
| 33.75 | 51.597 | 56.47 | -0.101 | 0.029 | 14.726 | 0.361 | -1.211 |
| 45 | 35.871 | 37.53 | 1.355 | -2.187 | 8.068 | -0.015 | -2.017 |

*Table A 5: Stress components of the thinnest part of the model 440 of model class I with different loads*

| **Mechanical load case** | | | | | | | |
|---|---|---|---|---|---|---|---|
| **Length [mm]** | **Von Mises stress [N/mm²]** | **Stress components [N/mm²]** | | | | | |
| | | **XX** | **XY** | **XZ** | **YY** | **YZ** | **ZZ** |
| 0 | 139.309 | 148.833 | 0.168 | 0.252 | 39.352 | -0.337 | -7.971 |
| 11.25 | 102.648 | 110.411 | 0.098 | -0.367 | 29.377 | -0.357 | -5.012 |
| 22.5 | 68.525 | 75.132 | -0.064 | -0.266 | 20.466 | -0.466 | -1.734 |
| 33.75 | 37.459 | 41.932 | -0.196 | -0.361 | 11.742 | -0.481 | 0.034 |
| 45 | 10.308 | 9.75 | -0.175 | -1.566 | 2.332 | -0.22 | -1.534 |
| **Thermical load case** | | | | | | | |
| **Length [mm]** | **Von Mises stress [N/mm²]** | **Stress components [N/mm²]** | | | | | |
| | | **XX** | **XY** | **XZ** | **YY** | **YZ** | **ZZ** |
| 0 | 8.162 | -8.276 | 0 | -0.009 | -0.236 | -0.009 | 0.003 |
| 11.25 | 4.072 | -4.136 | -0.002 | 0.048 | -0.073 | -0.007 | -0.057 |
| 22.5 | 0.2 | -0.179 | -0.006 | 0.04 | 0.031 | -0.005 | -0.118 |
| 33.75 | 3.603 | 3.594 | -0.01 | 0.023 | 0.107 | -0.002 | -0.115 |
| 45 | 7.081 | 7.181 | -0.015 | 0.052 | 0.187 | -0.001 | 0.017 |
| **Mechanic-thermal load case** | | | | | | | |

| Length [mm] | Von Mises stress [N/mm²] | Stress components [N/mm²] | | | | | |
|---|---|---|---|---|---|---|---|
| | | XX | XY | XZ | YY | YZ | ZZ |
| 0 | 131.468 | 140.557 | 0.168 | 0.243 | 39.116 | -0.346 | -7.967 |
| 11.25 | 98.755 | 106.275 | 0.096 | -0.319 | 29.305 | -0.364 | -5.069 |
| 22.5 | 68.431 | 74.953 | -0.069 | -0.226 | 20.497 | -0.471 | -1.852 |
| 33.75 | 40.98 | 45.526 | -0.206 | -0.337 | 11.849 | -0.484 | -0.08 |
| 45 | 17.009 | 16.931 | -0.19 | -1.514 | 2.518 | -0.22 | -1.517 |

*Table A 6: Stress components of the thinnest part of the model 450 of model class I with different loads*

| Mechanical load case | | | | | | | |
|---|---|---|---|---|---|---|---|
| Length [mm] | Von Mises stress [N/mm²] | Stress components [N/mm²] | | | | | |
| | | XX | XY | XZ | YY | YZ | ZZ |
| 0 | 166.357 | 179.021 | 0.204 | 0.442 | 47.717 | -0.653 | -8.049 |
| 11.25 | 115.314 | 124.967 | 0.12 | -0.662 | 33.509 | -0.552 | -4.557 |
| 22.5 | 68.289 | 75.777 | -0.112 | -0.529 | 20.901 | -0.689 | -0.677 |
| 33.75 | 25.466 | 29.334 | -0.338 | -0.638 | 8.489 | -0.713 | 1.037 |
| 45 | 13.912 | -16.476 | -0.405 | -2.468 | -5.129 | -0.276 | -1.971 |
| **Thermical load case** | | | | | | | |
| Length [mm] | Von Mises stress [N/mm²] | Stress components [N/mm²] | | | | | |
| | | XX | XY | XZ | YY | YZ | ZZ |
| 0 | 8.333 | -8.439 | -0.001 | -0.009 | -0.24 | -0.01 | 0.021 |
| 11.25 | 4.155 | -4.22 | -0.003 | 0.052 | -0.079 | -0.007 | -0.054 |
| 22.5 | 0.206 | -0.184 | -0.006 | 0.044 | 0.031 | -0.004 | -0.118 |
| 33.75 | 3.671 | 3.665 | -0.01 | 0.025 | 0.115 | -0.002 | -0.114 |
| 45 | 7.22 | 7.324 | -0.017 | 0.056 | 0.198 | -0.001 | 0.014 |
| **Mechanic-thermal load case** | | | | | | | |
| Length [mm] | Von Mises stress [N/mm²] | Stress components [N/mm²] | | | | | |
| | | XX | XY | XZ | YY | YZ | ZZ |
| 0 | 158.337 | 170.582 | 0.203 | 0.432 | 47.477 | -0.663 | -8.028 |
| 11.25 | 111.333 | 120.747 | 0.117 | -0.609 | 33.431 | -0.559 | -4.611 |
| 22.5 | 68.188 | 75.593 | -0.118 | -0.485 | 20.932 | -0.693 | -0.795 |
| 33.75 | 29.062 | 32.999 | -0.348 | -0.613 | 8.603 | -0.715 | 0.922 |
| 45 | 7.578 | -9.152 | -0.421 | -2.412 | -4.931 | -0.277 | -1.957 |

*Table A 7: Normal stress (ZZ) across the flange of model 400 of model class I with different loads*

| Length [mm] | Normal stress (ZZ) [N/mm²] | | |
|---|---|---|---|
| | Mechanical | Thermical | Mechanic-thermal |
| 0 | -16.323 | 0.035 | -16.288 |
| 1.39 | -15.847 | 0.038 | -15.809 |
| 2.78 | -15.352 | 0.041 | -15.311 |
| 4.17 | -14.866 | 0.044 | -14.822 |
| 5.56 | -14.413 | 0.047 | -14.367 |
| 7.01 | -13.887 | 0.05 | -13.837 |

| | | | |
|---|---|---|---|
| 8.46 | -13.386 | 0.053 | -13.333 |
| 9.91 | -12.892 | 0.056 | -12.836 |
| 11.359 | -12.387 | 0.059 | -12.328 |
| 14.151 | -11.471 | 0.064 | -11.407 |
| 16.943 | -10.558 | 0.07 | -10.488 |
| 19.734 | -9.657 | 0.076 | -9.581 |
| 22.526 | -8.778 | 0.082 | -8.696 |
| 24.638 | -8.116 | 0.086 | -8.03 |
| 26.75 | -7.463 | 0.09 | -7.373 |
| 28.863 | -6.818 | 0.095 | -6.723 |
| 30.975 | -6.176 | 0.099 | -6.077 |
| 33.089 | -5.529 | 0.103 | -5.425 |
| 35.203 | -4.892 | 0.108 | -4.784 |
| 37.317 | -4.26 | 0.112 | -4.148 |
| 39.431 | -3.628 | 0.117 | -3.512 |
| 41.66 | -2.988 | 0.121 | -2.867 |
| 43.889 | -2.335 | 0.126 | -2.21 |
| 46.118 | -1.683 | 0.13 | -1.553 |
| 48.347 | -1.043 | 0.133 | -0.91 |
| 51.576 | -0.116 | 0.13 | 0.014 |
| 54.806 | 0.807 | 0.128 | 0.935 |
| 58.035 | 1.727 | 0.126 | 1.853 |
| 61.264 | 2.645 | 0.124 | 2.769 |
| 63.224 | 3.23 | 0.123 | 3.352 |
| 65.184 | 3.805 | 0.121 | 3.926 |
| 67.144 | 4.376 | 0.12 | 4.496 |
| 69.104 | 4.946 | 0.119 | 5.065 |
| 71.708 | 5.745 | 0.117 | 5.862 |
| 74.311 | 6.56 | 0.115 | 6.675 |
| 76.915 | 7.383 | 0.113 | 7.497 |
| 79.519 | 8.204 | 0.111 | 8.316 |
| 81.791 | 8.966 | 0.11 | 9.076 |
| 84.062 | 9.731 | 0.108 | 9.84 |
| 86.334 | 10.509 | 0.107 | 10.616 |
| 88.606 | 11.308 | 0.105 | 11.413 |
| 90.75 | 12.075 | 0.104 | 12.179 |
| 92.894 | 12.848 | 0.102 | 12.951 |
| 95.038 | 13.636 | 0.101 | 13.737 |
| 97.182 | 14.448 | 0.094 | 14.542 |
| 99.185 | 15.184 | 0.088 | 15.272 |
| 101.189 | 15.942 | 0.082 | 16.024 |
| 103.193 | 16.721 | 0.075 | 16.797 |
| 105.197 | 17.521 | 0.069 | 17.59 |
| 106.908 | 18.203 | 0.064 | 18.267 |
| 108.62 | 18.894 | 0.058 | 18.952 |
| 110.331 | 19.598 | 0.053 | 19.65 |
| 112.043 | 20.319 | 0.047 | 20.367 |
| 113.806 | 21.035 | 0.042 | 21.077 |
| 115.569 | 21.777 | 0.036 | 21.814 |
| 117.333 | 22.537 | 0.031 | 22.568 |

| | | | |
|---|---|---|---|
| 119.096 | 23.305 | 0.025 | 23.331 |
| 120.366 | 23.861 | 0.021 | 23.882 |
| 121.636 | 24.422 | 0.017 | 24.44 |
| 122.907 | 24.989 | 0.013 | 25.003 |
| 124.177 | 25.561 | 0.009 | 25.57 |
| 125.554 | 26.184 | 0.005 | 26.189 |
| 126.931 | 26.814 | 0.001 | 26.815 |
| 128.308 | 27.45 | -0.004 | 27.446 |
| 129.685 | 28.09 | -0.008 | 28.082 |
| 131.821 | 29.089 | -0.015 | 29.074 |
| 133.956 | 30.103 | -0.021 | 30.082 |
| 136.092 | 31.129 | -0.028 | 31.101 |
| 138.228 | 32.165 | -0.035 | 32.131 |
| 140.83 | 33.451 | -0.043 | 33.409 |
| 143.433 | 34.752 | -0.068 | 34.684 |
| 146.036 | 36.071 | -0.123 | 35.948 |
| 148.639 | 37.412 | -0.178 | 37.234 |
| 151.135 | 38.676 | -0.231 | 38.445 |
| 153.631 | 39.961 | -0.284 | 39.677 |
| 156.127 | 41.289 | -0.337 | 40.952 |
| 158.623 | 42.687 | -0.39 | 42.297 |
| 160.71 | 43.763 | -0.434 | 43.329 |
| 162.797 | 44.797 | -0.478 | 44.319 |
| 164.884 | 45.876 | -0.522 | 45.354 |
| 166.97 | 47.087 | -0.566 | 46.52 |
| 169.378 | 48.133 | -0.617 | 47.515 |
| 171.786 | 49.249 | -0.669 | 48.581 |
| 174.194 | 50.46 | -0.72 | 49.74 |
| 176.602 | 51.787 | -0.771 | 51.016 |
| 177.975 | 52.525 | -0.8 | 51.725 |
| 179.347 | 53.329 | -0.829 | 52.5 |
| 180.72 | 54.251 | -0.858 | 53.393 |
| 182.092 | 55.342 | -0.887 | 54.456 |
| 184.069 | 56.288 | -0.929 | 55.359 |
| 186.046 | 57.345 | -0.971 | 56.375 |
| 188.023 | 58.776 | -1.012 | 57.763 |
| 190 | 60.841 | -1.054 | 59.786 |

*Table A 8: Normal stress (ZZ) across the flange of model 410 of model class I with different loads*

| **Length [mm]** | **Normal stress (ZZ) [N/mm²]** | | |
|---|---|---|---|
| | **Mechanical** | **Thermical** | **Mechanic-thermal** |
| 0 | -12.32 | -0.074 | -12.395 |
| 1.561 | -11.84 | -0.065 | -11.906 |
| 3.123 | -11.371 | -0.056 | -11.428 |
| 4.684 | -10.907 | -0.047 | -10.954 |
| 6.245 | -10.44 | -0.039 | -10.479 |
| 8.097 | -9.905 | -0.028 | -9.933 |

| | | | |
|---|---|---|---|
| 9.948 | -9.369 | -0.018 | -9.386 |
| 11.8 | -8.835 | -0.007 | -8.842 |
| 13.651 | -8.307 | 0.004 | -8.304 |
| 16.152 | -7.608 | 0.018 | -7.59 |
| 18.653 | -6.909 | 0.032 | -6.877 |
| 21.154 | -6.215 | 0.046 | -6.169 |
| 23.655 | -5.533 | 0.06 | -5.473 |
| 25.817 | -4.948 | 0.073 | -4.876 |
| 27.979 | -4.364 | 0.085 | -4.279 |
| 30.141 | -3.782 | 0.097 | -3.685 |
| 32.303 | -3.201 | 0.11 | -3.091 |
| 34.142 | -2.705 | 0.12 | -2.585 |
| 35.981 | -2.214 | 0.131 | -2.084 |
| 37.821 | -1.725 | 0.141 | -1.584 |
| 39.66 | -1.236 | 0.151 | -1.085 |
| 41.683 | -0.707 | 0.163 | -0.544 |
| 43.706 | -0.176 | 0.174 | -0.001 |
| 45.729 | 0.354 | 0.195 | 0.55 |
| 47.752 | 0.881 | 0.196 | 1.077 |
| 49.499 | 1.342 | 0.197 | 1.539 |
| 51.245 | 1.801 | 0.198 | 1.999 |
| 52.992 | 2.261 | 0.199 | 2.459 |
| 54.739 | 2.726 | 0.199 | 2.925 |
| 56.409 | 3.161 | 0.2 | 3.361 |
| 58.079 | 3.603 | 0.201 | 3.804 |
| 59.749 | 4.044 | 0.202 | 4.246 |
| 61.419 | 4.477 | 0.202 | 4.679 |
| 63.238 | 4.962 | 0.203 | 5.165 |
| 65.057 | 5.449 | 0.204 | 5.653 |
| 66.876 | 5.935 | 0.205 | 6.14 |
| 68.695 | 6.416 | 0.206 | 6.622 |
| 70.325 | 6.872 | 0.207 | 7.079 |
| 71.955 | 7.321 | 0.207 | 7.528 |
| 73.585 | 7.771 | 0.208 | 7.98 |
| 75.215 | 8.231 | 0.209 | 8.44 |
| 78.102 | 9.047 | 0.21 | 9.257 |
| 80.989 | 9.882 | 0.212 | 10.094 |
| 83.875 | 10.736 | 0.213 | 10.949 |
| 86.762 | 11.607 | 0.214 | 11.821 |
| 88.756 | 12.221 | 0.215 | 12.436 |
| 90.75 | 12.843 | 0.216 | 13.059 |
| 92.744 | 13.476 | 0.217 | 13.694 |
| 94.737 | 14.123 | 0.218 | 14.342 |
| 97.732 | 15.11 | 0.206 | 15.317 |
| 100.727 | 16.114 | 0.194 | 16.308 |
| 103.722 | 17.142 | 0.181 | 17.323 |
| 106.717 | 18.197 | 0.168 | 18.365 |
| 108.429 | 18.786 | 0.161 | 18.947 |
| 110.14 | 19.398 | 0.153 | 19.551 |
| 111.852 | 20.017 | 0.146 | 20.163 |

| | | | |
|---|---|---|---|
| 113.564 | 20.629 | 0.139 | 20.768 |
| 115.986 | 21.526 | 0.128 | 21.654 |
| 118.408 | 22.434 | 0.118 | 22.552 |
| 120.829 | 23.352 | 0.108 | 23.46 |
| 123.251 | 24.282 | 0.097 | 24.379 |
| 125.39 | 25.119 | 0.088 | 25.208 |
| 127.529 | 25.96 | 0.079 | 26.04 |
| 129.668 | 26.811 | 0.07 | 26.881 |
| 131.807 | 27.676 | 0.061 | 27.737 |
| 133.474 | 28.35 | 0.054 | 28.404 |
| 135.14 | 29.034 | 0.047 | 29.081 |
| 136.807 | 29.723 | 0.039 | 29.763 |
| 138.474 | 30.412 | 0.032 | 30.444 |
| 140.103 | 31.1 | 0.025 | 31.125 |
| 141.733 | 31.786 | 0.018 | 31.805 |
| 143.362 | 32.508 | -0.006 | 32.502 |
| 144.992 | 33.3 | -0.046 | 33.255 |
| 147.383 | 34.281 | -0.104 | 34.177 |
| 149.775 | 35.311 | -0.163 | 35.148 |
| 152.167 | 36.416 | -0.221 | 36.195 |
| 154.559 | 37.623 | -0.279 | 37.344 |
| 156.489 | 38.361 | -0.326 | 38.035 |
| 158.418 | 39.203 | -0.374 | 38.83 |
| 160.348 | 40.088 | -0.421 | 39.668 |
| 162.278 | 40.956 | -0.468 | 40.489 |
| 163.526 | 41.539 | -0.498 | 41.041 |
| 164.774 | 42.119 | -0.529 | 41.59 |
| 166.023 | 42.711 | -0.559 | 42.151 |
| 167.271 | 43.329 | -0.59 | 42.739 |
| 170.164 | 44.629 | -0.66 | 43.968 |
| 173.056 | 45.982 | -0.731 | 45.252 |
| 175.949 | 47.398 | -0.801 | 46.597 |
| 178.841 | 48.884 | -0.872 | 48.012 |
| 181.631 | 50.117 | -0.94 | 49.177 |
| 184.421 | 51.409 | -1.008 | 50.401 |
| 187.21 | 52.843 | -1.076 | 51.766 |
| 190 | 54.501 | -1.144 | 53.356 |

*Table A 9: Normal stress (ZZ) across the flange of model 420 of model class I with different loads*

| **Length [mm]** | **Normal stress (ZZ) [N/mm²]** | | |
|---|---|---|---|
| | **Mechanical** | **Thermical** | **Mechanic-thermal** |
| 0 | -7.772 | -0.17 | -7.941 |
| 2.369 | -7.238 | -0.149 | -7.386 |
| 4.737 | -6.713 | -0.127 | -6.84 |
| 7.106 | -6.193 | -0.106 | -6.299 |
| 9.474 | -5.675 | -0.085 | -5.76 |
| 11.646 | -5.205 | -0.066 | -5.271 |

| | | | |
|---|---|---|---|
| 13.817 | -4.732 | -0.047 | -4.779 |
| 15.989 | -4.255 | -0.027 | -4.282 |
| 18.16 | -3.772 | -0.008 | -3.78 |
| 20.051 | -3.376 | 0.009 | -3.367 |
| 21.942 | -2.968 | 0.026 | -2.942 |
| 23.833 | -2.552 | 0.043 | -2.51 |
| 25.724 | -2.131 | 0.059 | -2.072 |
| 27.709 | -1.686 | 0.077 | -1.609 |
| 29.695 | -1.235 | 0.095 | -1.14 |
| 31.681 | -0.777 | 0.112 | -0.664 |
| 33.667 | -0.31 | 0.13 | -0.18 |
| 35.56 | 0.132 | 0.147 | 0.278 |
| 37.453 | 0.577 | 0.164 | 0.741 |
| 39.346 | 1.026 | 0.181 | 1.206 |
| 41.239 | 1.478 | 0.197 | 1.675 |
| 42.764 | 1.841 | 0.211 | 2.052 |
| 44.29 | 2.204 | 0.225 | 2.428 |
| 45.816 | 2.566 | 0.238 | 2.804 |
| 47.342 | 2.929 | 0.252 | 3.181 |
| 49.654 | 3.48 | 0.257 | 3.737 |
| 51.967 | 4.031 | 0.262 | 4.293 |
| 54.28 | 4.569 | 0.266 | 4.834 |
| 56.592 | 5.076 | 0.27 | 5.346 |
| 57.919 | 5.421 | 0.273 | 5.694 |
| 59.245 | 5.739 | 0.275 | 6.014 |
| 60.572 | 6.05 | 0.278 | 6.327 |
| 61.898 | 6.376 | 0.28 | 6.656 |
| 64.212 | 6.927 | 0.285 | 7.212 |
| 66.525 | 7.489 | 0.289 | 7.778 |
| 68.839 | 8.055 | 0.293 | 8.348 |
| 71.152 | 8.621 | 0.298 | 8.918 |
| 73.232 | 9.139 | 0.301 | 9.44 |
| 75.312 | 9.661 | 0.305 | 9.966 |
| 77.392 | 10.188 | 0.309 | 10.497 |
| 79.472 | 10.72 | 0.313 | 11.033 |
| 81.088 | 11.125 | 0.316 | 11.441 |
| 82.705 | 11.545 | 0.319 | 11.864 |
| 84.322 | 11.968 | 0.322 | 12.29 |
| 85.938 | 12.385 | 0.325 | 12.711 |
| 88.242 | 13.001 | 0.33 | 13.331 |
| 90.546 | 13.621 | 0.334 | 13.955 |
| 92.85 | 14.253 | 0.338 | 14.591 |
| 95.154 | 14.906 | 0.341 | 15.247 |
| 97.047 | 15.423 | 0.331 | 15.754 |
| 98.939 | 15.953 | 0.321 | 16.274 |
| 100.832 | 16.488 | 0.311 | 16.799 |
| 102.725 | 17.021 | 0.301 | 17.321 |
| 105.06 | 17.706 | 0.288 | 17.994 |
| 107.395 | 18.403 | 0.276 | 18.679 |
| 109.73 | 19.105 | 0.263 | 19.368 |

| | | | |
|---|---|---|---|
| 112.065 | 19.806 | 0.251 | 20.057 |
| 113.741 | 20.334 | 0.242 | 20.575 |
| 115.416 | 20.859 | 0.233 | 21.092 |
| 117.091 | 21.393 | 0.224 | 21.616 |
| 118.767 | 21.944 | 0.215 | 22.158 |
| 120.732 | 22.583 | 0.204 | 22.788 |
| 122.697 | 23.226 | 0.194 | 23.419 |
| 124.661 | 23.871 | 0.183 | 24.054 |
| 126.626 | 24.52 | 0.173 | 24.692 |
| 128.333 | 25.061 | 0.163 | 25.225 |
| 130.039 | 25.634 | 0.154 | 25.788 |
| 131.745 | 26.218 | 0.145 | 26.363 |
| 133.451 | 26.793 | 0.136 | 26.929 |
| 134.911 | 27.294 | 0.128 | 27.422 |
| 136.371 | 27.802 | 0.12 | 27.922 |
| 137.831 | 28.312 | 0.112 | 28.424 |
| 139.291 | 28.82 | 0.105 | 28.925 |
| 141.2 | 29.512 | 0.094 | 29.606 |
| 143.109 | 30.198 | 0.07 | 30.268 |
| 145.018 | 30.892 | 0.015 | 30.907 |
| 146.927 | 31.61 | -0.039 | 31.571 |
| 148.496 | 32.162 | -0.084 | 32.078 |
| 150.065 | 32.734 | -0.129 | 32.605 |
| 151.634 | 33.322 | -0.174 | 33.148 |
| 153.202 | 33.921 | -0.219 | 33.702 |
| 155.128 | 34.637 | -0.275 | 34.363 |
| 157.053 | 35.365 | -0.33 | 35.035 |
| 158.979 | 36.097 | -0.385 | 35.712 |
| 160.904 | 36.826 | -0.44 | 36.386 |
| 162.699 | 37.521 | -0.492 | 37.029 |
| 164.494 | 38.218 | -0.543 | 37.675 |
| 166.288 | 38.921 | -0.594 | 38.327 |
| 168.083 | 39.635 | -0.646 | 38.989 |
| 169.825 | 40.313 | -0.696 | 39.617 |
| 171.568 | 41 | -0.746 | 40.254 |
| 173.31 | 41.695 | -0.796 | 40.899 |
| 175.052 | 42.395 | -0.846 | 41.55 |
| 176.933 | 43.139 | -0.9 | 42.239 |
| 178.814 | 43.896 | -0.953 | 42.942 |
| 180.695 | 44.655 | -1.007 | 43.648 |
| 182.576 | 45.408 | -1.061 | 44.347 |
| 184.432 | 46.167 | -1.115 | 45.052 |
| 186.288 | 46.923 | -1.168 | 45.755 |
| 188.144 | 47.682 | -1.221 | 46.461 |
| 190 | 48.446 | -1.274 | 47.172 |

*Table A 10: Normal stress (ZZ) across the flange of model 430 of model class I with different loads*

| Length [mm] | Normal stress (ZZ) [N/mm²] | | |
|---|---|---|---|
| | Mechanical | Thermical | Mechanic-thermal |
| 0 | -3.664 | -0.263 | -3.926 |
| 2.867 | -3.182 | -0.228 | -3.41 |
| 5.733 | -2.692 | -0.193 | -2.885 |
| 8.6 | -2.191 | -0.159 | -2.35 |
| 11.467 | -1.676 | -0.124 | -1.8 |
| 13.396 | -1.328 | -0.101 | -1.429 |
| 15.326 | -0.978 | -0.077 | -1.055 |
| 17.255 | -0.617 | -0.054 | -0.671 |
| 19.185 | -0.241 | -0.031 | -0.272 |
| 20.742 | 0.021 | -0.012 | 0.009 |
| 22.299 | 0.308 | 0.007 | 0.315 |
| 23.855 | 0.601 | 0.026 | 0.626 |
| 25.412 | 0.884 | 0.044 | 0.928 |
| 27.191 | 1.225 | 0.066 | 1.291 |
| 28.97 | 1.564 | 0.087 | 1.651 |
| 30.749 | 1.904 | 0.109 | 2.013 |
| 32.529 | 2.251 | 0.13 | 2.381 |
| 35.227 | 2.76 | 0.163 | 2.923 |
| 37.925 | 3.276 | 0.196 | 3.472 |
| 40.624 | 3.797 | 0.228 | 4.025 |
| 43.322 | 4.317 | 0.261 | 4.578 |
| 44.818 | 4.602 | 0.279 | 4.881 |
| 46.313 | 4.899 | 0.297 | 5.196 |
| 47.808 | 5.196 | 0.312 | 5.508 |
| 49.304 | 5.479 | 0.317 | 5.796 |
| 50.949 | 5.818 | 0.322 | 6.14 |
| 52.595 | 6.151 | 0.327 | 6.478 |
| 54.24 | 6.48 | 0.333 | 6.813 |
| 55.885 | 6.808 | 0.338 | 7.146 |
| 58.728 | 7.388 | 0.347 | 7.734 |
| 61.571 | 7.975 | 0.356 | 8.33 |
| 64.415 | 8.564 | 0.364 | 8.929 |
| 67.258 | 9.153 | 0.373 | 9.526 |
| 69.461 | 9.649 | 0.38 | 10.029 |
| 71.665 | 10.125 | 0.387 | 10.512 |
| 73.868 | 10.598 | 0.394 | 10.992 |
| 76.071 | 11.087 | 0.401 | 11.488 |
| 78.656 | 11.654 | 0.409 | 12.064 |
| 81.24 | 12.231 | 0.417 | 12.648 |
| 83.825 | 12.815 | 0.425 | 13.241 |
| 86.41 | 13.407 | 0.434 | 13.841 |
| 89.252 | 14.063 | 0.442 | 14.505 |
| 92.095 | 14.73 | 0.451 | 15.181 |
| 94.937 | 15.406 | 0.46 | 15.867 |
| 97.78 | 16.09 | 0.443 | 16.533 |

| | | | |
|---|---|---|---|
| 99.017 | 16.385 | 0.434 | 16.82 |
| 100.254 | 16.688 | 0.426 | 17.114 |
| 101.491 | 16.99 | 0.418 | 17.409 |
| 102.728 | 17.286 | 0.41 | 17.697 |
| 104.04 | 17.618 | 0.402 | 18.02 |
| 105.352 | 17.952 | 0.393 | 18.346 |
| 106.664 | 18.285 | 0.385 | 18.67 |
| 107.976 | 18.611 | 0.376 | 18.988 |
| 109.973 | 19.124 | 0.363 | 19.487 |
| 111.969 | 19.64 | 0.35 | 19.99 |
| 113.965 | 20.152 | 0.338 | 20.49 |
| 115.961 | 20.655 | 0.325 | 20.979 |
| 118.069 | 21.217 | 0.311 | 21.528 |
| 120.176 | 21.772 | 0.297 | 22.069 |
| 122.283 | 22.328 | 0.284 | 22.611 |
| 124.391 | 22.896 | 0.27 | 23.166 |
| 125.608 | 23.225 | 0.262 | 23.487 |
| 126.825 | 23.56 | 0.254 | 23.814 |
| 128.042 | 23.895 | 0.246 | 24.142 |
| 129.259 | 24.23 | 0.238 | 24.468 |
| 131.157 | 24.747 | 0.226 | 24.973 |
| 133.055 | 25.268 | 0.214 | 25.481 |
| 134.953 | 25.788 | 0.201 | 25.99 |
| 136.851 | 26.304 | 0.189 | 26.493 |
| 139.767 | 27.152 | 0.17 | 27.322 |
| 142.682 | 27.999 | 0.146 | 28.145 |
| 145.598 | 28.84 | 0.051 | 28.892 |
| 148.513 | 29.674 | -0.044 | 29.63 |
| 150.115 | 30.154 | -0.096 | 30.058 |
| 151.716 | 30.627 | -0.148 | 30.479 |
| 153.317 | 31.099 | -0.201 | 30.898 |
| 154.919 | 31.575 | -0.253 | 31.322 |
| 156.529 | 32.056 | -0.305 | 31.75 |
| 158.14 | 32.545 | -0.358 | 32.187 |
| 159.75 | 33.026 | -0.41 | 32.615 |
| 161.361 | 33.482 | -0.463 | 33.018 |
| 163.176 | 34.087 | -0.522 | 33.565 |
| 164.991 | 34.646 | -0.581 | 34.064 |
| 166.807 | 35.204 | -0.641 | 34.563 |
| 168.622 | 35.807 | -0.7 | 35.107 |
| 170.934 | 36.518 | -0.775 | 35.742 |
| 173.247 | 37.243 | -0.851 | 36.392 |
| 175.559 | 37.979 | -0.926 | 37.053 |
| 177.872 | 38.723 | -1.002 | 37.721 |
| 179.364 | 39.187 | -1.05 | 38.136 |
| 180.856 | 39.671 | -1.099 | 38.572 |
| 182.348 | 40.162 | -1.148 | 39.014 |
| 183.84 | 40.645 | -1.197 | 39.449 |
| 185.38 | 41.174 | -1.247 | 39.927 |
| 186.92 | 41.689 | -1.297 | 40.392 |

| | | | |
|---|---|---|---|
| 188.46 | 42.217 | -1.347 | 40.87 |
| 190 | 42.786 | -1.398 | 41.388 |

*Table A 11: Normal stress (ZZ) across the flange of model 440 of model class I with different loads*

| Length [mm] | Normal stress (ZZ) [N/mm²] | | |
|---|---|---|---|
| | Mechanical | Thermical | Mechanic-thermal |
| 0 | 0.49 | -0.353 | 0.137 |
| 2.097 | 0.726 | -0.321 | 0.405 |
| 4.193 | 0.964 | -0.29 | 0.675 |
| 6.29 | 1.21 | -0.258 | 0.952 |
| 8.386 | 1.469 | -0.226 | 1.243 |
| 10.087 | 1.682 | -0.2 | 1.483 |
| 11.789 | 1.901 | -0.174 | 1.728 |
| 13.49 | 2.125 | -0.148 | 1.977 |
| 15.191 | 2.351 | -0.122 | 2.229 |
| 17.012 | 2.597 | -0.094 | 2.503 |
| 18.833 | 2.85 | -0.066 | 2.784 |
| 20.654 | 3.108 | -0.039 | 3.069 |
| 22.475 | 3.369 | -0.011 | 3.358 |
| 24.369 | 3.647 | 0.018 | 3.665 |
| 26.263 | 3.928 | 0.047 | 3.975 |
| 28.156 | 4.211 | 0.076 | 4.287 |
| 30.05 | 4.496 | 0.105 | 4.601 |
| 31.877 | 4.781 | 0.132 | 4.913 |
| 33.703 | 5.067 | 0.16 | 5.227 |
| 35.529 | 5.355 | 0.188 | 5.543 |
| 37.355 | 5.643 | 0.216 | 5.859 |
| 39.412 | 5.995 | 0.247 | 6.242 |
| 41.468 | 6.336 | 0.278 | 6.614 |
| 43.525 | 6.677 | 0.31 | 6.986 |
| 45.581 | 7.027 | 0.341 | 7.368 |
| 47.634 | 7.372 | 0.371 | 7.743 |
| 49.688 | 7.725 | 0.38 | 8.105 |
| 51.741 | 8.083 | 0.389 | 8.472 |
| 53.794 | 8.445 | 0.397 | 8.842 |
| 55.557 | 8.758 | 0.405 | 9.163 |
| 57.32 | 9.069 | 0.412 | 9.481 |
| 59.083 | 9.383 | 0.42 | 9.803 |
| 60.846 | 9.707 | 0.428 | 10.135 |
| 62.309 | 9.97 | 0.434 | 10.404 |
| 63.772 | 10.233 | 0.44 | 10.673 |
| 65.236 | 10.498 | 0.446 | 10.944 |
| 66.699 | 10.765 | 0.453 | 11.218 |
| 68.352 | 11.065 | 0.46 | 11.524 |
| 70.005 | 11.37 | 0.467 | 11.836 |
| 71.658 | 11.672 | 0.474 | 12.146 |
| 73.31 | 11.966 | 0.481 | 12.447 |

| | | | |
|---|---|---|---|
| 75.725 | 12.423 | 0.491 | 12.914 |
| 78.14 | 12.88 | 0.502 | 13.382 |
| 80.556 | 13.341 | 0.512 | 13.853 |
| 82.971 | 13.807 | 0.522 | 14.33 |
| 84.554 | 14.103 | 0.529 | 14.632 |
| 86.138 | 14.409 | 0.536 | 14.945 |
| 87.721 | 14.713 | 0.543 | 15.256 |
| 89.305 | 15.007 | 0.549 | 15.556 |
| 91.19 | 15.38 | 0.557 | 15.937 |
| 93.075 | 15.747 | 0.565 | 16.312 |
| 94.96 | 16.113 | 0.574 | 16.686 |
| 96.845 | 16.484 | 0.56 | 17.043 |
| 98.508 | 16.808 | 0.547 | 17.355 |
| 100.172 | 17.131 | 0.534 | 17.665 |
| 101.836 | 17.454 | 0.521 | 17.976 |
| 103.499 | 17.781 | 0.509 | 18.289 |
| 104.906 | 18.056 | 0.498 | 18.554 |
| 106.313 | 18.333 | 0.487 | 18.82 |
| 107.72 | 18.61 | 0.476 | 19.087 |
| 109.127 | 18.886 | 0.466 | 19.352 |
| 110.605 | 19.178 | 0.454 | 19.632 |
| 112.084 | 19.47 | 0.443 | 19.913 |
| 113.563 | 19.761 | 0.432 | 20.193 |
| 115.041 | 20.049 | 0.421 | 20.47 |
| 116.533 | 20.352 | 0.409 | 20.761 |
| 118.025 | 20.651 | 0.398 | 21.049 |
| 119.516 | 20.95 | 0.386 | 21.336 |
| 121.008 | 21.25 | 0.375 | 21.625 |
| 123.251 | 21.693 | 0.358 | 22.051 |
| 125.495 | 22.142 | 0.341 | 22.483 |
| 127.738 | 22.59 | 0.324 | 22.913 |
| 129.982 | 23.03 | 0.306 | 23.337 |
| 132.559 | 23.555 | 0.287 | 23.841 |
| 135.135 | 24.078 | 0.267 | 24.345 |
| 137.712 | 24.603 | 0.247 | 24.85 |
| 140.289 | 25.131 | 0.228 | 25.358 |
| 141.786 | 25.434 | 0.216 | 25.65 |
| 143.283 | 25.742 | 0.182 | 25.925 |
| 144.78 | 26.053 | 0.128 | 26.181 |
| 146.278 | 26.365 | 0.073 | 26.439 |
| 148.147 | 26.778 | 0.006 | 26.784 |
| 150.016 | 27.192 | -0.062 | 27.129 |
| 151.885 | 27.609 | -0.13 | 27.478 |
| 153.754 | 28.032 | -0.198 | 27.834 |
| 156.464 | 28.668 | -0.297 | 28.372 |
| 159.175 | 29.319 | -0.395 | 28.924 |
| 161.886 | 29.994 | -0.494 | 29.501 |
| 164.596 | 30.706 | -0.592 | 30.114 |
| 167.224 | 31.362 | -0.688 | 30.674 |
| 169.851 | 32.088 | -0.783 | 31.304 |

| | | | |
|---|---|---|---|
| 172.478 | 32.825 | -0.879 | 31.946 |
| 175.106 | 33.516 | -0.974 | 32.542 |
| 177.473 | 34.211 | -1.06 | 33.151 |
| 179.841 | 34.962 | -1.146 | 33.816 |
| 182.209 | 35.594 | -1.232 | 34.362 |
| 184.577 | 35.934 | -1.318 | 34.616 |
| 185.932 | 36.532 | -1.368 | 35.165 |
| 187.288 | 37.034 | -1.417 | 35.617 |
| 188.644 | 37.457 | -1.466 | 35.991 |
| 190 | 37.815 | -1.515 | 36.3 |

*Table A 12: Normal stress (ZZ) across the flange of model 450 of model class I with different loads*

| **Length [mm]** | **Normal stress (ZZ) [N/mm²]** | | |
|---|---|---|---|
| | **Mechanical** | **Thermical** | **Mechanic-thermal** |
| 0 | 5.046 | -0.495 | 4.551 |
| 1.821 | 5.185 | -0.46 | 4.724 |
| 3.642 | 5.289 | -0.425 | 4.863 |
| 5.463 | 5.392 | -0.391 | 5.001 |
| 7.284 | 5.528 | -0.356 | 5.173 |
| 8.903 | 5.646 | -0.325 | 5.322 |
| 10.523 | 5.764 | -0.294 | 5.47 |
| 12.142 | 5.885 | -0.263 | 5.622 |
| 13.761 | 6.014 | -0.232 | 5.781 |
| 15.878 | 6.174 | -0.192 | 5.982 |
| 17.995 | 6.361 | -0.151 | 6.209 |
| 20.112 | 6.558 | -0.111 | 6.447 |
| 22.228 | 6.751 | -0.07 | 6.681 |
| 24.307 | 6.971 | -0.031 | 6.94 |
| 26.386 | 7.194 | 0.009 | 7.203 |
| 28.465 | 7.423 | 0.049 | 7.471 |
| 30.544 | 7.659 | 0.088 | 7.747 |
| 33.339 | 7.991 | 0.142 | 8.132 |
| 36.133 | 8.331 | 0.195 | 8.526 |
| 38.927 | 8.681 | 0.248 | 8.929 |
| 41.721 | 9.042 | 0.302 | 9.344 |
| 43.102 | 9.228 | 0.328 | 9.556 |
| 44.484 | 9.412 | 0.355 | 9.767 |
| 45.865 | 9.598 | 0.381 | 9.979 |
| 47.246 | 9.788 | 0.407 | 10.195 |
| 48.398 | 9.945 | 0.416 | 10.361 |
| 49.55 | 10.104 | 0.42 | 10.525 |
| 50.702 | 10.265 | 0.425 | 10.69 |
| 51.854 | 10.425 | 0.429 | 10.855 |
| 53.842 | 10.707 | 0.437 | 11.145 |
| 55.831 | 10.99 | 0.445 | 11.436 |
| 57.819 | 11.277 | 0.453 | 11.729 |
| 59.807 | 11.568 | 0.461 | 12.029 |

| | | | |
|---|---|---|---|
| 61.717 | 11.846 | 0.468 | 12.314 |
| 63.626 | 12.124 | 0.476 | 12.6 |
| 65.536 | 12.405 | 0.483 | 12.889 |
| 67.445 | 12.689 | 0.491 | 13.18 |
| 69.928 | 13.052 | 0.501 | 13.553 |
| 72.411 | 13.42 | 0.511 | 13.931 |
| 74.894 | 13.79 | 0.52 | 14.311 |
| 77.376 | 14.158 | 0.53 | 14.688 |
| 79.936 | 14.532 | 0.54 | 15.072 |
| 82.496 | 14.914 | 0.551 | 15.464 |
| 85.056 | 15.296 | 0.561 | 15.857 |
| 87.616 | 15.672 | 0.571 | 16.242 |
| 88.984 | 15.885 | 0.576 | 16.461 |
| 90.353 | 16.086 | 0.582 | 16.668 |
| 91.722 | 16.288 | 0.587 | 16.875 |
| 93.091 | 16.501 | 0.592 | 17.093 |
| 94.51 | 16.7 | 0.598 | 17.298 |
| 95.929 | 16.904 | 0.588 | 17.492 |
| 97.347 | 17.108 | 0.57 | 17.678 |
| 98.766 | 17.306 | 0.553 | 17.858 |
| 100.469 | 17.555 | 0.531 | 18.087 |
| 102.171 | 17.8 | 0.51 | 18.31 |
| 103.874 | 18.045 | 0.489 | 18.534 |
| 105.577 | 18.297 | 0.467 | 18.764 |
| 106.909 | 18.476 | 0.451 | 18.927 |
| 108.242 | 18.663 | 0.434 | 19.097 |
| 109.574 | 18.851 | 0.417 | 19.269 |
| 110.907 | 19.036 | 0.401 | 19.437 |
| 113.372 | 19.377 | 0.37 | 19.747 |
| 115.836 | 19.717 | 0.339 | 20.056 |
| 118.301 | 20.06 | 0.308 | 20.367 |
| 120.765 | 20.406 | 0.277 | 20.683 |
| 123.157 | 20.723 | 0.247 | 20.97 |
| 125.549 | 21.046 | 0.217 | 21.263 |
| 127.941 | 21.368 | 0.187 | 21.555 |
| 130.333 | 21.685 | 0.157 | 21.843 |
| 132.657 | 21.993 | 0.128 | 22.121 |
| 134.981 | 22.302 | 0.099 | 22.401 |
| 137.304 | 22.612 | 0.07 | 22.682 |
| 139.628 | 22.921 | 0.041 | 22.962 |
| 141.833 | 23.218 | 0.013 | 23.231 |
| 144.039 | 23.515 | -0.066 | 23.449 |
| 146.244 | 23.816 | -0.168 | 23.648 |
| 148.45 | 24.125 | -0.27 | 23.855 |
| 150.618 | 24.421 | -0.37 | 24.051 |
| 152.786 | 24.725 | -0.47 | 24.255 |
| 154.954 | 25.034 | -0.57 | 24.464 |
| 157.123 | 25.348 | -0.67 | 24.678 |
| 158.517 | 25.549 | -0.734 | 24.815 |
| 159.912 | 25.757 | -0.799 | 24.958 |

| | | | |
|---|---|---|---|
| 161.306 | 25.958 | -0.863 | 25.095 |
| 162.701 | 26.138 | -0.928 | 25.21 |
| 164.614 | 26.486 | -1.016 | 25.471 |
| 166.527 | 26.791 | -1.104 | 25.687 |
| 168.44 | 27.1 | -1.192 | 25.908 |
| 170.353 | 27.464 | -1.281 | 26.183 |
| 172.065 | 27.697 | -1.36 | 26.338 |
| 173.777 | 27.99 | -1.439 | 26.552 |
| 175.489 | 28.285 | -1.518 | 26.767 |
| 177.201 | 28.522 | -1.597 | 26.926 |
| 178.783 | 28.907 | -1.67 | 27.237 |
| 180.366 | 29.223 | -1.743 | 27.48 |
| 181.948 | 29.53 | -1.816 | 27.714 |
| 183.53 | 29.884 | -1.889 | 27.996 |
| 185.148 | 30.237 | -1.963 | 28.273 |
| 186.765 | 30.582 | -2.038 | 28.544 |
| 188.383 | 30.942 | -2.113 | 28.829 |
| 190 | 31.338 | -2.187 | 29.151 |

*Table A 13: Normal stress (YY) of the thinnest point of the model 420_20 of model class I*

| **Length [mm]** | **Normal stress (YY) [N/mm²]** | | |
|---|---|---|---|
| | **Mechanical** | **Thermical** | **Mechanic-thermal** |
| 0 | 85.511 | -7.005 | 78.506 |
| 11.25 | 81.589 | -3.409 | 78.18 |
| 22.5 | 77.859 | -0.028 | 77.831 |
| 33.75 | 74.439 | 3.185 | 77.624 |
| 45 | 71.444 | 6.279 | 77.723 |

*Table A 14: Normal stress (ZZ) across the flange of model 420_20 of model class I*

| **Length [mm]** | **Normal stress (ZZ) [N/mm²]** | | |
|---|---|---|---|
| | **Mechanical** | **Thermical** | **Mechanic-thermal** |
| 0 | 2.258 | 0.243 | 2.5 |
| 1.092 | 2.36 | 0.242 | 2.602 |
| 2.184 | 2.459 | 0.241 | 2.701 |
| 3.275 | 2.561 | 0.242 | 2.803 |
| 4.367 | 2.668 | 0.247 | 2.915 |
| 7.623 | 3.007 | 0.242 | 3.249 |
| 10.878 | 3.36 | 0.242 | 3.602 |
| 14.133 | 3.733 | 0.244 | 3.977 |
| 17.389 | 4.13 | 0.247 | 4.377 |
| 19.036 | 4.335 | 0.249 | 4.584 |
| 20.684 | 4.545 | 0.251 | 4.796 |
| 22.331 | 4.761 | 0.253 | 5.014 |
| 23.978 | 4.981 | 0.256 | 5.237 |
| 25.486 | 5.185 | 0.258 | 5.443 |
| 26.993 | 5.393 | 0.261 | 5.654 |

| | | | |
|---|---|---|---|
| 28.501 | 5.606 | 0.262 | 5.868 |
| 30.008 | 5.822 | 0.264 | 6.086 |
| 31.698 | 6.065 | 0.266 | 6.331 |
| 33.387 | 6.314 | 0.268 | 6.581 |
| 35.076 | 6.567 | 0.27 | 6.837 |
| 36.765 | 6.824 | 0.272 | 7.095 |
| 38.534 | 7.096 | 0.274 | 7.37 |
| 40.302 | 7.373 | 0.276 | 7.649 |
| 42.07 | 7.654 | 0.278 | 7.931 |
| 43.839 | 7.939 | 0.28 | 8.218 |
| 45.361 | 8.185 | 0.282 | 8.467 |
| 46.882 | 8.435 | 0.283 | 8.718 |
| 48.404 | 8.686 | 0.285 | 8.971 |
| 49.926 | 8.938 | 0.287 | 9.225 |
| 52.011 | 9.29 | 0.289 | 9.579 |
| 54.097 | 9.647 | 0.291 | 9.939 |
| 56.182 | 10.008 | 0.291 | 10.299 |
| 58.268 | 10.37 | 0.291 | 10.661 |
| 59.636 | 10.613 | 0.291 | 10.904 |
| 61.005 | 10.855 | 0.291 | 11.146 |
| 62.373 | 11.098 | 0.291 | 11.389 |
| 63.741 | 11.343 | 0.29 | 11.634 |
| 66.488 | 11.844 | 0.29 | 12.134 |
| 69.236 | 12.348 | 0.288 | 12.636 |
| 71.983 | 12.854 | 0.287 | 13.141 |
| 74.73 | 13.365 | 0.285 | 13.65 |
| 77.438 | 13.875 | 0.283 | 14.158 |
| 80.146 | 14.385 | 0.281 | 14.665 |
| 82.853 | 14.897 | 0.276 | 15.173 |
| 85.561 | 15.416 | 0.269 | 15.685 |
| 86.831 | 15.657 | 0.266 | 15.923 |
| 88.101 | 15.898 | 0.263 | 16.162 |
| 89.371 | 16.141 | 0.26 | 16.401 |
| 90.642 | 16.385 | 0.257 | 16.642 |
| 92.125 | 16.66 | 0.253 | 16.913 |
| 93.609 | 16.942 | 0.248 | 17.19 |
| 95.093 | 17.223 | 0.244 | 17.467 |
| 96.576 | 17.496 | 0.239 | 17.735 |
| 98.367 | 17.838 | 0.233 | 18.072 |
| 100.157 | 18.177 | 0.227 | 18.405 |
| 101.947 | 18.515 | 0.221 | 18.736 |
| 103.738 | 18.852 | 0.215 | 19.066 |
| 105.3 | 19.146 | 0.209 | 19.354 |
| 106.861 | 19.435 | 0.203 | 19.637 |
| 108.423 | 19.722 | 0.196 | 19.918 |
| 109.985 | 20.01 | 0.189 | 20.199 |
| 112.023 | 20.388 | 0.178 | 20.566 |
| 114.061 | 20.761 | 0.167 | 20.928 |
| 116.099 | 21.125 | 0.155 | 21.281 |
| 118.137 | 21.478 | 0.144 | 21.622 |

| | | | |
|---|---|---|---|
| 119.478 | 21.722 | 0.136 | 21.858 |
| 120.819 | 21.96 | 0.128 | 22.088 |
| 122.16 | 22.19 | 0.12 | 22.31 |
| 123.501 | 22.413 | 0.11 | 22.524 |
| 125.226 | 22.694 | 0.102 | 22.796 |
| 126.951 | 22.975 | 0.092 | 23.067 |
| 128.675 | 23.24 | 0.083 | 23.323 |
| 130.4 | 23.475 | 0.075 | 23.549 |
| 131.593 | 23.714 | 0.067 | 23.781 |
| 132.786 | 23.918 | 0.06 | 23.978 |
| 133.979 | 24.09 | 0.053 | 24.144 |
| 135.172 | 24.231 | 0.047 | 24.278 |
| 136.922 | 24.539 | 0.034 | 24.573 |
| 138.671 | 24.823 | 0.021 | 24.844 |
| 140.42 | 25.097 | 0.009 | 25.106 |
| 142.17 | 25.378 | -0.004 | 25.374 |
| 144.504 | 25.767 | -0.023 | 25.744 |
| 146.839 | 26.112 | -0.04 | 26.072 |
| 149.174 | 26.429 | -0.056 | 26.373 |
| 151.508 | 26.731 | -0.073 | 26.658 |
| 154.28 | 27.051 | -0.092 | 26.96 |
| 157.052 | 27.366 | -0.11 | 27.256 |
| 159.823 | 27.666 | -0.127 | 27.539 |
| 162.595 | 27.941 | -0.143 | 27.798 |
| 165.497 | 28.224 | -0.161 | 28.063 |
| 168.4 | 28.474 | -0.181 | 28.292 |
| 171.302 | 28.704 | -0.201 | 28.503 |
| 174.204 | 28.929 | -0.22 | 28.71 |
| 175.613 | 28.995 | -0.233 | 28.762 |
| 177.021 | 29.077 | -0.244 | 28.832 |
| 178.429 | 29.159 | -0.253 | 28.906 |
| 179.837 | 29.229 | -0.26 | 28.969 |
| 181.925 | 29.33 | -0.273 | 29.057 |
| 184.013 | 29.417 | -0.284 | 29.133 |
| 186.102 | 29.494 | -0.295 | 29.199 |
| 188.19 | 29.565 | -0.306 | 29.259 |
| 188.642 | 29.583 | -0.31 | 29.273 |
| 189.095 | 29.6 | -0.313 | 29.287 |
| 189.547 | 29.615 | -0.315 | 29.3 |
| 190 | 29.63 | -0.317 | 29.313 |

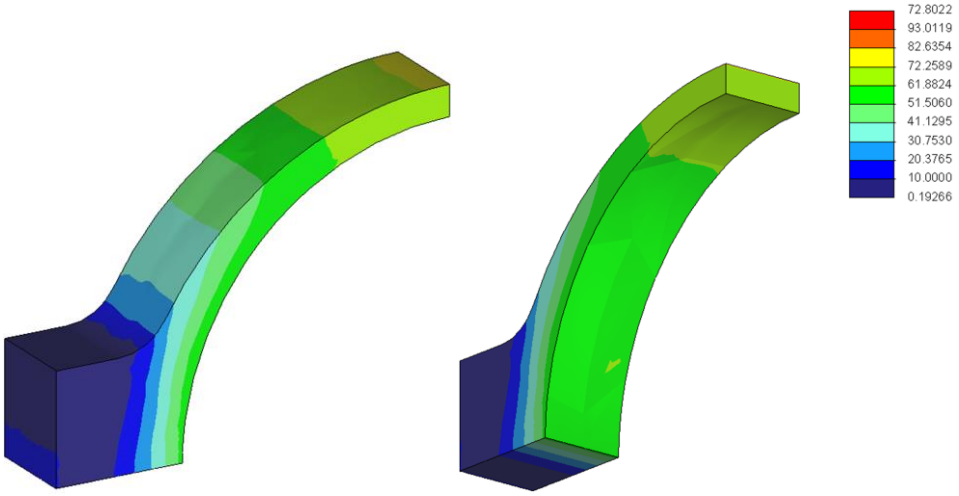


*Figure A 1: Von Mises stress of model 410 of model class I*

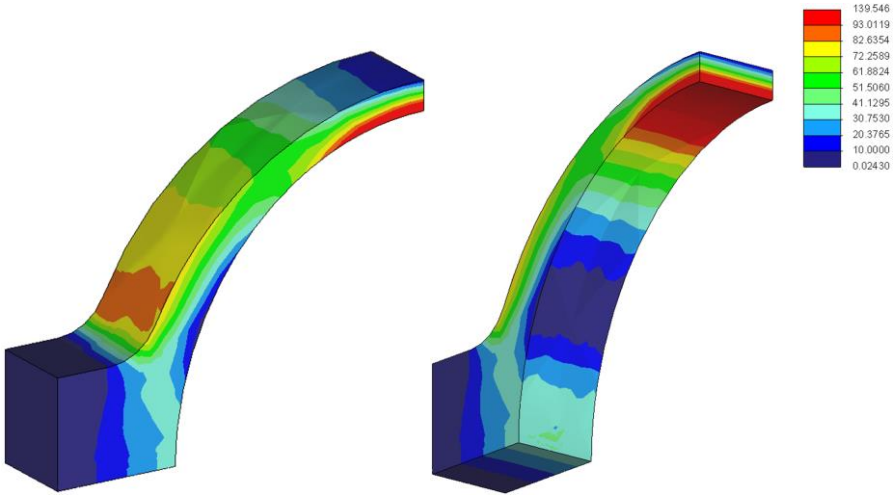


*Figure A 2: Von Mises stress of model 440 of model class I*

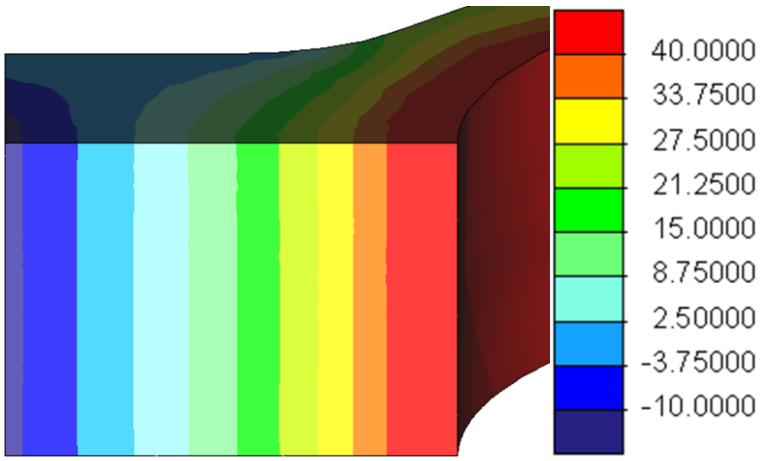


*Figure A 3: Normal stress (ZZ) across the flange of model 410 of model class I with mechanical load*

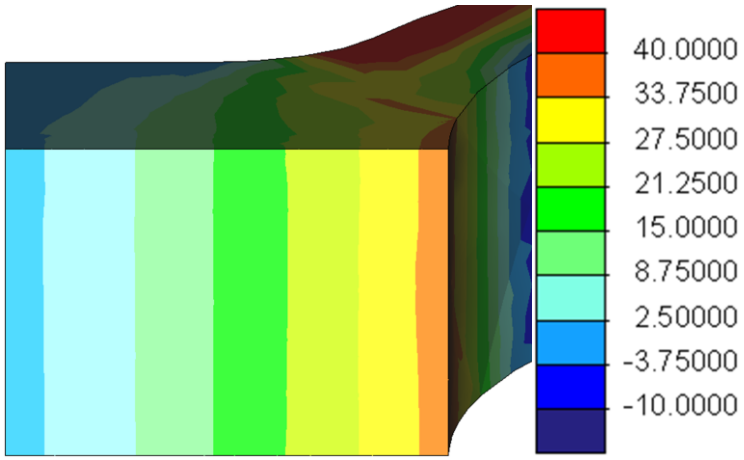


*Figure A 4: Normal stress (ZZ) across the flange of model 440 of model class I with mechanical load*

## Appendix B for chapter 4.2

*Table B 1: Normal stress (YY) of the thinnest part of model 400 of model class II*

| Length [mm] | Normal stress (YY) [N/mm²] | | |
|---|---|---|---|
| | Mechanical | Thermical | Mechanic-thermal |
| 0 | 36.755 | -10.218 | 26.537 |
| 11.25 | 54.694 | -5.081 | 49.612 |
| 22.5 | 71.81 | -0.125 | 71.685 |
| 33.75 | 88.539 | 4.621 | 93.159 |
| 45 | 105.31 | 9.127 | 114.437 |

*Table B 2: Normal stress (YY) of the thinnest part of model 410 of model class II*

| Length [mm] | Normal stress (YY) [N/mm²] | | |
|---|---|---|---|
| | Mechanical | Thermical | Mechanic-thermal |
| 0 | 67.384 | -10.338 | 57.046 |
| 11.25 | 70.276 | -5.135 | 65.141 |
| 22.5 | 73.011 | -0.124 | 72.887 |
| 33.75 | 75.864 | 4.672 | 80.536 |
| 45 | 79.113 | 9.227 | 88.34 |

*Table B 3: Normal stress (YY) of the thinnest part of model 420 of model class II*

| Length [mm] | Normal stress (ZZ) [N/mm²] | | |
|---|---|---|---|
| | Mechanic | Thermical | Mechanic-thermal |
| 0 | 98.59 | -10.45 | 88.141 |
| 11.25 | 86.138 | -5.185 | 80.952 |
| 22.5 | 74.177 | -0.122 | 74.055 |
| 33.75 | 62.858 | 4.721 | 67.579 |
| 45 | 52.329 | 9.324 | 61.653 |

*Table B 4: Normal stress (YY) of the thinnest part of model 430 of model class II*

| Length [mm] | Normal stress (YY) [N/mm²] | | |
|---|---|---|---|
| | Mechanical | Thermical | Mechanic-thermal |
| 0 | 130.354 | -10.574 | 119.78 |
| 11.25 | 102.267 | -5.244 | 97.023 |
| 22.5 | 75.308 | -0.121 | 75.187 |
| 33.75 | 49.524 | 4.779 | 54.303 |
| 45 | 24.962 | 9.44 | 34.401 |

*Table B 5: Normal stress (YY) of the thinnest part of model 440 of model class II*

| Length [mm] | Normal stress (YY) [N/mm²] | | |
|---|---|---|---|
| | Mechanical | Thermical | Mechanic-thermal |
| 0 | 162.664 | -10.697 | 151.967 |
| 11.25 | 118.654 | -5.306 | 113.348 |
| 22.50 | 76.403 | -0.121 | 76.281 |
| 33.75 | 35.866 | 4.838 | 40.704 |
| 45 | -3.000 | 9.553 | 6.552 |

*Table B 6: Normal stress (YY) of the thinnest part of model 450 of model class II*

| Length [mm] | Normal stress (YY) [N/mm²] | | |
|---|---|---|---|
| | Mechanical | Thermical | Mechanic-thermal |
| 0 | 195.672 | -10.830 | 184.842 |
| 11.25 | 135.376 | -5.369 | 130.006 |
| 22.50 | 77.451 | -0.119 | 77.332 |
| 33.75 | 21.771 | 4.904 | 26.674 |
| 45 | -31.794 | 9.683 | -22.111 |

*Table B 7: Normal stress (ZZ) across the flange with working load and bolt force of model 400 of model class II*

| Working load | | Bolt force | | Working load and bolt force | |
|---|---|---|---|---|---|
| Length [mm] | Normal stress [N/mm²] | Length [mm] | Normal stress [N/mm²] | Length [mm] | Normal stress [N/mm²] |
| 0 | -14.339 | 0 | 5.71 | 0 | -8.703 |
| 1.696 | -13.747 | 1.821 | 4.848 | 1.71 | -8.898 |
| 3.393 | -13.155 | 3.641 | 3.988 | 3.419 | -9.107 |
| 5.089 | -12.597 | 5.462 | 3.121 | 5.129 | -9.33 |
| 6.785 | -12.105 | 7.283 | 2.234 | 6.838 | -9.568 |
| 9.182 | -11.205 | 8.806 | 1.498 | 8.975 | -9.897 |
| 11.578 | -10.391 | 10.33 | 0.747 | 11.112 | -10.244 |
| 13.975 | -9.618 | 11.853 | -0.007 | 13.249 | -10.612 |
| 16.372 | -8.839 | 13.377 | -0.756 | 15.385 | -11.003 |
| 19.337 | -7.915 | 16.423 | -2.312 | 16.682 | -11.247 |
| 22.302 | -6.997 | 19.47 | -3.881 | 17.979 | -11.501 |
| 25.267 | -6.087 | 22.516 | -5.467 | 19.276 | -11.762 |
| 28.232 | -5.189 | 25.562 | -7.075 | 20.573 | -12.024 |
| 30.495 | -4.488 | 27.613 | -8.161 | 21.83 | -12.299 |
| 32.758 | -3.792 | 29.664 | -9.249 | 23.086 | -12.569 |
| 35.02 | -3.09 | 31.715 | -10.341 | 24.342 | -12.836 |
| 37.283 | -2.371 | 33.765 | -11.435 | 25.599 | -13.105 |
| 39.174 | -1.815 | 35.069 | -12.133 | 27.576 | -13.547 |
| 41.065 | -1.252 | 36.373 | -12.832 | 29.554 | -13.995 |
| 42.956 | -0.686 | 37.677 | -13.53 | 31.531 | -14.448 |
| 44.847 | -0.126 | 38.98 | -14.228 | 33.509 | -14.904 |
| 46.917 | 0.49 | 39.952 | -14.749 | 34.984 | -15.252 |
| 48.987 | 1.106 | 40.923 | -15.269 | 36.459 | -15.599 |

| | | | | | |
|---|---|---|---|---|---|
| 51.058 | 1.725 | 41.894 | -15.788 | 37.933 | -15.945 |
| 53.128 | 2.348 | 42.865 | -16.309 | 39.408 | -16.292 |
| 54.92 | 2.889 | 45.159 | -17.526 | 40.442 | -16.54 |
| 56.712 | 3.436 | 47.453 | -18.745 | 41.476 | -16.783 |
| 58.504 | 3.989 | 49.747 | -19.959 | 42.509 | -17.025 |
| 60.296 | 4.548 | 52.042 | -21.157 | 43.543 | -17.266 |
| 61.697 | 4.987 | 53.982 | -22.17 | 44.935 | -17.585 |
| 63.098 | 5.432 | 55.923 | -23.175 | 46.326 | -17.905 |
| 64.498 | 5.882 | 57.864 | -24.17 | 47.718 | -18.222 |
| 65.899 | 6.334 | 59.805 | -25.152 | 49.109 | -18.53 |
| 67.788 | 6.952 | 61.759 | -26.153 | 50.746 | -18.889 |
| 69.677 | 7.579 | 63.713 | -27.129 | 52.382 | -19.25 |
| 71.566 | 8.214 | 65.667 | -28.09 | 54.019 | -19.597 |
| 73.455 | 8.858 | 67.621 | -29.049 | 55.655 | -19.916 |
| 75.049 | 9.406 | 68.927 | -29.672 | 57.005 | -20.201 |
| 76.643 | 9.96 | 70.233 | -30.294 | 58.355 | -20.476 |
| 78.238 | 10.524 | 71.538 | -30.914 | 59.705 | -20.738 |
| 79.832 | 11.099 | 72.844 | -31.534 | 61.055 | -20.983 |
| 82.347 | 12.001 | 76.037 | -33.003 | 62.638 | -21.276 |
| 84.862 | 12.933 | 79.23 | -34.437 | 64.221 | -21.553 |
| 87.377 | 13.885 | 82.423 | -35.834 | 65.804 | -21.817 |
| 89.892 | 14.849 | 85.616 | -37.187 | 67.387 | -22.073 |
| 92.421 | 15.855 | 88.064 | -38.207 | 68.944 | -22.3 |
| 94.951 | 16.888 | 90.512 | -39.207 | 70.502 | -22.521 |
| 97.481 | 17.948 | 92.96 | -40.169 | 72.06 | -22.734 |
| 100.01 | 19.036 | 95.408 | -41.074 | 73.617 | -22.934 |
| 102.269 | 20.04 | 97.605 | -41.915 | 74.886 | -23.08 |
| 104.527 | 21.057 | 99.802 | -42.705 | 76.155 | -23.212 |
| 106.786 | 22.091 | 101.999 | -43.474 | 77.423 | -23.333 |
| 109.045 | 23.146 | 104.196 | -44.249 | 78.692 | -23.449 |
| 111.177 | 24.16 | 105.572 | -44.707 | 80.229 | -23.566 |
| 113.31 | 25.19 | 106.949 | -45.169 | 81.766 | -23.683 |
| 115.443 | 26.235 | 108.325 | -45.62 | 83.303 | -23.78 |
| 117.575 | 27.299 | 109.701 | -46.045 | 84.839 | -23.838 |
| 119.799 | 28.433 | 111.321 | -46.634 | 87.329 | -23.933 |
| 122.023 | 29.584 | 112.941 | -47.19 | 89.818 | -23.994 |
| 124.247 | 30.768 | 114.561 | -47.733 | 92.307 | -23.992 |
| 126.471 | 32 | 116.181 | -48.284 | 94.796 | -23.9 |
| 129.322 | 33.594 | 117.891 | -48.866 | 96.944 | -23.864 |
| 132.173 | 35.245 | 119.6 | -49.454 | 99.093 | -23.738 |
| 135.024 | 36.945 | 121.31 | -50.051 | 101.241 | -23.572 |
| 137.875 | 38.688 | 123.02 | -50.659 | 103.389 | -23.412 |
| 139.93 | 39.964 | 124.488 | -51.196 | 105.018 | -23.222 |
| 141.985 | 41.266 | 125.957 | -51.742 | 106.647 | -23.034 |
| 144.04 | 42.593 | 127.426 | -52.302 | 108.275 | -22.821 |
| 146.095 | 43.941 | 128.895 | -52.88 | 109.904 | -22.556 |
| 147.76 | 45.036 | 132.2 | -54.213 | 112.073 | -22.323 |
| 149.426 | 46.144 | 135.505 | -55.657 | 114.242 | -22.018 |
| 151.092 | 47.262 | 138.811 | -57.193 | 116.411 | -21.673 |
| 152.757 | 48.388 | 142.116 | -58.806 | 118.58 | -21.318 |

| | | | | | |
|---|---|---|---|---|---|
| 154.395 | 49.507 | 144.888 | -60.334 | 119.863 | -21.097 |
| 156.033 | 50.638 | 147.66 | -61.947 | 121.145 | -20.873 |
| 157.671 | 51.775 | 150.432 | -63.66 | 122.427 | -20.647 |
| 159.309 | 52.917 | 153.203 | -65.491 | 123.709 | -20.417 |
| 162.155 | 54.925 | 156.195 | -67.59 | 125.258 | -20.139 |
| 165.001 | 56.955 | 159.186 | -69.891 | 126.808 | -19.859 |
| 167.847 | 58.994 | 162.177 | -72.373 | 128.358 | -19.581 |
| 170.692 | 61.025 | 165.168 | -75.013 | 129.907 | -19.312 |
| 172.713 | 62.51 | 166.526 | -76.292 | 131.58 | -19.015 |
| 174.734 | 63.989 | 167.883 | -77.617 | 133.253 | -18.725 |
| 176.754 | 65.457 | 169.241 | -78.986 | 134.926 | -18.446 |
| 178.775 | 66.907 | 170.598 | -80.396 | 136.599 | -18.185 |
| 180.202 | 67.975 | 172.802 | -82.793 | 138.071 | -17.945 |
| 181.628 | 69.037 | 175.006 | -85.301 | 139.542 | -17.729 |
| 183.055 | 70.097 | 177.21 | -87.923 | 141.014 | -17.515 |
| 184.481 | 71.159 | 179.414 | -90.663 | 142.485 | -17.28 |
| 185.861 | 72.198 | 182.061 | -94.123 | 145.346 | -16.978 |
| 187.241 | 73.239 | 184.707 | -97.772 | 148.206 | -16.736 |
| 188.62 | 74.282 | 187.354 | -101.616 | 151.067 | -16.574 |
| 190 | 75.323 | 190 | -105.66 | 153.928 | -16.512 |
| | | | | 156.644 | -16.524 |
| | | | | 159.361 | -16.726 |
| | | | | 162.077 | -17.076 |
| | | | | 164.794 | -17.534 |
| | | | | 166.242 | -17.887 |
| | | | | 167.691 | -18.279 |
| | | | | 169.139 | -18.716 |
| | | | | 170.588 | -19.204 |
| | | | | 172.106 | -19.771 |
| | | | | 173.624 | -20.385 |
| | | | | 175.142 | -21.053 |
| | | | | 176.66 | -21.784 |
| | | | | 178.176 | -22.557 |
| | | | | 179.691 | -23.383 |
| | | | | 181.207 | -24.268 |
| | | | | 182.722 | -25.215 |
| | | | | 184.542 | -26.398 |
| | | | | 186.361 | -27.667 |
| | | | | 188.181 | -29.017 |
| | | | | 190 | -30.44 |

*Table B 8: Normal stress (ZZ) across the flange of model 400-450 of model class II with mechanical load*

| **Model** | **400** | **410** | **420** | **430** | **440** | **450** |
|---|---|---|---|---|---|---|
| **Length [mm]** | **Normal stress (ZZ) [N/mm²]** | | | | | |
| 0 | -8.703 | -4.687 | -0.641 | 3.499 | 7.712 | 12.002 |
| 1.71 | -8.898 | -4.993 | -1.051 | 2.977 | 7.079 | 11.256 |
| 3.419 | -9.107 | -5.309 | -1.471 | 2.45 | 6.443 | 10.512 |

| | | | | | | |
|---|---|---|---|---|---|---|
| 5.129 | -9.33 | -5.636 | -1.899 | 1.918 | 5.806 | 9.77 |
| 6.838 | -9.568 | -5.974 | -2.336 | 1.381 | 5.168 | 9.03 |
| 8.975 | -9.897 | -6.422 | -2.897 | 0.699 | 4.366 | 8.105 |
| 11.112 | -10.244 | -6.884 | -3.471 | 0.011 | 3.561 | 7.183 |
| 13.249 | -10.612 | -7.362 | -4.057 | -0.686 | 2.753 | 6.264 |
| 15.385 | -11.003 | -7.858 | -4.657 | -1.391 | 1.942 | 5.346 |
| 16.682 | -11.247 | -8.163 | -5.026 | -1.821 | 1.449 | 4.79 |
| 17.979 | -11.501 | -8.477 | -5.399 | -2.254 | 0.956 | 4.236 |
| 19.276 | -11.762 | -8.795 | -5.775 | -2.689 | 0.462 | 3.682 |
| 20.573 | -12.024 | -9.113 | -6.157 | -3.127 | -0.033 | 3.129 |
| 21.83 | -12.299 | -9.442 | -6.53 | -3.553 | -0.514 | 2.594 |
| 23.086 | -12.569 | -9.764 | -6.903 | -3.979 | -0.992 | 2.062 |
| 24.342 | -12.836 | -10.083 | -7.275 | -4.403 | -1.469 | 1.532 |
| 25.599 | -13.105 | -10.402 | -7.647 | -4.825 | -1.943 | 1.006 |
| 27.576 | -13.547 | -10.922 | -8.236 | -5.494 | -2.691 | 0.177 |
| 29.554 | -13.995 | -11.445 | -8.831 | -6.164 | -3.437 | -0.647 |
| 31.531 | -14.448 | -11.97 | -9.428 | -6.834 | -4.182 | -1.467 |
| 33.509 | -14.904 | -12.497 | -10.025 | -7.502 | -4.923 | -2.281 |
| 34.984 | -15.252 | -12.896 | -10.475 | -8.003 | -5.475 | -2.886 |
| 36.459 | -15.599 | -13.292 | -10.922 | -8.5 | -6.024 | -3.488 |
| 37.933 | -15.945 | -13.687 | -11.367 | -8.996 | -6.57 | -4.085 |
| 39.408 | -16.292 | -14.081 | -11.814 | -9.49 | -7.114 | -4.68 |
| 40.442 | -16.54 | -14.363 | -12.125 | -9.836 | -7.494 | -5.095 |
| 41.476 | -16.783 | -14.64 | -12.434 | -10.179 | -7.871 | -5.508 |
| 42.509 | -17.025 | -14.914 | -12.742 | -10.52 | -8.246 | -5.918 |
| 43.543 | -17.266 | -15.187 | -13.049 | -10.86 | -8.621 | -6.327 |
| 44.935 | -17.585 | -15.55 | -13.456 | -11.312 | -9.119 | -6.872 |
| 46.326 | -17.905 | -15.913 | -13.864 | -11.764 | -9.615 | -7.415 |
| 47.718 | -18.222 | -16.272 | -14.268 | -12.212 | -10.108 | -7.954 |
| 49.109 | -18.53 | -16.625 | -14.665 | -12.653 | -10.594 | -8.486 |
| 50.746 | -18.889 | -17.033 | -15.129 | -13.169 | -11.163 | -9.109 |
| 52.382 | -19.25 | -17.442 | -15.588 | -13.679 | -11.725 | -9.725 |
| 54.019 | -19.597 | -17.839 | -16.038 | -14.18 | -12.278 | -10.332 |
| 55.655 | -19.916 | -18.21 | -16.469 | -14.665 | -12.818 | -10.929 |
| 57.005 | -20.201 | -18.534 | -16.835 | -15.072 | -13.268 | -11.423 |
| 58.355 | -20.476 | -18.848 | -17.192 | -15.471 | -13.71 | -11.91 |
| 59.705 | -20.738 | -19.15 | -17.536 | -15.858 | -14.141 | -12.386 |
| 61.055 | -20.983 | -19.435 | -17.861 | -16.226 | -14.555 | -12.847 |
| 62.638 | -21.276 | -19.774 | -18.254 | -16.67 | -15.05 | -13.396 |
| 64.221 | -21.553 | -20.099 | -18.634 | -17.102 | -15.535 | -13.937 |
| 65.804 | -21.817 | -20.412 | -19.003 | -17.524 | -16.011 | -14.468 |
| 67.387 | -22.073 | -20.716 | -19.361 | -17.934 | -16.475 | -14.989 |
| 68.944 | -22.3 | -20.995 | -19.697 | -18.324 | -16.921 | -15.493 |
| 70.502 | -22.521 | -21.266 | -20.024 | -18.704 | -17.357 | -15.986 |
| 72.06 | -22.734 | -21.529 | -20.343 | -19.079 | -17.787 | -16.475 |
| 73.617 | -22.934 | -21.783 | -20.657 | -19.45 | -18.218 | -16.969 |
| 74.886 | -23.08 | -21.971 | -20.89 | -19.728 | -18.542 | -17.341 |
| 76.155 | -23.212 | -22.145 | -21.112 | -19.996 | -18.859 | -17.707 |
| 77.423 | -23.333 | -22.311 | -21.328 | -20.26 | -19.173 | -18.074 |
| 78.692 | -23.449 | -22.475 | -21.546 | -20.529 | -19.493 | -18.448 |

| | | | | | | |
|---|---|---|---|---|---|---|
| 80.229 | -23.566 | -22.642 | -21.767 | -20.806 | -19.831 | -18.846 |
| 81.766 | -23.683 | -22.815 | -22.001 | -21.1 | -20.188 | -19.268 |
| 83.303 | -23.78 | -22.97 | -22.221 | -21.383 | -20.536 | -19.684 |
| 84.839 | -23.838 | -23.086 | -22.4 | -21.626 | -20.848 | -20.065 |
| 87.329 | -23.933 | -23.281 | -22.705 | -22.039 | -21.37 | -20.703 |
| 89.818 | -23.994 | -23.444 | -22.979 | -22.423 | -21.868 | -21.319 |
| 92.307 | -23.992 | -23.55 | -23.2 | -22.759 | -22.324 | -21.899 |
| 94.796 | -23.9 | -23.574 | -23.345 | -23.028 | -22.721 | -22.426 |
| 96.944 | -23.864 | -23.63 | -23.499 | -23.282 | -23.08 | -22.893 |
| 99.093 | -23.738 | -23.607 | -23.583 | -23.476 | -23.388 | -23.318 |
| 101.241 | -23.572 | -23.548 | -23.637 | -23.643 | -23.675 | -23.727 |
| 103.389 | -23.412 | -23.496 | -23.698 | -23.819 | -23.971 | -24.145 |
| 105.018 | -23.222 | -23.393 | -23.686 | -23.9 | -24.148 | -24.42 |
| 106.647 | -23.034 | -23.295 | -23.68 | -23.989 | -24.334 | -24.706 |
| 108.275 | -22.821 | -23.172 | -23.65 | -24.054 | -24.498 | -24.971 |
| 109.904 | -22.556 | -22.999 | -23.568 | -24.067 | -24.61 | -25.183 |
| 112.073 | -22.323 | -22.892 | -23.598 | -24.234 | -24.916 | -25.634 |
| 114.242 | -22.018 | -22.718 | -23.561 | -24.335 | -25.158 | -26.021 |
| 116.411 | -21.673 | -22.506 | -23.487 | -24.403 | -25.369 | -26.38 |
| 118.58 | -21.318 | -22.286 | -23.409 | -24.468 | -25.581 | -26.742 |
| 119.863 | -21.097 | -22.147 | -23.355 | -24.5 | -25.702 | -26.953 |
| 121.145 | -20.873 | -22.006 | -23.301 | -24.533 | -25.823 | -27.166 |
| 122.427 | -20.647 | -21.864 | -23.246 | -24.566 | -25.946 | -27.381 |
| 123.709 | -20.417 | -21.719 | -23.189 | -24.599 | -26.07 | -27.598 |
| 125.258 | -20.139 | -21.545 | -23.122 | -24.64 | -26.222 | -27.862 |
| 126.808 | -19.859 | -21.369 | -23.055 | -24.682 | -26.376 | -28.131 |
| 128.358 | -19.581 | -21.198 | -22.993 | -24.731 | -26.537 | -28.407 |
| 129.907 | -19.312 | -21.037 | -22.941 | -24.789 | -26.709 | -28.694 |
| 131.58 | -19.015 | -20.858 | -22.885 | -24.855 | -26.897 | -29.009 |
| 133.253 | -18.725 | -20.688 | -22.836 | -24.93 | -27.096 | -29.335 |
| 134.926 | -18.446 | -20.53 | -22.802 | -25.018 | -27.309 | -29.675 |
| 136.599 | -18.185 | -20.391 | -22.786 | -25.126 | -27.541 | -30.034 |
| 138.071 | -17.945 | -20.261 | -22.766 | -25.216 | -27.743 | -30.349 |
| 139.542 | -17.729 | -20.155 | -22.77 | -25.329 | -27.967 | -30.685 |
| 141.014 | -17.515 | -20.05 | -22.774 | -25.443 | -28.19 | -31.021 |
| 142.485 | -17.28 | -19.927 | -22.758 | -25.535 | -28.392 | -31.334 |
| 145.346 | -16.978 | -19.847 | -22.898 | -25.893 | -28.967 | -32.13 |
| 148.206 | -16.736 | -19.827 | -23.093 | -26.299 | -29.585 | -32.963 |
| 151.067 | -16.574 | -19.879 | -23.35 | -26.758 | -30.248 | -33.833 |
| 153.928 | -16.512 | -20.017 | -23.678 | -27.275 | -30.958 | -34.738 |
| 156.644 | -16.524 | -20.244 | -24.105 | -27.898 | -31.773 | -35.748 |
| 159.361 | -16.726 | -20.623 | -24.656 | -28.616 | -32.659 | -36.803 |
| 162.077 | -17.076 | -21.127 | -25.314 | -29.426 | -33.621 | -37.921 |
| 164.794 | -17.534 | -21.726 | -26.065 | -30.323 | -34.666 | -39.117 |
| 166.242 | -17.887 | -22.142 | -26.55 | -30.877 | -35.291 | -39.813 |
| 167.691 | -18.279 | -22.591 | -27.066 | -31.457 | -35.937 | -40.527 |
| 169.139 | -18.716 | -23.081 | -27.617 | -32.068 | -36.608 | -41.261 |
| 170.588 | -19.204 | -23.614 | -28.207 | -32.713 | -37.309 | -42.018 |
| 172.106 | -19.771 | -24.222 | -28.87 | -33.428 | -38.078 | -42.844 |
| 173.624 | -20.385 | -24.867 | -29.565 | -34.171 | -38.87 | -43.687 |

| | | | | | | |
|---|---|---|---|---|---|---|
| 175.142 | -21.053 | -25.559 | -30.302 | -34.951 | -39.696 | -44.56 |
| 176.66 | -21.784 | -26.306 | -31.093 | -35.781 | -40.566 | -45.474 |
| 178.176 | -22.557 | -27.09 | -31.904 | -36.619 | -41.437 | -46.378 |
| 179.691 | -23.383 | -27.92 | -32.762 | -37.504 | -42.349 | -47.322 |
| 181.207 | -24.268 | -28.804 | -33.668 | -38.43 | -43.299 | -48.298 |
| 182.722 | -25.215 | -29.747 | -34.623 | -39.396 | -44.281 | -49.298 |
| 184.542 | -26.398 | -30.907 | -35.796 | -40.578 | -45.473 | -50.506 |
| 186.361 | -27.667 | -32.149 | -37.038 | -41.819 | -46.718 | -51.759 |
| 188.181 | -29.017 | -33.461 | -38.341 | -43.112 | -48.005 | -53.047 |
| 190 | -30.44 | -34.834 | -39.696 | -44.449 | -49.327 | -54.361 |

*Table B 9: Normal stress (YY) of the thinnest part of model 420_20 of model class II*

| Length [mm] | Normal stress (YY) [N/mm²] | | |
|---|---|---|---|
| | Mechanical | Thermical | Mechanic-thermal |
| 0 | 104.222 | -8.927 | 95.294 |
| 11.25 | 90.502 | -4.365 | 86.137 |
| 22.50 | 77.287 | 0.018 | 77.304 |
| 33.75 | 64.782 | 4.203 | 68.984 |
| 45 | 53.193 | 8.169 | 61.362 |

*Table B 10: Normal stress (ZZ) across the flange of model 420_20 of model class II*

| Length [mm] | Normal stress (ZZ) [N/mm²] | | |
|---|---|---|---|
| | Mechanical | Thermical | Mechanic-thermal |
| 0 | 10.713 | -6.987 | 3.726 |
| 2.505 | 9.749 | -6.508 | 3.241 |
| 5.009 | 8.717 | -6.01 | 2.708 |
| 7.514 | 7.674 | -5.522 | 2.153 |
| 10.019 | 6.676 | -5.074 | 1.602 |
| 12.377 | 5.683 | -4.65 | 1.034 |
| 14.735 | 4.712 | -4.245 | 0.467 |
| 17.093 | 3.714 | -3.857 | -0.143 |
| 19.452 | 2.641 | -3.482 | -0.841 |
| 21.908 | 1.717 | -3.094 | -1.377 |
| 24.364 | 0.745 | -2.72 | -1.975 |
| 26.821 | -0.248 | -2.359 | -2.606 |
| 29.277 | -1.234 | -2.009 | -3.243 |
| 31.495 | -2.141 | -1.706 | -3.847 |
| 33.714 | -3.034 | -1.409 | -4.443 |
| 35.932 | -3.915 | -1.114 | -5.029 |
| 38.151 | -4.784 | -0.821 | -5.605 |
| 41.081 | -5.936 | -0.458 | -6.394 |
| 44.012 | -7.077 | -0.111 | -7.188 |
| 46.943 | -8.224 | 0.211 | -8.013 |
| 49.874 | -9.395 | 0.501 | -8.894 |
| 52.384 | -10.375 | 0.76 | -9.615 |
| 54.893 | -11.343 | 1.007 | -10.336 |
| 57.402 | -12.294 | 1.236 | -11.058 |

| | | | |
|---|---|---|---|
| 59.912 | -13.226 | 1.439 | -11.787 |
| 61.726 | -13.868 | 1.6 | -12.268 |
| 63.54 | -14.529 | 1.738 | -12.79 |
| 65.354 | -15.172 | 1.868 | -13.305 |
| 67.168 | -15.763 | 2.001 | -13.762 |
| 69.658 | -16.681 | 2.121 | -14.56 |
| 72.149 | -17.519 | 2.234 | -15.285 |
| 74.639 | -18.29 | 2.326 | -15.965 |
| 77.129 | -19.007 | 2.383 | -16.624 |
| 78.585 | -19.442 | 2.404 | -17.038 |
| 80.042 | -19.853 | 2.419 | -17.434 |
| 81.498 | -20.239 | 2.426 | -17.813 |
| 82.955 | -20.601 | 2.427 | -18.173 |
| 85.068 | -21.097 | 2.415 | -18.682 |
| 87.181 | -21.574 | 2.384 | -19.19 |
| 89.294 | -21.984 | 2.348 | -19.635 |
| 91.407 | -22.283 | 2.321 | -19.961 |
| 92.801 | -22.686 | 2.214 | -20.472 |
| 94.195 | -22.993 | 2.124 | -20.868 |
| 95.589 | -23.248 | 2.05 | -21.198 |
| 96.983 | -23.498 | 1.986 | -21.512 |
| 98.202 | -23.692 | 1.874 | -21.818 |
| 99.422 | -23.878 | 1.8 | -22.078 |
| 100.641 | -24.039 | 1.712 | -22.328 |
| 101.86 | -24.162 | 1.557 | -22.605 |
| 104.173 | -24.622 | 1.37 | -23.253 |
| 106.485 | -25.018 | 1.151 | -23.867 |
| 108.798 | -25.371 | 0.942 | -24.429 |
| 111.11 | -25.707 | 0.786 | -24.921 |
| 113.117 | -26.13 | 0.571 | -25.559 |
| 115.123 | -26.476 | 0.361 | -26.115 |
| 117.13 | -26.786 | 0.159 | -26.627 |
| 119.136 | -27.104 | -0.032 | -27.136 |
| 120.76 | -27.346 | -0.184 | -27.53 |
| 122.383 | -27.595 | -0.344 | -27.939 |
| 124.007 | -27.85 | -0.5 | -28.35 |
| 125.631 | -28.108 | -0.64 | -28.748 |
| 128.809 | -28.638 | -0.899 | -29.537 |
| 131.987 | -29.165 | -1.101 | -30.266 |
| 135.165 | -29.724 | -1.275 | -30.999 |
| 138.344 | -30.35 | -1.453 | -31.804 |
| 140.023 | -30.683 | -1.497 | -32.18 |
| 141.703 | -31.037 | -1.56 | -32.597 |
| 143.383 | -31.385 | -1.626 | -33.011 |
| 145.063 | -31.701 | -1.679 | -33.38 |
| 146.875 | -32.189 | -1.667 | -33.856 |
| 148.687 | -32.64 | -1.684 | -34.325 |
| 150.499 | -33.089 | -1.694 | -34.783 |
| 152.312 | -33.569 | -1.659 | -35.228 |
| 154.003 | -34.039 | -1.683 | -35.722 |

| | | | |
|---|---|---|---|
| 155.694 | -34.517 | -1.665 | -36.182 |
| 157.385 | -35.019 | -1.644 | -36.663 |
| 159.076 | -35.563 | -1.655 | -37.218 |
| 160.927 | -36.204 | -1.593 | -37.798 |
| 162.778 | -36.848 | -1.539 | -38.387 |
| 164.629 | -37.532 | -1.464 | -38.996 |
| 166.48 | -38.291 | -1.342 | -39.634 |
| 167.876 | -38.797 | -1.298 | -40.095 |
| 169.271 | -39.325 | -1.239 | -40.565 |
| 170.667 | -39.922 | -1.11 | -41.032 |
| 172.063 | -40.633 | -0.855 | -41.488 |
| 175.359 | -41.911 | -0.807 | -42.718 |
| 178.655 | -43.352 | -0.602 | -43.954 |
| 181.951 | -44.899 | -0.294 | -45.193 |
| 185.247 | -46.496 | 0.067 | -46.43 |
| 186.435 | -47.048 | 0.179 | -46.869 |
| 187.623 | -47.61 | 0.321 | -47.289 |
| 188.812 | -48.178 | 0.475 | -47.703 |
| 190 | -48.747 | 0.622 | -48.125 |

*Table B 11: Normal stress (YY) of the thinnest part of model narrow-flange*

| **Length [mm]** | **Normal stress (YY) [N/mm²]** | | |
|---|---|---|---|
| | **Mechanical** | **Thermical** | **Mechanic-thermal** |
| 0 | 84.412 | -11.646 | 72.766 |
| 11.25 | 81.112 | -5.732 | 75.381 |
| 22.5 | 77.935 | 0.069 | 78.004 |
| 33.75 | 75.136 | 5.621 | 80.757 |
| 45 | 72.972 | 10.788 | 83.760 |

*Table B 12: Normal stress (ZZ) across the flange of model narrow-flange*

| **Length [mm]** | **Normal stress (ZZ) [N/mm²]** | | |
|---|---|---|---|
| | **Mechanical** | **Thermical** | **Mechanic-thermal** |
| 0 | -23.068 | -5.272 | -28.34 |
| 1.784 | -23.871 | -4.741 | -28.612 |
| 3.568 | -24.685 | -4.232 | -28.917 |
| 5.351 | -25.525 | -3.745 | -29.27 |
| 7.135 | -26.407 | -3.282 | -29.689 |
| 8.736 | -26.896 | -2.921 | -29.817 |
| 10.337 | -27.458 | -2.571 | -30.029 |
| 11.938 | -28.054 | -2.236 | -30.29 |
| 13.539 | -28.641 | -1.925 | -30.566 |
| 15.38 | -29.269 | -1.603 | -30.872 |
| 17.222 | -29.867 | -1.307 | -31.173 |
| 19.063 | -30.431 | -1.033 | -31.464 |
| 20.904 | -30.958 | -0.778 | -31.736 |
| 23.026 | -31.544 | -0.528 | -32.072 |
| 25.148 | -32.071 | -0.299 | -32.37 |

| | | | |
|---|---|---|---|
| 27.271 | -32.547 | -0.092 | -32.639 |
| 29.393 | -32.981 | 0.092 | -32.889 |
| 30.913 | -33.275 | 0.202 | -33.074 |
| 32.434 | -33.553 | 0.3 | -33.253 |
| 33.954 | -33.81 | 0.388 | -33.422 |
| 35.474 | -34.046 | 0.468 | -33.578 |
| 37.321 | -34.327 | 0.541 | -33.786 |
| 39.167 | -34.584 | 0.601 | -33.983 |
| 41.013 | -34.82 | 0.646 | -34.174 |
| 42.859 | -35.042 | 0.672 | -34.37 |
| 44.427 | -35.222 | 0.688 | -34.534 |
| 45.995 | -35.392 | 0.69 | -34.701 |
| 47.562 | -35.557 | 0.683 | -34.874 |
| 49.13 | -35.72 | 0.67 | -35.05 |
| 50.15 | -35.803 | 0.66 | -35.143 |
| 51.169 | -35.897 | 0.643 | -35.254 |
| 52.188 | -35.995 | 0.624 | -35.371 |
| 53.208 | -36.094 | 0.606 | -35.488 |
| 54.959 | -36.251 | 0.569 | -35.683 |
| 56.711 | -36.419 | 0.533 | -35.886 |
| 58.462 | -36.596 | 0.487 | -36.109 |
| 60.214 | -36.782 | 0.413 | -36.369 |
| 62.738 | -36.954 | 0.353 | -36.601 |
| 65.261 | -37.205 | 0.285 | -36.92 |
| 67.785 | -37.498 | 0.222 | -37.276 |
| 70.309 | -37.797 | 0.179 | -37.618 |
| 72.156 | -38.02 | 0.155 | -37.865 |
| 74.003 | -38.27 | 0.139 | -38.132 |
| 75.851 | -38.514 | 0.131 | -38.382 |
| 77.698 | -38.715 | 0.133 | -38.582 |
| 79.387 | -39.003 | 0.167 | -38.836 |
| 81.077 | -39.312 | 0.203 | -39.109 |
| 82.766 | -39.629 | 0.247 | -39.382 |
| 84.455 | -39.941 | 0.306 | -39.635 |
| 86.128 | -40.28 | 0.376 | -39.904 |
| 87.802 | -40.649 | 0.457 | -40.192 |
| 89.475 | -41.025 | 0.553 | -40.471 |
| 91.148 | -41.383 | 0.669 | -40.714 |
| 93.27 | -41.924 | 0.83 | -41.094 |
| 95.392 | -42.479 | 1.019 | -41.46 |
| 97.513 | -43.065 | 1.229 | -41.836 |
| 99.635 | -43.696 | 1.458 | -42.238 |
| 101.278 | -44.199 | 1.662 | -42.537 |
| 102.921 | -44.7 | 1.874 | -42.827 |
| 104.563 | -45.209 | 2.102 | -43.108 |
| 106.206 | -45.735 | 2.355 | -43.38 |
| 107.548 | -46.15 | 2.573 | -43.577 |
| 108.889 | -46.639 | 2.801 | -43.838 |
| 110.23 | -47.048 | 3.042 | -44.006 |
| 111.572 | -47.225 | 3.302 | -43.923 |

| | | | |
|---|---|---|---|
| 113.679 | -48.139 | 3.688 | -44.451 |
| 115.786 | -48.974 | 4.134 | -44.84 |
| 117.893 | -49.799 | 4.617 | -45.182 |
| 120 | -50.68 | 5.112 | -45.568 |

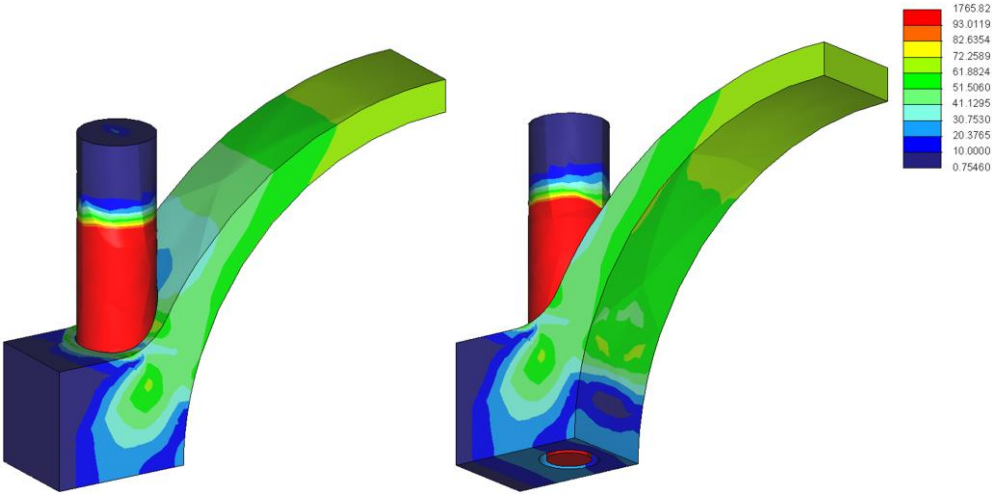


*Figure B 1: Von Mises stress of model 410 model class II*

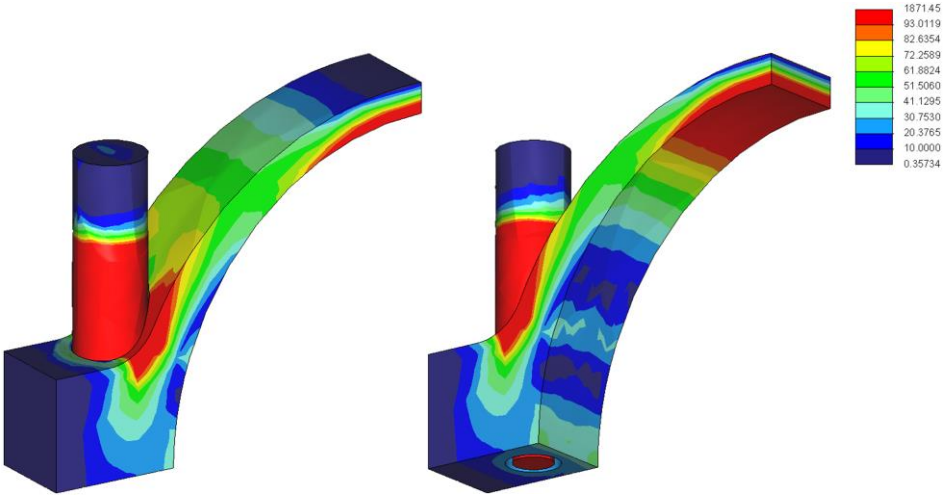


*Figure B 2: Von Mises stress of model 440 of model class II*

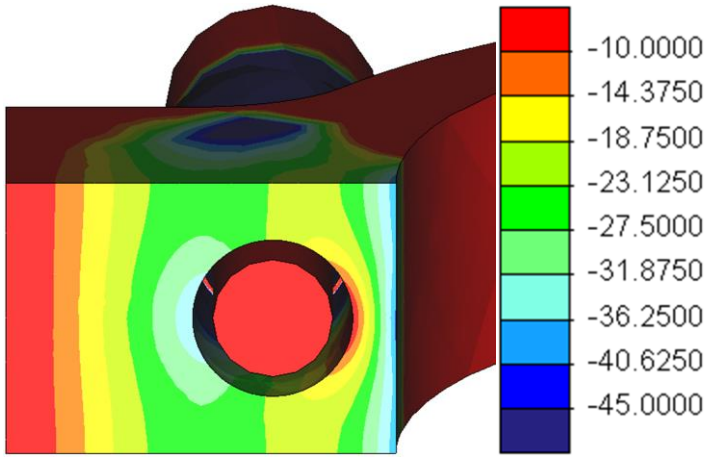


*Figure B 3: Normal stress (ZZ) across the flange of model 410 of model class II with mechanical load*

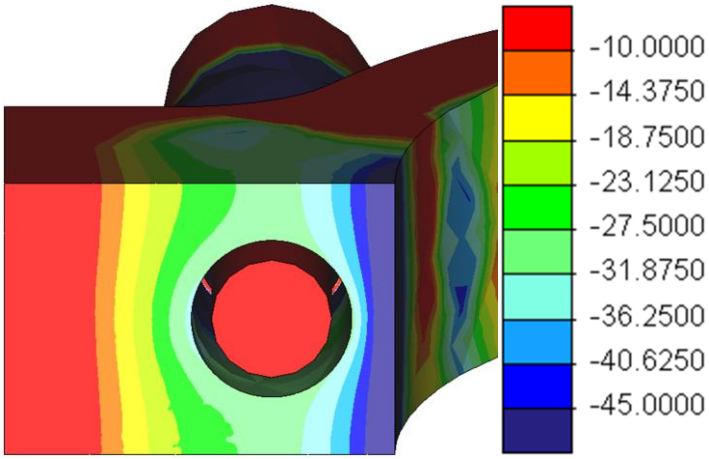


*Figure B 4: Normal stress (ZZ) across the flange of model 440 of model class II with mechanical load*

# Affidavit

I assure that I have written this thesis myself. No further sources or aids were used than those explicitly stated. All citations in this work are labeled as such.

This thesis will be published in September 2015 on: www.theseus.fi

Hamburg, 14.08.2015

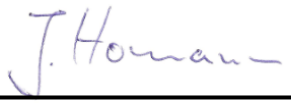

(Place, Date) (Jochen Homann)